

**SMART CAR SEAT DESIGN FOR SAFETY AND
COMFORT**

**GÜVENLİK VE KONFOR İÇİN AKILLI ARABA
KOLTUĞU TASARIMI**

CANSU KARABEYOĞLU

ASSIST. PROF. DR. SELÇUK HİMMETOĞLU

Thesis Supervisor

Submitted to Graduate School of Science and Engineering of Hacettepe University
as a Partial Fulfillment to the Requirements
for the Award of the Degree of Master of Sciences
in Mechanical Engineering

2019

This work named “**Smart Car Seat Design For Safety and Comfort**” by CANSU **KARABEYOĞLU** has been approved as a thesis for the degree of **MASTER OF SCIENCE IN MECHANICAL ENGINEERING** by the below mentioned Examining Committee Members.

Assoc. Prof. Dr. Selahattin Çağlar BAŞLAMIŞLI

Head

.....



Assist. Prof. Dr. Selçuk HİMMETOĞLU

Supervisor

.....


Assoc. Prof. Dr. Can Ulaş DOĞRUER

Member

.....


Assoc. Prof. Dr. Mehmet Bülent ÖZER

Member

.....


Assist. Prof. Dr. Özgür ÜNVER

Member

.....


This thesis has been approved as a thesis for the degree of **MASTER OF SCIENCE IN MECHANICAL ENGINEERING** by a Board of Directors of the Institute for Graduate School of Science and Engineering at the date of / /..... .

Prof. Dr. Menemşe GÜMÜŞDERELİOĞLU

Director of the Institute of Graduate School of Science and
Engineering

ETHICS

In this thesis study, prepared in accordance with the spelling rules of Institute of Graduate Studies in Science of Hacettepe University,

I declare that

- all the information and documents have been obtained in the base of the academic rules
- all audio-visual and written information and results have been presented according to the rules of scientific ethics
- in case of using others Works, related studies have been cited in accordance with the scientific standards
- all cited studies have been fully referenced
- I did not do any distortion in the data set
- and any part of this thesis has not been presented as another thesis study at this or any other university

17/07/2019



CANSU KARABEYOđLU

YAYINLANMA FİKRİ MÜLKİYET HAKLARI BEYANI

Enstitü tarafından onaylanan lisansüstü tezimin/raporumun tamamını veya herhangi bir kısmını, basılı (kağıt) ve elektronik formatta arşivleme ve aşağıda verilen koşullarla kullanıma açma iznini Hacettepe üniversitesine verdiğimi bildiririm. Bu izinle Üniversiteye verilen kullanım hakları dışındaki tüm fikri mülkiyet haklarım bende kalacak, tezimin tamamının ya da bir bölümünün gelecekteki çalışmalarda (makale, kitap, lisans ve patent vb.) kullanım hakları bana ait olacaktır.

Tezin kendi orijinal çalışmam olduğunu, başkalarının haklarını ihlal etmediğimi ve tezimin tek yetkili sahibi olduğumu beyan ve taahhüt ederim. Tezimde yer alan telif hakkı bulunan ve sahiplerinden yazılı izin alınarak kullanması zorunlu metinlerin yazılı izin alarak kullandığımı ve istenildiğinde suretlerini Üniversiteye teslim etmeyi taahhüt ederim.

Yükseköğretim Kurulu tarafından yayınlanan "*Lisansüstü Tezlerin Elektronik Ortamda Toplanması, Düzenlenmesi ve Erişime Açılmasına İlişkin Yönerge*" kapsamında tezim aşağıda belirtilen koşullar haricince YÖK Ulusal Tez Merkezi / H. Ü. Kütüphaneleri Açık Erişim Sisteminde erişime açılır.

- Enstitü / Fakülte yönetim kurulu kararı ile tezimin erişime açılması mezuniyet tarihimden itibaren 2 yıl ertelenmiştir.
- Enstitü / Fakülte yönetim kurulu gerekçeli kararı ile tezimin erişime açılması mezuniyet tarihimden itibaren ay ertelenmiştir.
- Tezim ile ilgili gizlilik kararı verilmiştir.

17.07.2019

(İmza)


CANSU KARABEYOĞLU

ABSTRACT

SMART CAR SEAT DESIGN FOR SAFETY AND COMFORT

Cansu KARABEYOĞLU

Master of Science, Department of Mechanical Engineering

Supervisor: Assist. Prof. Dr. Selçuk Himmetođlu

July 2019, 89 pages

In this work of thesis, whiplash injury and its relation with rear end accidents are studied. After brief explanation on what whiplash injury is and its effects on both people's health and economy, injury mechanism is studied. Injury criteria on the subject of whiplash injuries are explained, and the major factors affecting the whiplash injury risk in rear end collisions are discussed. Alternative car seat and head restraint designs for reducing the whiplash injury risk are considered and physical properties of such head restraint design are optimized as a reference for further design studies.

Keywords: vehicle rear impact, whiplash injury, head restraint design, car seat

ÖZET

GÜVENLİK VE KONFOR İÇİN AKILLI ARABA KOLTUĞU TASARIMI

Cansu KARABEYOĞLU

Yüksek Lisans, Makina Mühendisliği Bölümü

Tez Danışmanı: Dr. Öğr. Üyesi Selçuk Himmetoğlu

Temmuz 2019, 89 sayfa

Bu tez çalışmasında, boyun incinmesi ve araçlarda arkadan çarpışmalarla ilişkisi incelenmiştir. Boyun incinmesi ve bunun insan sağlığına ve ekonomiye etkileriyle ilgili kısa bir açıklamadan sonra, yaralanma mekanizması incelenmiştir. Boyun incinmesi konusunda yaralanma kriterleri açıklanarak, arkadan çarpışmalarda boyun incinmelerine neden olan ana faktörler hakkında bilgi verilmiştir. Boyun yaralanması riskini azaltacak alternatif araç koltuğu ve koltuk başlığı tasarımları değerlendirilerek, konuyla ilgili bir koltuk başlığı tasarımı, ileri çalışmalara referans olması için optimize edilmiştir.

Anahtar Kelimeler: arkadan çarpışmalar, boyun yaralanması, koltuk başlığı tasarımı, araba koltuğu

ACKNOWLEDGEMENTS

First of all, I would like to express my sincere gratitude to my supervisor Assist. Prof. Dr. Selçuk Himmetoğlu for his continuous support for my study. He helped me throughout my research and writing of this thesis with his guidance and motivation, and steered me in the right direction when I needed.

Besides my advisor, I would like to thank the rest of my thesis committee for their insightful comments and suggestions.

I would also like to thank our research assistants, technicians Hasan Çelikli and Selamet Çöçü, and students of Mechanical Engineering Department who helped with the preparation of the experiment setups. I also thank all the volunteer students of our school who participated in the experiments. The experiments could not have been successfully completed without their help.

My sincere thanks also go to my friends and coworkers who helped me with their unique perspectives and motivated me during both the research and writing of this thesis.

Finally, I would like to thank my family for their never-ending support and continuous encouragement throughout my years of study. This accomplishment would not have been possible without them.

TABLE OF CONTENTS

ABSTRACT	i
ÖZET.....	ii
ACKNOWLEDGEMENTS	iii
TABLE OF CONTENTS	iv
LIST OF FIGURES.....	vii
LIST OF TABLES	x
1. INTRODUCTION.....	1
2. GENERAL INFORMATION	2
2.1. Whiplash Injury.....	2
2.2. Injury Criteria and Thresholds	3
2.2.1. The Neck Injury Criterion (NIC)	3
2.2.2. The Nij Criterion.....	4
2.2.3. The Nkm Criterion	4
2.2.4. The Intervertebral Neck Injury Criterion (IV-NIC).....	5
2.2.5. The Neck Displacement Criterion (NDC).....	5
2.2.6. The Lower Neck Load Index (LNL)	6
2.3. Affecting Factors.....	8
2.3.1. Crash Severity	8
2.3.2. Seating Position.....	8
2.3.3. Occupant Related Factors.....	9
2.3.4. Seat Design and Head Restraint Geometry	9
3. EXPERIMENTAL STUDIES.....	12
3.1. Seatback Angle Study	12
3.1.1. Experiment Results and Discussion	15
3.2. Head Range of Motion and Torso Extension Study.....	16
3.2.1. Measurement Device.....	19
3.2.2. Range of Motion Measurement.....	21
3.2.3. Results of the Experiments.....	24
4. COMPUTATIONAL STUDIES	35

4.1. Mechanical Properties of the Car Seat.....	36
4.1.1. Head Restraint Model	36
4.1.2. Energy absorber at the bottom of the seat pan.....	37
4.1.3. Head-restraint damper at the top of the seatback.....	37
4.1.4. Recliner Mechanical Properties	38
4.1.5. Seat Foam Mechanical Properties.....	39
4.1.6. Seatpan Angle of the Seat and H-Point Height.....	40
4.2. Adjusted Seating Positions at 15°, 20°, 25° and 30° Seatback Angles	41
4.3. Selection of the Optimized Car Seat.....	42
4.3.1. Seatpan damper is locked + recliner breakaway is removed (RONB):	43
4.3.2. Seatpan damper is locked + recliner with breakaway (ROWB):	44
4.3.3. Seatpan damper is active + recliner breakaway is removed (RSNB):	44
4.3.4. Seatpan damper is active + recliner with breakaway (RSWB):.....	45
4.3.5. Seatpan damper is active + recliner is locked (SOLR):.....	45
4.4. Performance of the Car Seat at Various Severities of Crash Pulses	46
4.4.1. At 15° Seatback Angle.....	46
4.4.2. At 20° Seatback Angle.....	47
4.4.3. At 25° Seatback Angle.....	47
4.4.4. At 30° Seatback Angle.....	48
4.5. Adaptation of the Head Restraint Model to the Simulations	49
4.5.1. Simulations with Locked Head Restraint	50
4.5.2. Damping Simulations	51
4.5.3. Performance on High and Low Severity Crash Pulses	54
4.5.4. Comparison with the Experimental Results.....	56
5. RESULTS AND DISCUSSION	64
5.1. Comparison of the Seat's Performance with and without the New HR design.....	64
5.1.1. TR16 Test Standards (Low Severity Crash)	64
5.1.2. IIWPG Test Standards (Medium Severity Crash)	67
5.1.3. TR24 Test Standards (High Severity Crash)	71
5.2. Discussion.....	74
6. CONCLUSION.....	77
7. REFERENCES	78

APPENDIX	83
APPENDIX 1 – RANGE OF MOTION STUDY OF NECK.....	83
CURRICULUM VITAE	89

LIST OF FIGURES

Figure 1 - IIWPG neck force classification [26].....	6
Figure 2 - Typical driving posture of a 50th percentile male, showing various reference points [52].....	7
Figure 3 - Height (H) and backset (B) of the head restraint	9
Figure 4 - An example car seat for seatback angle measurement.....	12
Figure 5 - Scale for seatback angle fixed on the seat's recliner	13
Figure 6 - Seatback angle wrt occupant height.....	14
Figure 7 - Seatback angle wrt occupant height for male occupants	14
Figure 8 - Seatback angle wrt occupant height for female occupants	15
Figure 9 - Measurement of the markers with the 3D measurement device	16
Figure 10 - Protrusion motion and measured reference points P1/P2 [59].....	17
Figure 11 - Neutral and reclined seating positions for torso ROM measurements.....	18
Figure 12 - 3 reference points necessary for determination of the head circle [58]	18
Figure 13 - Drawing of the head circle and neck with 5 reference points	19
Figure 14 - Solid model of the 3D measurement device	19
Figure 15 - Neutral position of the head	22
Figure 16 - Flexion position of the head.....	22
Figure 17 - Extension position of the head	23
Figure 18 - Calculation of the head motion through CATIA with measured coordinates	24
Figure 19 - Vertical and horizontal lines as used in the calculations	25
Figure 20 - Horizontal distance traveled by head geometrical center wrt occupant height	27
Figure 21 - Horizontal distance traveled by head geometrical center wrt occupant sitting height	27
Figure 22 - Vertical distance traveled by head geometrical center wrt occupant height	28
Figure 23 - Vertical distance traveled by head geometrical center wrt occupant sitting height	28
Figure 24 - Horizontal distance traveled by head geometrical center wrt occupant height (For female subjects)	29

Figure 25 - Horizontal distance traveled by head geometrical center wrt occupant height (For male subjects)	29
Figure 26 - Horizontal distance traveled by head geometrical center wrt occupant sitting height (For female subjects)	30
Figure 27 - Horizontal distance traveled by head geometrical center wrt occupant sitting height (For male subjects)	30
Figure 28 - Vertical distance traveled by head geometrical center wrt occupant height (For female subjects)	31
Figure 29 - Vertical distance traveled by head geometrical center wrt occupant height (For male subjects)	31
Figure 30 - Vertical distance traveled by head geometrical center wrt occupant sitting height (For female subjects)	32
Figure 31 - Vertical distance traveled by head geometrical center wrt occupant sitting height (For male subjects)	32
Figure 32 - Normal (Gaussian) distribution comparison of horizontal distance traveled by head geometrical center	33
Figure 33 - Normal (Gaussian) distribution comparison of horizontal distance traveled by head geometrical center for female occupants	33
Figure 34 - Normal (Gaussian) distribution comparison of horizontal distance traveled by head geometrical center for male occupants	34
Figure 35 - Hysteresis model for the head-restraint	36
Figure 36 - Head restraint mechanical properties	36
Figure 37 - Mechanical properties of the energy absorber at the bottom of the seat pan	37
Figure 38 - Stiffness properties of the head restraint damper	37
Figure 39 - Basic representation of the head restraint damper position	38
Figure 40 - Stiffness properties of the recliner mechanism	38
Figure 41 - Stiffness properties of the foam	39
Figure 42 - Damping properties of the foam	40
Figure 43 - H-Point and seatpan angle	41
Figure 44 - Adjusting the seatback angle in the simulation	41
Figure 45 - Reference seating positions at various seatback angles	42
Figure 46 - Simulation for RONB seat	43
Figure 47 - Simulation for ROWB seat	44
Figure 48 - Simulation for RSNB seat	44

Figure 49 - Simulation for RSWB seat.....	45
Figure 50 - Simulation for SOLR seat.....	45
Figure 51 - Adjusting the head restraint position	49
Figure 52 - Simulation with locked head restraint at 30° seatback angle.....	50
Figure 53 - Adjusting the damping ratio and stiffness for the head restraint	51
Figure 54 - Seatback 30° optimizations.....	52
Figure 55 - Seatback 25° optimizations.....	52
Figure 56 - Seatback 20° optimizations.....	53
Figure 57 - Seatback 15° optimizations.....	54
Figure 58 - Original seating position	57
Figure 59 - Adjusted seating position.....	58
Figure 60 - Reclined position representing rear crash	58
Figure 61 - Vectorial representation of the specified coordinates	59
Figure 62 - Given angles of the specified vectors	60
Figure 63 - TR16 Crash Pulse Fsh Comparison	65
Figure 64 - TR16 Crash Pulse Ftn Comparison.....	65
Figure 65 - TR16 Crash Pulse Nkm Comparison.....	66
Figure 66 - TR16 Crash Pulse Torso Orientation Comparison	66
Figure 67 - TR16 Crash Pulse NIC Comparison	67
Figure 68 - IIWPG Crash Pulse Fsh Comparison.....	68
Figure 69 - IIWPG Crash Pulse Ftn Comparison	69
Figure 70 - IIWPG Crash Pulse Nkm Comparison.....	69
Figure 71 - IIWPG Crash Pulse Torso Orientation Comparison	70
Figure 72 - IIWPG Crash Pulse NIC Comparison.....	70
Figure 73 - TR24 Crash Pulse Fsh Comparison	72
Figure 74 - TR24 Crash Pulse Ftn Comparison.....	72
Figure 75 - TR24 Crash Pulse Nkm Comparison.....	73
Figure 76 - TR24 Crash Pulse Torso Orientation Comparison	73
Figure 77 - TR24 Crash Pulse NIC Comparison	74
Figure 78- The variation in the combined flexion– extension range of motions for voluntary sagittal rotations of the human thoracic and lumbar vertebrae [52].....	76

LIST OF TABLES

Table 1 - Average SB (seatback) Angle and Standard deviation of Seatback Angles for people of various Statures	13
Table 2 - Torso Extension Experiment Results.....	26
Table 3 – Horizontal (Δy) and vertical (Δz) distances traveled by head geometrical center in simulations.....	60
Table 4 - Different damping values comparison (Δy horizontal and Δz vertical distances).....	61
Table 5 - Simulation results for TR16 crash pulse with the original car seat design.....	64
Table 6 – Simulation results for TR16 crash pulse with the new HR design	64
Table 7 - Simulation results for IIWPG crash pulse with the original car seat design ...	67
Table 8 - Simulation results for IIWPG crash pulse with the new HR design.....	68
Table 9 - Simulation results for TR24 crash pulse with the original car seat design.....	71
Table 10 - Simulation results for TR24 crash pulse with the new HR design	71

1. INTRODUCTION

This work focuses on the importance of the seat design in rear end accidents and considers possible smart seat designs for decreasing the injury risk. In case of rear end collisions, head and neck injuries are the most frequent injury types to occur, and they are considered the main injury mechanism for that type of accidents. Whiplash injuries are one of the most common injury types in car accidents. During rear-end collisions; the occupant's torso is first pressed into the seatback, then at the second part of the collision pushed from the seatback. During the whole movement the neck is exposed to a motion similar to whiplash motion. This motion can cause large loads to arise in the neck due to head inertia, and these large loads can result in whiplash injuries [1]. Most of the time this type of injuries heals after a short duration, but long-term problems can also occur in some of the injured occupants, therefore making this type of injury significant in terms of frequency and long term health issues [2]. It can be caused by impacts from all directions, but it is most commonly caused by rear end collisions [3].

With the increasing number of vehicles and traffic density, car accidents are becoming even more important topic. According to data on traffic accident analysis done in Japan, rear-end crashes cause 4% of fatalities, and about 50% of total injuries. Of these rear-end crashes, 77% result in neck injuries, and majority of these injuries are whiplash injuries [4]. So, even though rear-end crashes don't constitute a high fatality risk, whiplash injuries produce an increasing amount of health and economic problems. Besides cost reported by insurance companies (which makes over 80% of the total cost of personal injury claims in England), with further unaccounted medical costs and the cost of lost working days because of whiplash injuries amount to a high financial loss for the economy. Additionally, they can cause painful symptoms and disablements for up to many years following the crash [5].

2. GENERAL INFORMATION

2.1. Whiplash Injury

Since rear-end collisions are considered to be the main reason for whiplash injuries in car accidents, many biomechanical experiments have been done for studying whiplash injury. In case of a rear-end collision, first the pelvis is accelerated rearwards and due to passenger posture and a delay caused by seatback structure, movement of the upper torso comes after. This movement unsynchronization between the upper torso and the pelvis causes a small rotation motion of the torso, which causes the flexion of the neck. As the upper torso moves backwards with respect to head, horizontal translation motion occurs between the cervical spine base and the head. This motion applies compression, shear, and tensional forces in the lower vertebrae [6]. The term “whiplash injury” comes from the whiplash-like motion of the neck causing the injury, and is commonly used as a general diagnosis for injuries around the neck. There are various theories on the injury mechanisms and the injury region. Possible injury mechanisms are excessive neck loads, abnormal vertebra motion, pressure pulses in the spinal canal or local hyperextension/flexion. Possible regions for the whiplash injury include facet joint, muscle, ligament, disc, artery, Central Nervous System [1].

Normally considered as minor injuries, whiplash injuries are classified as AIS1 (Abbreviated Injury Scale 1) type injuries by the Association for the Advancement of Automotive Medicine [7]. The Quebec Task Force also made a different classification of Whiplash Associated Disorders (WAD). WAD is further separated into 4 groups by their severity based classification, in which WAD Grade 1 is the mildest grade where symptoms are stiffness, pain, tenderness or irritation in the neck area without physical signs. In WAD Grade 2, musculoskeletal signs include signs as reduced range of motion of the neck and tenderness. In WAD Grade 3, neurological signs comprise reduced or absent deep tendon reflexes, weakness and decreased sensory functions [8]. Usually grades 2 and 3 symptoms last longer than Grade 1 injuries. Some symptoms, such as shoulder pain, upper back pain, dizziness, headache, jaw and facial pain, sleep disturbance, impaired concentration, memory loss, and difficulty in swallowing etc. can be observed in all grades and doesn't affect the grading of the injury [9][10].

2.2. Injury Criteria and Thresholds

As there isn't a common consensus on how exactly whiplash injuries work, there isn't a single correct injury criteria on the study of whiplash injuries. Considering the injury mechanism, and the general characteristics of the whiplash injuries, several injury criteria have been suggested in the literature. These injury criteria are mainly designed to be used in crash tests with dummies. Testing in simulated experiments is necessary for car safety systems and the special apparatus and sensors such as load cells and accelerometers that are attached to dummies allow quantifying the injury risk with the help of these criteria. Injury criteria should be based on injury mechanisms, but due to the fact that medical diagnosis techniques are inconclusive in showing the structural components associated with injury, no standard evaluation exists for whiplash injury mechanisms. Whiplash injury may exist at different locations of the neck affecting different types of soft tissues due to a combination of different injury mechanisms [11]. Defining injury threshold values for short and long-term symptoms is therefore difficult. Considering the limitations and the urgent need for whiplash prevention systems, most of the proposed injury criteria measure the loading of the neck in a global manner by measuring the overall forces and moments and/or calculating the relative kinematics between several regions of the head and neck. In general, injury criteria for whiplash are suggested and approved based on experimental research. Nevertheless, they are important instruments for study and evolution of safety systems. In the following part, major proposed neck injury criteria are listed and explained:

2.2.1. The Neck Injury Criterion (NIC)

The Neck Injury Criterion is one of the major criteria on the topic of neck injuries. The formula (which is proposed by Boström [12]) is based on Aldman's pressure gradient hypothesis [13] and Örtengren and Svensson's biological experiments [14] [15]. According to the formula, NIC is calculated as;

$$NIC = 0.2a_{rel} + v_{rel}^2$$

Where a_{rel} can be defined as relative horizontal acceleration between the occipital joint and T1, and v_{rel} can be defined as relative horizontal velocity between the occipital joint and T1.

The NIC is calculated at the point of maximum retraction. Boström proposed the NIC_{max} value, which is the maximum amount NIC can be in the first 150 ms of the crash, in his article on the topic [16]. The NIC that is formulated for the use with Hybrid III dummy tests is named as NIC50. The level of tolerance identified for NIC, NIC_{max} and NIC50 is found to be $15 \text{ m}^2/\text{s}^2$. Kullgren studied real life accident reports and mathematical simulations, and found that NIC_{max} can be used to evaluate whiplash injury risk for tests with BioRID dummies [17]. For $NIC=15$ approximately 20% long term (effects lasting more than a month) neck injury risk was reported. Linder reconstructed real world rear end collisions with sled tests and compared the results with regards to known injury outcomes for frontal seat occupants [18]. The results showed that the long term whiplash injury risk was less than 10% for $NIC_{max} < 16.7$.

2.2.2. The N_{ij} Criterion

The N_{ij} was presented for evaluating severe neck injuries caused by frontal collisions, including accidents with deployed airbags, by the US National Highway Traffic Safety Administration [19] [20]. It combines the moment and force effects at the occipital condyles and is related to both the levels of tolerance for bending moment and axial compression.

2.2.3. The N_{km} Criterion

The N_{km} criterion was proposed to evaluate neck injuries in rear end accidents. It is evaluated from the N_{ij} , and like N_{ij} uses the effects of both shear forces and moments [21]. The N_{km} is calculated as:

$$N_{km} = \frac{F_x}{F_{int}} + \frac{M_y}{M_{int}}$$

Where F_x is the shear force and M_y is the flexion/extension moment measured by the load cells on the upper neck. F_{int} and M_{int} are the critical intercept values, and their values can be shown as F_{int} (anterior) = F_{int} (posterior) = 845 N, M_{int} (flexion) = 88.1 Nm, M_{int} (extension) = 47.5 Nm [21].

4 different load enquiries that can be acquired are; N_{fa} for flexion and anterior (positive x direction), N_{fp} for flexion and posterior (negative x direction), N_{ea} for extension and anterior, and N_{ep} for extension and posterior. For each load case, the injury threshold value of 1.0 applies.

Studying real-life accident reports and mathematical simulations, Kullgren showed that N_{km} is also applicable on prediction of whiplash injury risk on tests with BioRID dummy [17]. An approximate 20% long term neck injury risk was found for $N_{km}=0.8$. In the sled tests that Linder reconstructed based on real world data on rear end accident, he recorded that the risk of long-term whiplash injury was less than 10% for $N_{km}<0.37$ [18].

2.2.4. The Intervertebral Neck Injury Criterion (IV-NIC)

The IV-NIC is formulated by Panjabi it is based on the hypothesis that the injury occurs when intervertebral extension/flexion exceeds neck's physiological limits [23]. It can be defined as the physiological range of motion $\Theta_{\text{physiological}}$ and the part of the intervertebral motion Θ_{trauma} under traumatic loads. The IV-NIC can be calculated as:

$$IV - NIC = \frac{\Theta_{\text{trauma},i}}{\Theta_{\text{physiological},i}}$$

No threshold value is proposed for IV-NIC, and the criterion cannot be used with the existing test dummies [20].

2.2.5. The Neck Displacement Criterion (NDC)

The NDC is based on the angular and linear displacement response data of the head relative to T1, and it is proposed by Viano and Davidsson after their study with volunteer tests [24]. The criterion is shown as corridors of the z vs. angular displacements, and x vs. angular displacements of the occipital condyle of the head with respect to T1. Performance guidelines are proposed for Hybrid III and BioRID dummies at low speed rear end collisions as excellent, good, acceptable and poor. In his study, Kullgren found that NDC is less applicable than the previous methods at evaluating whiplash injury risk with BioRID dummy [22]. In accordance to Schmitt's study, the NDC is still on debate, and the proposed corridors can't be considered exact as of now [21].

2.2.6. The Lower Neck Load Index (LNL)

The Lower Neck Load Index (LNL) is calculated with the 3 force and 2 moment components measured at load cells on the lower neck [25]. The LNL can be calculated as:

$$LNL = \left| \frac{\sqrt{M_{y_{lower}}^2 + M_{x_{lower}}^2}}{C_{moment}} \right| + \left| \frac{\sqrt{F_{y_{lower}}^2 + F_{x_{lower}}^2}}{C_{shear}} \right| + \left| \frac{F_{z_{lower}}}{C_{tension}} \right|$$

Where F_i and M_i are the specified force and moment components. The proposed intercept values can be shown as $C_{moment} = 15$, $C_{shear} = 250$, and $C_{tension} = 900$ for RID dummy.

2.2.7. F_{tn} And F_{sh} Criterion

For the evaluation of the forces affecting the upper neck, IIWPG neck force classification is used. Since the positive normal and positive shear forces affecting the head at the upper neck are positive by definition, upper neck rearward shear force (F_{sh}) is considered as negative shear force at the upper neck, and tension force (F_{tn}) is negative by definition. As for the positive shear forces at the upper neck, the denotation $F_{sh}^{(+)}$ is used. The IIWPG neck force classification can be seen in the figure below:

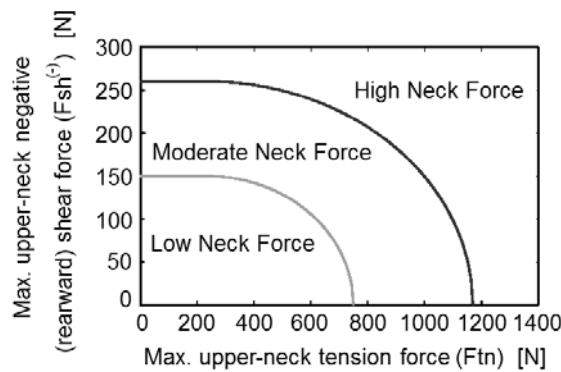


Figure 1 - IIWPG neck force classification [26]

When evaluating the injury risk with respect to F_{sh} or F_{tn} , magnitude of the greatest shear and tension forces are used.

2.2.2.8. Neck Distortion Index (NDI)

In addition to previously mentioned injury criteria, neck intervertebral motions are also tracked to control the neck motion of the model. The criterion is based on the upper and lower neck intervertebral rotations and is calculated with the formula given below [27]:

$$NDI = -\theta_{OC/C1} + \theta_{C7/T1}$$

where $\theta_{OC/C1}$ and $\theta_{C7/T1}$ are intervertebral rotations between the upper neck (occipital condyles (OC)) and C7 and between T1 and C7 respectively (Figure 2). OC is the joint between the skull and the first cervical vertebra (C1). C7 is the seventh cervical vertebra. T1 is the first thoracic vertebra. In the criterion, flexion (-) and extension (+) states of the upper neck is represented by $\theta_{OC/C1}$ and lower neck is represented by $\theta_{C7/T1}$. NDI basically identifies the protrusion and retraction type of deformations in the upper and lower neck during the rear impacts. Positive value of NDI indicates retraction and is usually the indication of S-shape deformation, where in the upper neck flexion is observed, and in the lower neck extension is observed. As for negative values, protrusion type of deformation can be seen in the neck. While there isn't a specified threshold for NDI value for injury assessment, the aim is keeping the NDI value as low as possible.

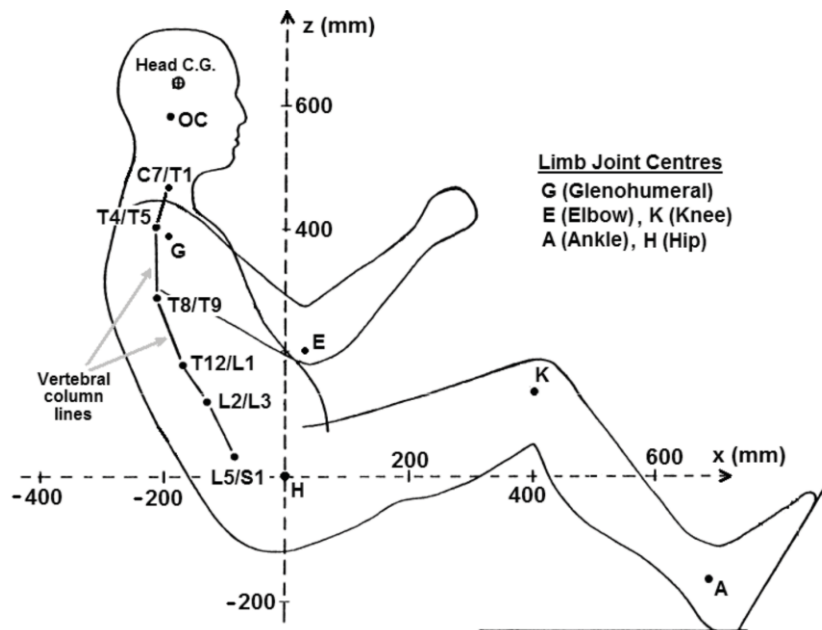


Figure 2 - Typical driving posture of a 50th percentile male, showing various reference points [52]

2.3. Affecting Factors

2.3.1. Crash Severity

It's been shown in several studies that there's a correlation between the severity of the impact and whiplash injury risk. The crash characteristic mainly used for classifying the crash severity, Delta-V, can be explained as the area under the time-acceleration curve of the collided vehicle during the accident [28]. Also in addition to delta-V, the mean or peak acceleration values of the curve is also said to better indicate the severity of rear impacts. The most frequent rear impact form that whiplash injuries happen is found to be a 0° to 5° angled collision with nearly full overlap (50% to 100%) and in delta-V's around 9 to 25 kph [29]. According to the aggregated distribution of various impact severities, 90% of the inspected rear-end collisions recorded to be occurring at speeds with delta-V smaller than 22 kph, and 78% of which happening at delta-V smaller than 15 kph. Also in relation to the injury risk related to the acceleration, it is recorded that the risk of long-term whiplash injury is close to 100% at average acceleration of 7g or higher. At average vehicle accelerations below 5g, it's found that the long term injury risk was lower [17]. As the mean acceleration went below 3g, the injury risk has come closer to zero. Overall, it can be concluded that majority of the whiplash injuries happen at low severities.

2.3.2. Seating Position

The whiplash injury risk can also be correlated with the car seat the occupant is sitting on. It's been reported in several studies that occupants in front seats have a higher risk of whiplash injury compared to the rear-seat occupants [30][3]. But according to the later studies with more inclusive research, generalization is found to be inaccurate for female occupants [31]. In the complete study done on all neck injuries that occurred on rear end collisions between 1990–1999 (as they've been reported to the insurance company Folksam), the males are found to have a smaller risk of whiplash injury in the rear seats than in the frontal seats, while the female occupants had a significantly higher risk of injury in the rear seat. Permanent disability risk for female drivers was also about 3 times higher than for male drivers. Similarly for female occupants on front passenger seats, permanent disability risk was 1.5 times higher than for male occupants, and 5 times higher than female occupants on rear seats.

2.3.3. Occupant Related Factors

The risk of whiplash injury has also been shown to be related to age and stature of the occupant, their initial position during the impact, and the awareness of an upcoming collision. It's seen that, for both men and women, the injury risk is increased as the stature is increased [3][32][33]. When the comparison is made between male and female drivers, risk of injury is found to be 2 times higher for the female drivers, while the mass of the occupants have a much smaller effect on the risk of injury [33][34]. Rotating the head in course of the accident is also recorded to be the cause of a higher risk of long term symptoms following an accident [33][34]. When a comparison is made between different age groups, whiplash injury risk is found to be highest in middle age people, and decrease with older age [3][33][37].

2.3.4. Seat Design and Head Restraint Geometry

Many studies show that HR (head restraint) geometry is the most effective factor on whiplash mitigation. HR geometry is defined in terms of backset and HR height. Height (H) of the HR can be defined as the vertical space between the top of the head and top of the head restraint, while backset (B) can be defined as the horizontal space between the front of the HR and the back of the head. Szabo in his extensive literature survey, recorded several types of studies including dummies, epidemiological studies, mathematical model and volunteer studies on rear end collisions. All the studies validated that providing a high positioned head restraint that is also near the backside of the head was the most efficient way for whiplash mitigation [38].

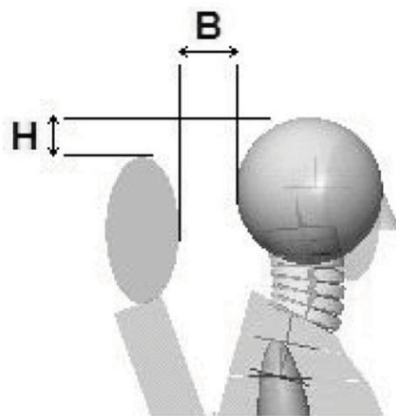


Figure 3 - Height (H) and backset (B) of the head restraint

A common comparison regarding the effect of seatbacks against whiplash injuries is between stiff and yielding seatbacks. Stiff seatbacks increase occupant retention in high severity impacts, which helps prevent further backwards movement, but they also apply higher forces on occupants and might increase rebound [39][40]. Stiffer seatbacks are harder to deform and can help decreasing the risk of occupant hitting the rear interior of the car, but might increase rebound risk which is in rear accidents also reported to be possible cause of injury even in low severity collisions [41]. Yielding seatbacks can control occupant energy from the impact, limit forces on the occupant and decrease rebound, but they also generate larger seat back rotations and increase the head contact time to head restraint [42][43].

As a conclusion, if a good head restraint geometry can be provided, seat designs that decreases the head contact time and/or have efficient energy absorption can mitigate the risk of whiplash injury [44][45].

Stiffness and yielding characteristics of seatbacks are primarily managed by the properties of the recliner mechanism, which is located between the seat pan and the seatback. Effectiveness of suspension and foam of the seatback have also been studied. To see the effects of the seatback foam characteristics on risk of whiplash injury, crash tests have been carried out with various seatbacks with different foam combinations [47]. The examinations showed that there was little to no differences between seats with similar HR geometries. In the tests, the seat that provided the worst result was the seat with the poor HR geometry. The results showed that the geometrical properties of the seat were much more effective in reducing the whiplash injury risk compared to foam properties.

Tests were conducted on the effects of the compliance of the upper and lower regions of the seatback [48]. Adjustments on the regional compliance was done by adding steel plates and decreasing the thickness of the foam for decreased compliance, and taking out the suspension springs and locally tearing the foam for increased compliance. In the tests where same HR geometry were used with different regional compliances, the seat with the increased compliance at both upper and lower regions performed the best at reducing the whiplash injury risk. Comparing the effectiveness of the regional compliance between the upper and lower parts showed no significant differences, though in general increasing compliance on the upper part of the seatback seemed to be more favorable.

Additionally, another author made tests where several seat properties such as HR geometry, seat frame stiffness, seat pan foam compliance, and seatback foam and suspension compliance were modified to study their effects on NIC [49]. On the tests, it is found that decreasing the backset and increasing the compliance of the upper seatback was more effective at reducing NIC. Among all, decreasing the backset found to be significantly more influential.

When the studies are taken into consideration, it can be concluded that if the upper torso of the occupant is allowed to edge into the seatback more with respect to the lower torso, the risk of injury decreases, if the seat also has a head restraint with good geometry. Although, in the seats where this idea was applied in Toyota which called the WIL seat (Whiplash Injury Lessening), insurance statistics showed that the WIL seat was not effective at whiplash mitigation, on the opposite; a 15% increase in risk of whiplash injury was seen [50]. On the other hand, the Whiplash Protection System (WHIPS) of Volvo uses equal compliance along the seatback, but it also has a recliner mechanism that absorbs energy, therefore controlling the recline of the seatback. Whiplash injury data from real world accident statistics shows the that the WHIPS is quite effective at whiplash mitigation, and the system obtains the highest scores in sled tests [44][45][50].

Overall, only changing the foam characteristics was not effective [47], but when it applied with a modified seatback suspension, some improvements were seen in reducing injury risks [42][48][49]. Though the improvements we not significant and results were unclear in some cases, and making big changes on the suspension and foam properties of the seatback can also affect comfort or may not be suitable for production [47][49]. Also considering the variation in stature of the occupants, such modifications might not be suitable or effective for everyone.

3. EXPERIMENTAL STUDIES

3.1. Seatback Angle Study

Although the seatback angle is adjusted at an angle of 25° for most vehicle safety studies, seating position of drivers and passengers can vary greatly in practical driving conditions. To investigate the average seatback angle for people of different statures, and to shape the base for our studies regarding safety and comfort of the car seat for people of various statures, an experiment on average driving seatback angle has been conducted.



Figure 4 - An example car seat for seatback angle measurement

72 subjects (62 male / 10 female) took place in the experiment. In the experiment the subjects were not allowed to play with the up-and-down motion of the seat-pan. In the experimental process, the subject assumes a normal seating posture with the Frankfort plane of the head oriented horizontally (i.e. the subject looks ahead as if he/she is driving the car). Subject is asked to change the seatback angle to their preferred comfortable driving position, and the seatback angle for each subject is recorded.



Figure 5 - Scale for seatback angle fixed on the seat's recliner

The scale used for measuring the seatback angle is fixed to the center of the recliner mechanism that is used for adjusting the seatback angle and is the center of rotation of the seatback.

From the various data collected from the experiment; occupant statistics, calculated average seatback angle and standard deviations of the results can be found as below;

Table 1 - Average SB (seatback) Angle and Standard deviation of Seatback Angles for people of various Statures

	Average Height (m)	Seatback Angle(°)	SD of Seatback Angles
Males	1.79	22.74	4.84
Females	1.64	21.44	6.06
Total	1.77	22.56	5.00

The seat angle distributions as a result of these experiments with respect to specified criteria are given in the following figures:

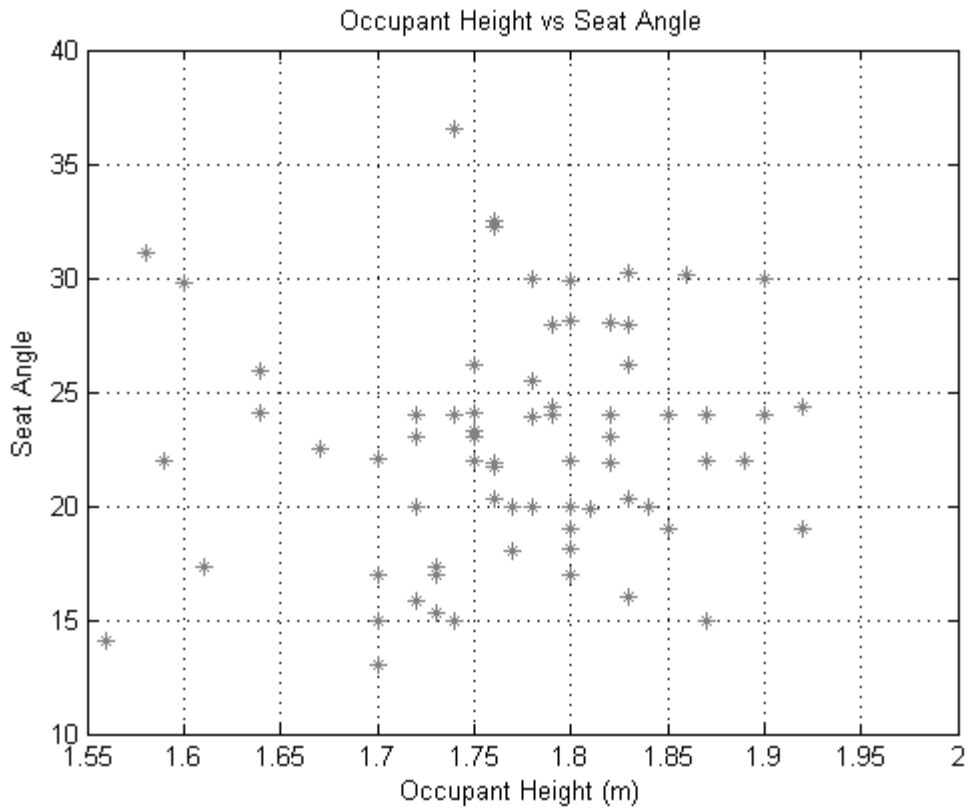


Figure 6 - Seatback angle wrt occupant height

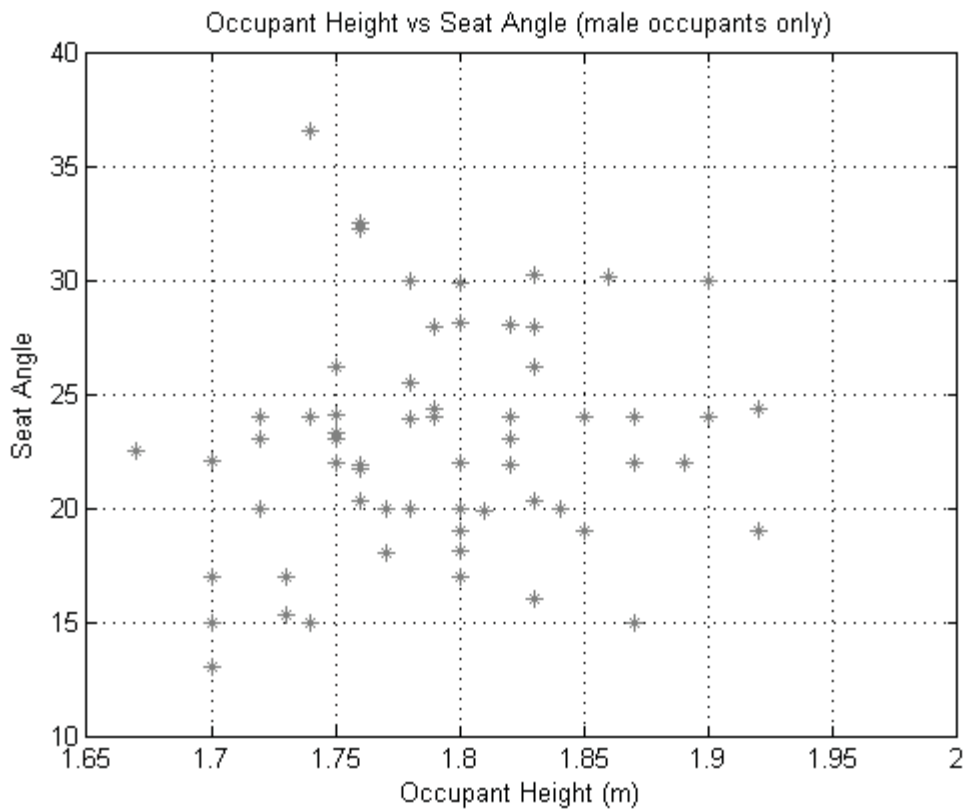


Figure 7 - Seatback angle wrt occupant height for male occupants

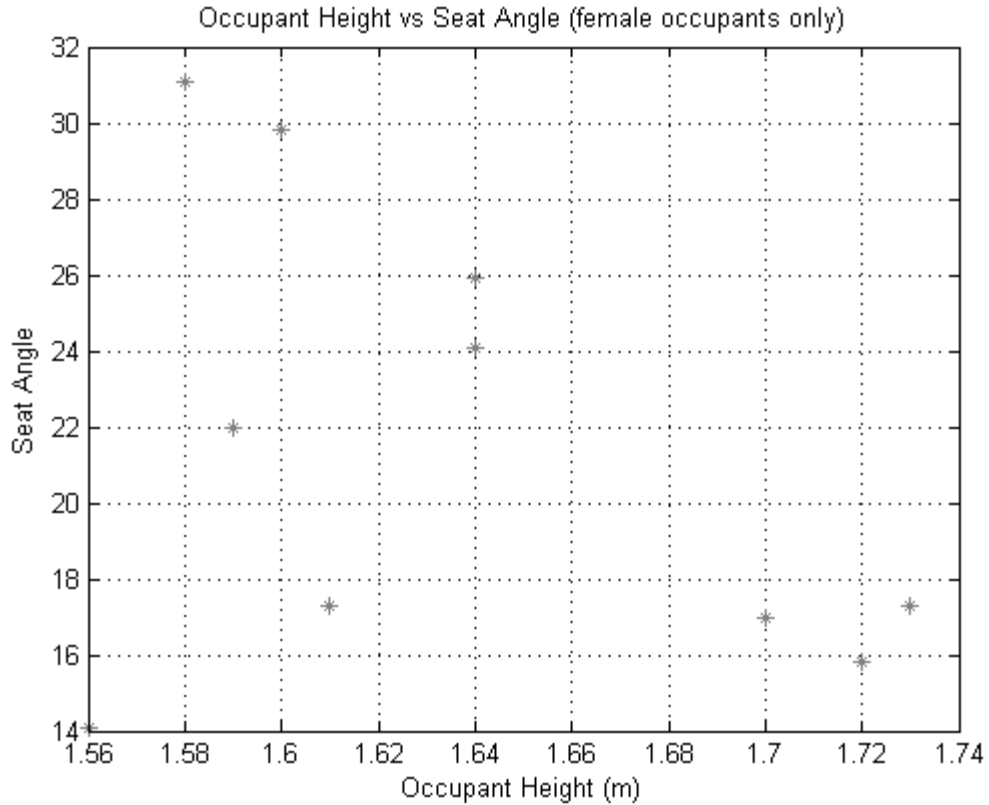


Figure 8 - Seatback angle wrt occupant height for female occupants

3.1.1. Experiment Results and Discussion

It can be seen from the experiments that while the preferred seatback angle doesn't have a clear relation to occupant height, the preferred seatback angle is found to be close to average of 22° for both male and female occupants. Those results also support the experiments done by M. Kolich which investigates the average seatback angle preferred by occupants of different ages and statures and how it affects the comfort of the car seats that are optimized for average male occupant sitting at SB (seatback) angle of 25° [51]. M. Kolich has done a pilot experiment on 140 people (45 female and 95 male) and a following main study on 66 people (33 female and 33 male) on different types of vehicles. Both experiments shown that the average seatback angle preferred by 80 to 85 percent of occupants of various sizes were between 21° and 22° on all vehicle types, which is more upright than the 25° used for vehicle seat optimizations and tests [51]. This condition can especially create comfort issues for occupants sitting more upright and can interfere with their preferred sitting position.

The results showed that how seatback angle and backset also affects the comfort of the seat, and were taken under consideration throughout the following studies.

3.2. Head Range of Motion and Torso Extension Study

Another experiment has been conducted on torso and neck range of motion and safe head motion interval in rear end collisions. The experiment related to head ROM was based on the motion of torso allowed by cervical spine's spinal ROM and irrelevant to neck's ROM. Neck extension, flexion, and protrusion motions are measured on people of various heights. The horizontal and vertical distances traveled by head in case of a rear and collision are also measured and calculated at seatback angles of 15, 20, 25 and 30 degrees. A 3D measurement device is designed for the experiment. With the device that's designed for measuring several specific points on a human body while sitting, experiments are conducted with people of different sizes to find an average safe head movement interval at various seatback angles.



Figure 9 - Measurement of the markers with the 3D measurement device

People with no known previous spinal injuries that limit spine motion have been chosen for the experiment. During the experiments, the seat pan is kept fixed for all subjects and the subject was not allowed to change the up-and-down motion adjustment of the seat-pan.

For the experiment, subjects were told to wear T-shirts with no collars (i.e. undershirt or a similar type of clothing) so that the markers can be attached easily on the chest and the back of the neck. People with long hair are asked to tie their hair up to provide visibility of the markers.

The Frankfort plane is determined with a ruler and marked with a make-up pencil at the start of the experiment. When viewed in the sagittal plane, the Frankfort plane appears as a line that passes through the external ear canal and across the top of the lower bone of the eye socket. The flexion and extension range of motion (ROM) of the neck is measured by taking pictures of the Frankfort plane when the neck is voluntarily flexed / extended by the subject maximally. ROM is found by measuring the change in angle with the help of a computer program.

After the flexion/extension measurements, 2 markers are fixated on the subject for 2 specific points; T1 vertebra and the top edge of the sternum, where it meets the clavicles. The head-neck of the subject is bent forward so as to locate the C7 vertebra spinous process more easily. After locating the C7, T1 vertebra spinous process is located (right below the C7 vertebra), and markers are fixated to the 2 aforementioned points (Figure 2).

For the measurements, the subject assumes a normal seating posture on the car seat with the Frankfort plane of the head oriented horizontally (i.e. the subject looks ahead as if he/she is driving the car). Protrusion ROM is found by measuring the coordinates of the tip of the nose of the subject firstly on a neutral position, and secondly after they are asked to move their head horizontally forward while their body is kept stationary.

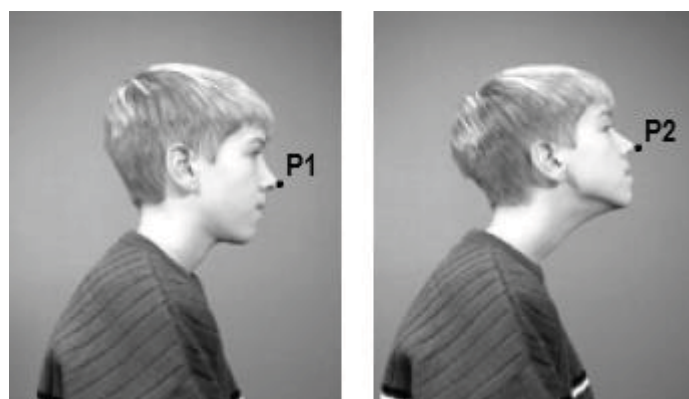


Figure 10 - Protrusion motion and measured reference points P1/P2 [59]



Figure 11 - Neutral and reclined seating positions for torso ROM measurements

For the measurement for a safe movement interval during rear impacts, subject sits in a neutral position. Ear tragus (C) and the extremist points of brow (H1) and the back of the head (H2) are measured for determining head circle.

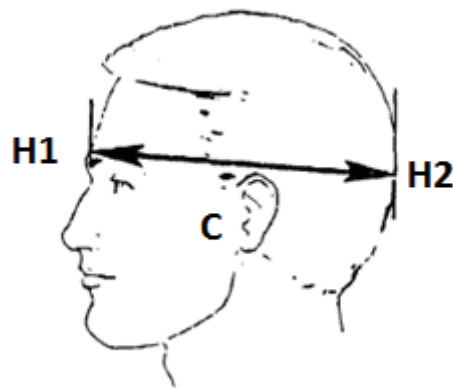


Figure 12 - 3 reference points necessary for determination of the head circle [58]

Firstly the positions of the two markers and the tragus are measured at the neutral position. Then the subject is asked to push their body backwards to the seat as in the case of a rear impact. Two marker points are measured again, and the relative points of the head circle in each position is measured and calculated with the help of a computer program after the experiment. Measurements are repeated for preferred seatback angles (15° to 30° with 5° increments). It is checked before each experiment that seat platform has not moved during sessions. Since the seat and platform assembly is quite heavy, the seat cannot be moved easily.



Figure 13 - Drawing of the head circle and neck with 5 reference points

3.2.1. Measurement Device

Measurements for the experiment are done by a measurement device built specifically for determining the coordinates of the required points in a 3D coordinate system. It consists of a vertical sliding body used for measuring the z coordinate, and two horizontal planes for measuring the x and y coordinates. Y axis carries the pointer which is used for spotting the point to be measured. In the following parts, that pointer is going to be referred as marker.

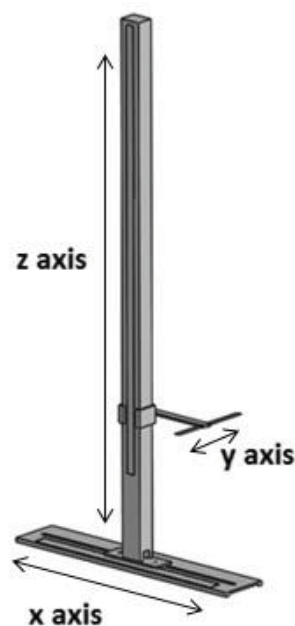


Figure 14 - Solid model of the 3D measurement device

The base that's used for measuring the x coordinate has a slot which the vertical profile slides on. There's a 500 mm ruler on the side of the base, and with the help of the pointer at the bottom of the sliding profile it can be seen where the point is on the x axis. The difference on the x axis between the pointer on the x axis and the marker is taken into consideration in our coordinate calculations. The calculations used for determining the coordinates will be explained in the following parts.

Z coordinate is found with the 1000 mm ruler on the sliding profile. The pointer slides freely on the z axis with the slider it's carried on. Like the previous axis, the height difference between the floor and the 0 point of the ruler is taken into consideration in the calculations.

Y axis has a 200 mm ruler and a pointer at its tip. It slides on the flat bar fixed to the slider on the z axis. Y coordinate of the point is determined as the previous processes.

For the coordinate calculation, ground point at the center of the sliding profile where the ruler on the x axis shows zero selected as center (0,0,0). The horizontal difference between the marker and the center is found 20 mm on the x axis and 470 mm on the y axis.

Vertical difference between the center point and the zero of the ruler on the z axis is 76,5 mm. If we name the values the rulers shows as x, y and z on x, y and z rulers respectively, the coordinates of the point that marker shows is found as;

$$A_x = 200 - x$$

$$A_y = 470 - y$$

$$A_z = 76,5 + z$$

After finding the required coordinates, we can find the distance between two points using the formula;

$$d = \sqrt{(A_x - B_x)^2 + (A_y - B_y)^2 + (A_z - B_z)^2}$$

3.2.1.1. Accuracy of the Device

The accuracy of the device is tested with a measurement experiment. For the test, a ruler of 20 cm is measured on 3D coordinate system, with one or two axes kept fixed and others changed. For the three experiments, measured first and second coordinates are;

1.

x1=175,8 cm	y1=454,6 cm	z1=80,8 cm
x2=155,9 cm	y2=454,6 cm	z2=80,8 cm

The difference between two points;

$$d = \sqrt{(175,8 - 155,9)^2 + (454,6 - 454,6)^2 + (80,8 - 80,8)^2} = 19,9 \text{ cm}$$

2.

x1=153,4 cm	y1=460,1 cm	z1=81,5 cm
x2=171,3 cm	y2=469,5 cm	z2=81,5 cm

The difference between two points;

$$d = \sqrt{(153,4 - 171,3)^2 + (460,1 - 469,5)^2 + (81,5 - 81,5)^2} = 20,2 \text{ cm}$$

3.

x1=151,4 cm	y1=457,1 cm	z1=98,6 cm
x2=168,9 cm	y2=457,1 cm	z2=108,5 cm

The difference between two points;

$$d = \sqrt{(151,4 - 168,9)^2 + (457,1 - 457,1)^2 + (98,6 - 108,5)^2} = 20,1 \text{ cm}$$

From the experiment, it is seen that the device's accuracy is adequate (± 0.2 cm), and could be reliably used for the further experiments.

3.2.2. Range of Motion Measurement

The flexion and extension ROM of the neck is measured by taking pictures of the Frankfort plane when the neck is voluntarily flexed / extended by the subject. Photos of the subject is taken in neutral sitting position first, and then with their neck flexed maximally and with their neck extended maximally. ROM is found by measuring the change in angle at each position with the help of the computer program, CATIA.

In the program, the angle of the Frankfort plane with respect to horizontal plane is measured firstly for the subject's neutral position, and then flexion and extension positions. Results are compared to find the flexion and extension ranges of motion of the subject.



Figure 15 - Neutral position of the head



Figure 16 - Flexion position of the head



Figure 17 - Extension position of the head

Flexion and extension ranges of motion of the subject in the figures can be found as;

Flexion ROM: $41,696^{\circ} + 9,4^{\circ} = 51,096^{\circ}$

Extension ROM: $71,319^{\circ} - 9,4^{\circ} = 61,919^{\circ}$

Safe movement interval of the head in case of rear impacts is also found with the help of the computer program CATIA. Each measured point coordinate for the neutral sitting position is marked and fixed on the computer program first. With the marked coordinates, we can determine the head circle and T1 vertebra - sternum – tragus triangle. Then, the coordinates of the second position is marked on the program, and the previously determined triangle is moved to the second positions of the T1 vertebra and sternum markers. The head circle is carried with the triangle, since it is assumed that no motion occurs in the neck during the process. After that, the horizontal and vertical distances between the centers of the head circle at each position is measured to obtain the distance that the head can travel during the impact, without any motion observed in the neck. The measurements are repeated for each preferred angle as explained above.

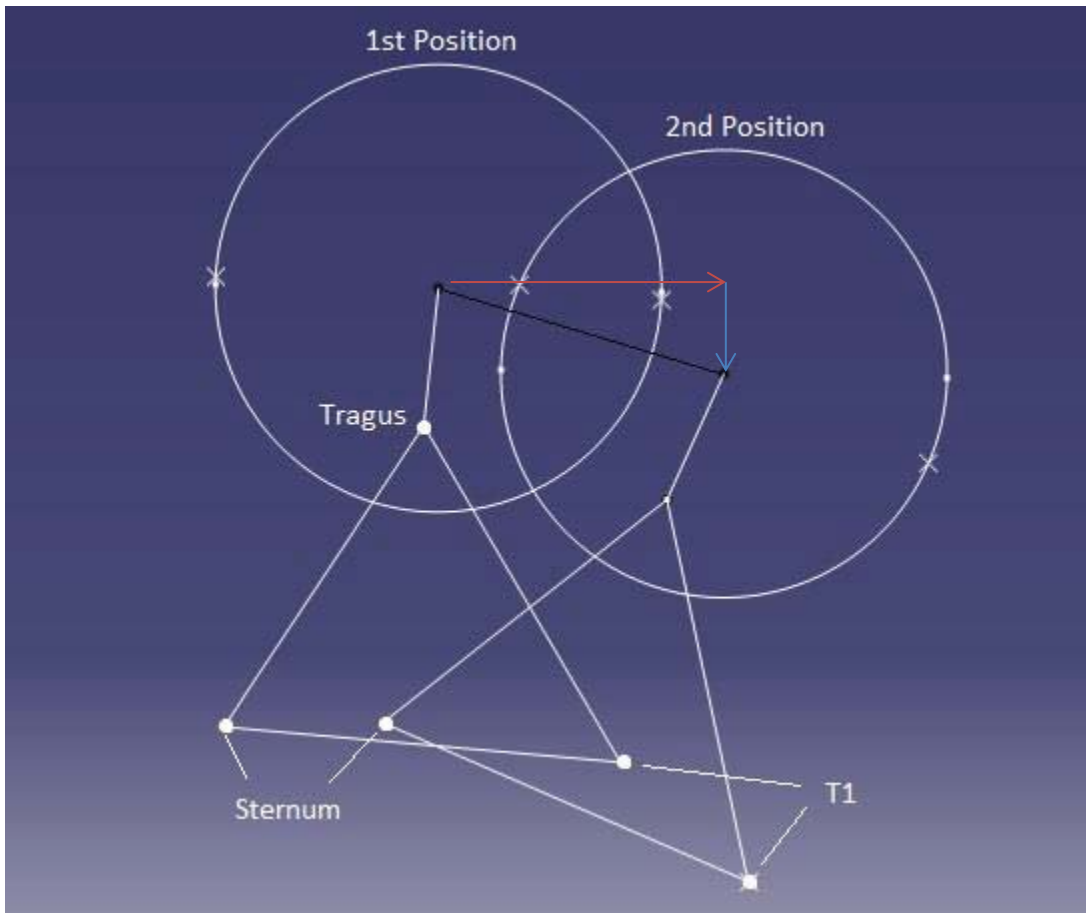


Figure 18 - Calculation of the head motion through CATIA with measured coordinates

3.2.3. Results of the Experiments

The measurements have been studied with the help of MATLAB and the results are plotted on graphs and compared between each other with respect to subject's height and sitting height. Results of flexion/extension and protrusion experiments are plotted separately. To observe the effects of gender to neck ROM, results of male and female subject also separately studied. Effects of occupant's gender, weight, height and sitting height has been considered. Age factor couldn't be studied due to subjects being all from similar age group (young adult). Horizontal and vertical distances traveled by the center of the head in case of rear end impacts are plotted in groups for each seatback angle for better comparison of the effects of the seatback angle. For the graphics regarding neck ROM wrt occupant weight, height and sitting height, see Appendix 1. Numerical results and the graphs regarding horizontal and vertical distances traveled by head geometrical center can be found on the table below.

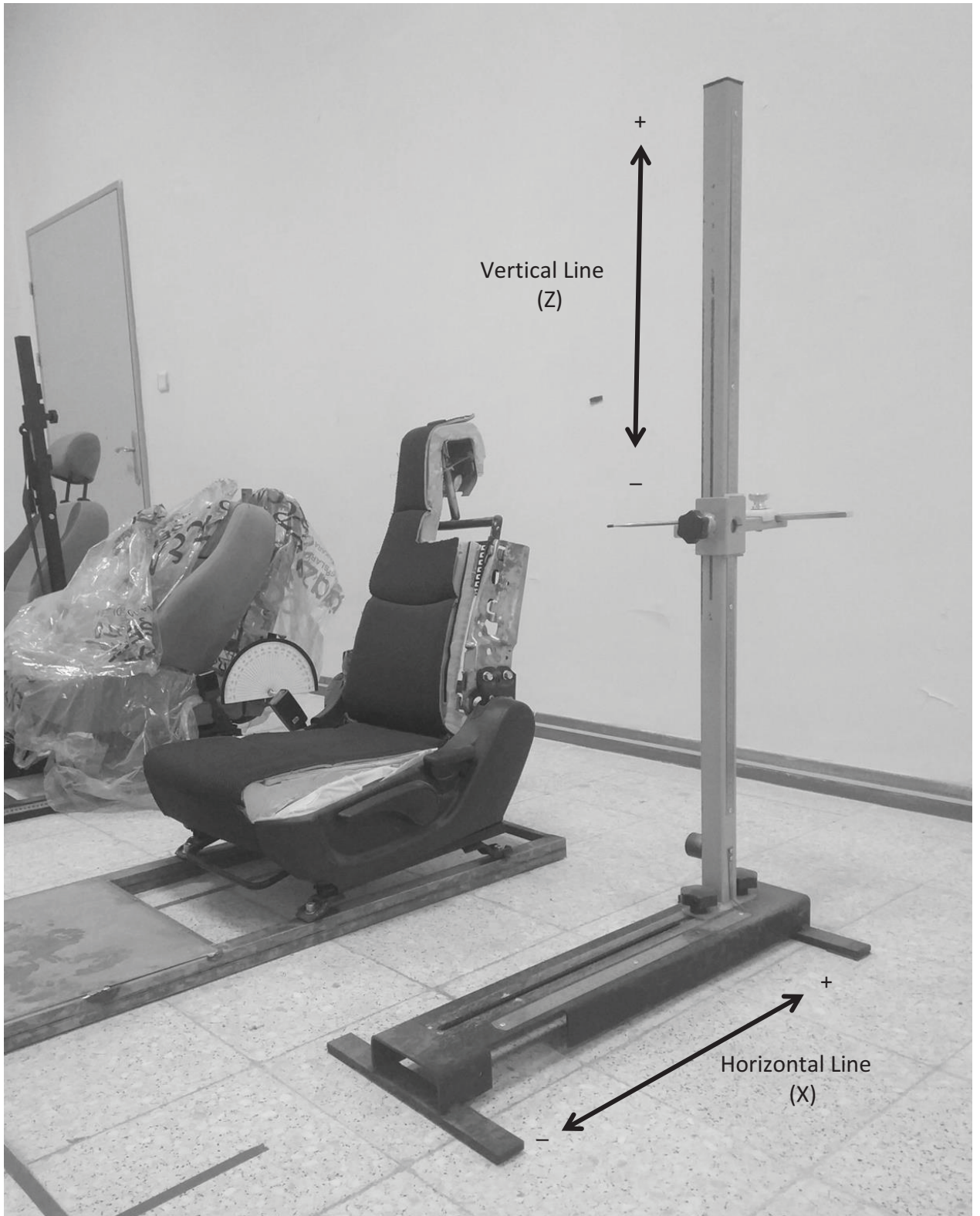


Figure 19 - Vertical and horizontal lines as used in the calculations

Table 2 - Torso Extension Experiment Results

	All Subjects	Female Subjects	Male Subjects
Number of Subjects	38	19	19
Average Weight	71,37	58,58	84,16
SD of Weight	17,91	8,94	15,29
Average Height	172,25	164,95	179,55
SD of Height	11,15	7,58	9,24
Average Sitting Height	89,98	87,05	92,92
SD of Sitting Height	4,70	3,00	4,26
Average Horizontal Head Displacement (All Angles)	10,62	10,14	11,11
SD of Horizontal Head Displacement (All Angles)	3,57	3,47	3,62
Average Vertical Head Displacement (All Angles)	-1,36	-1,35	-1,37
SD of Vertical Head Displacement (All Angles)	1,27	1,05	1,46
Average Horizontal Head Displacement (15°)	12,40	12,38	12,43
SD of Horizontal Head Displacement (15°)	3,28	3,02	3,60
Average Vertical Head Displacement (15°)	-0,37	-0,74	0,01
SD of Vertical Head Displacement (15°)	1,04	0,76	1,17
Average Horizontal Head Displacement (20°)	10,00	10,03	9,97
SD of Horizontal Head Displacement (20°)	3,58	3,57	3,69
Average Vertical Head Displacement (20°)	-1,11	-0,98	-1,24
SD of Vertical Head Displacement (20°)	0,82	0,97	0,62
Average Horizontal Head Displacement (25°)	10,24	9,39	11,09
SD of Horizontal Head Displacement (25°)	3,51	3,41	3,50
Average Vertical Head Displacement (25°)	-1,76	-1,59	-1,94
SD of Vertical Head Displacement (25°)	1,03	1,08	0,97
Average Horizontal Head Displacement (30°)	9,85	8,77	10,93
SD of Horizontal Head Displacement (30°)	3,41	2,97	3,55
Average Vertical Head Displacement (30°)	-2,21	-2,10	-2,31
SD of Vertical Head Displacement (30°)	1,34	0,84	1,72

By studying the resulting data from the table, it can be said that in general, horizontal head displacement value is higher for male occupants than for female occupants, while the vertical head displacement average seemed to vary. Although the reason behind this can be that male occupants have a higher average height and sitting height.

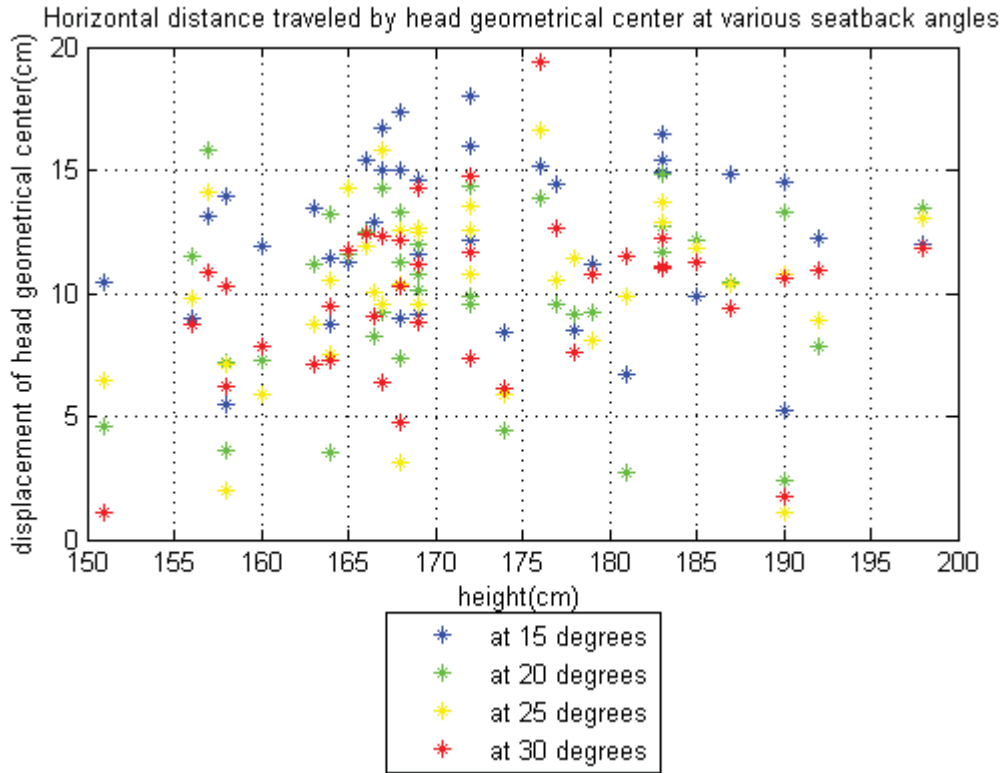


Figure 20 - Horizontal distance traveled by head geometrical center wrt occupant height

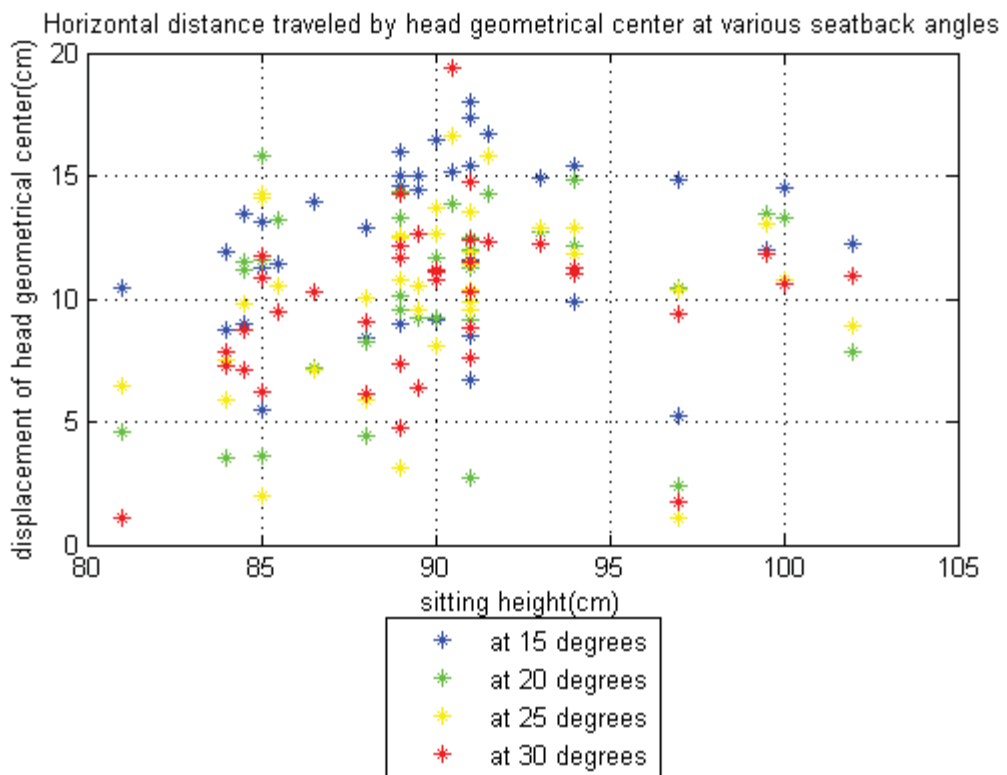


Figure 21 - Horizontal distance traveled by head geometrical center wrt occupant sitting height

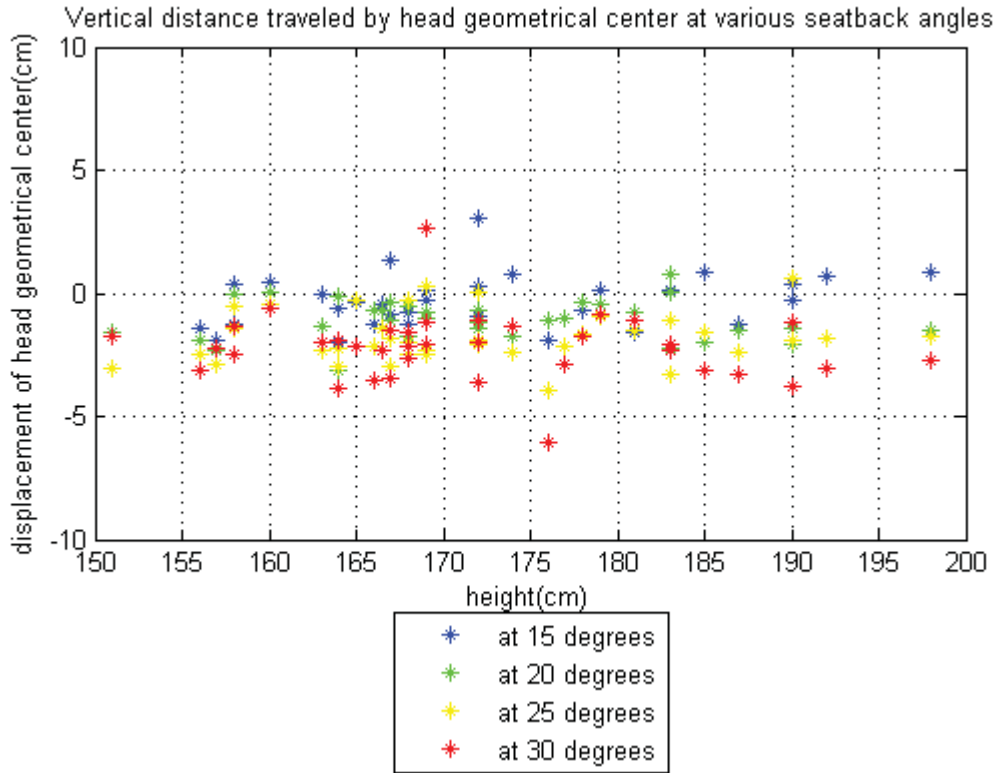


Figure 22 - Vertical distance traveled by head geometrical center wrt occupant height

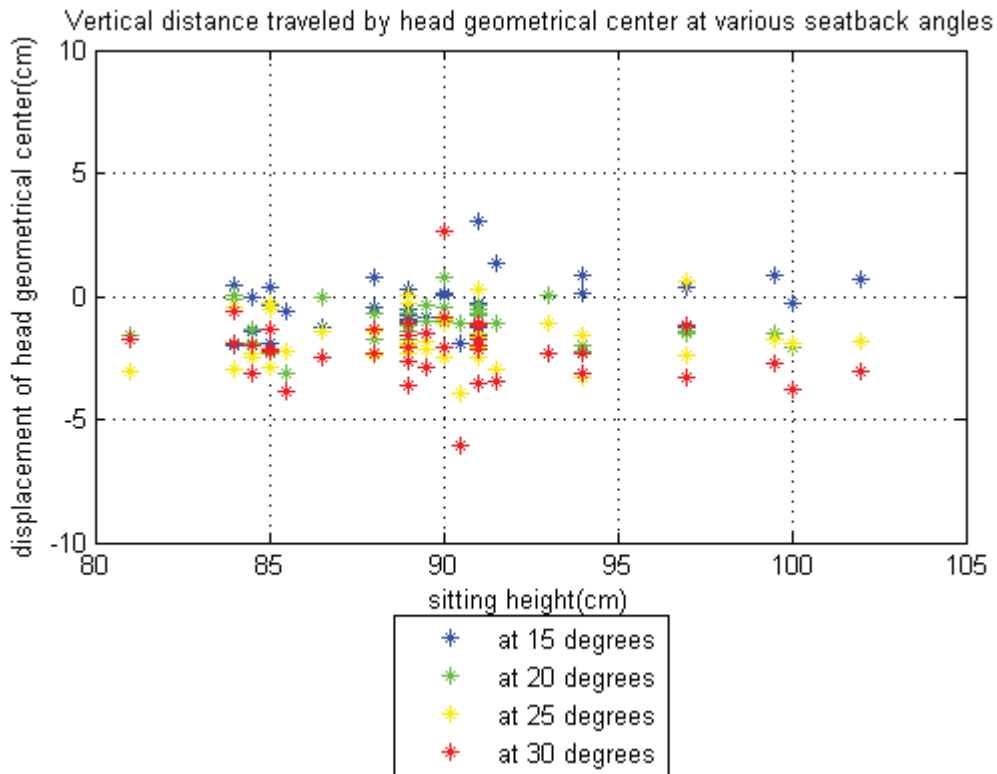


Figure 23 - Vertical distance traveled by head geometrical center wrt occupant sitting height

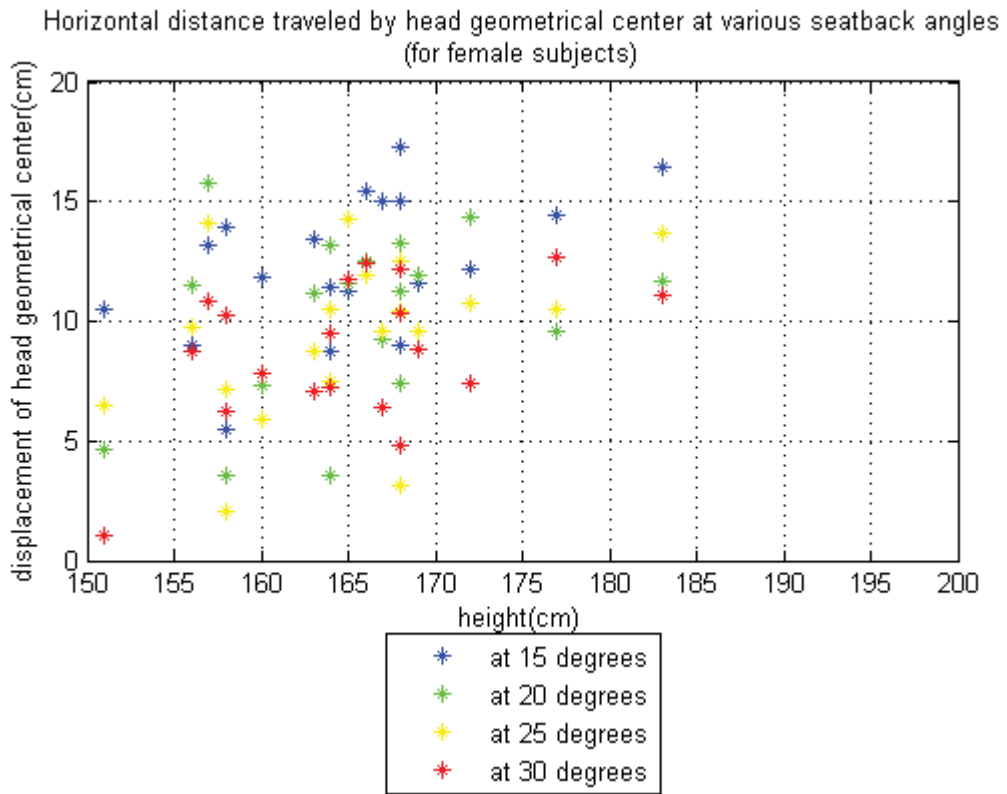


Figure 24 - Horizontal distance traveled by head geometrical center wrt occupant height
(For female subjects)

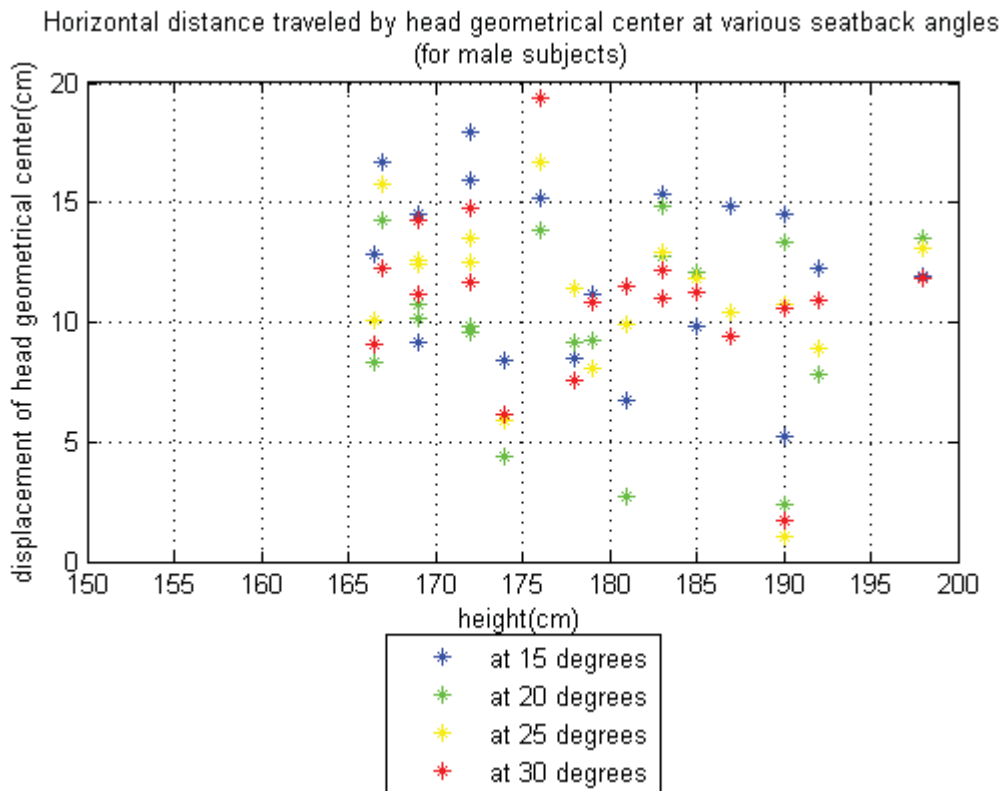


Figure 25 - Horizontal distance traveled by head geometrical center wrt occupant height
(For male subjects)

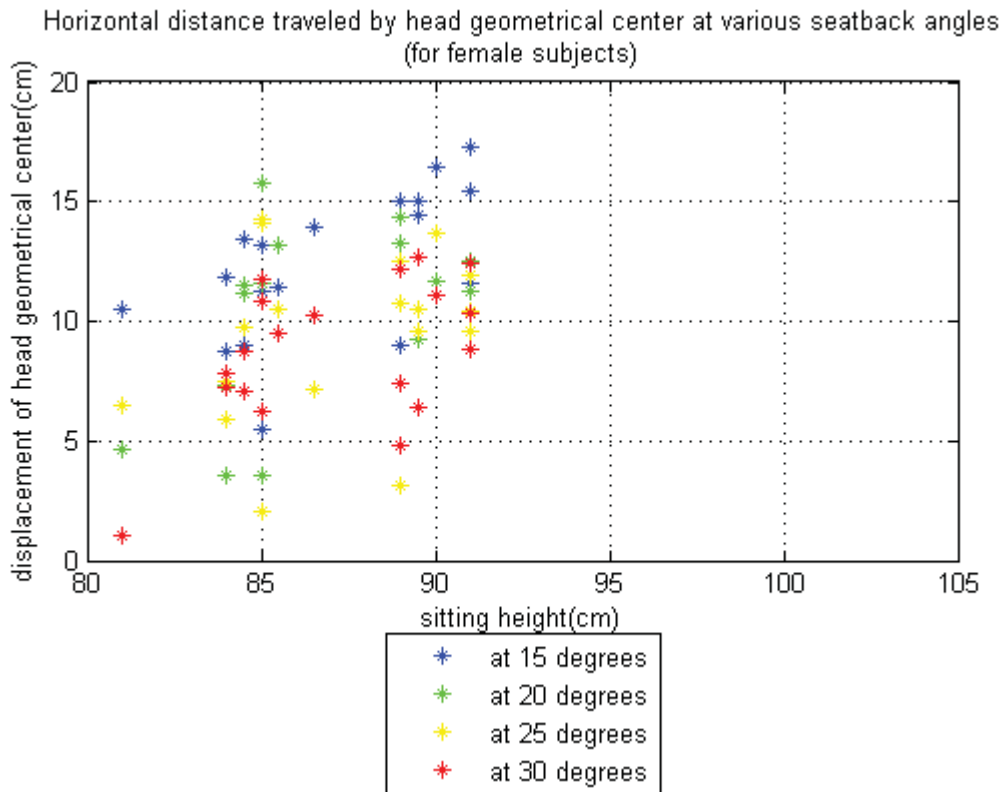


Figure 26 - Horizontal distance traveled by head geometrical center wrt occupant sitting height (For female subjects)

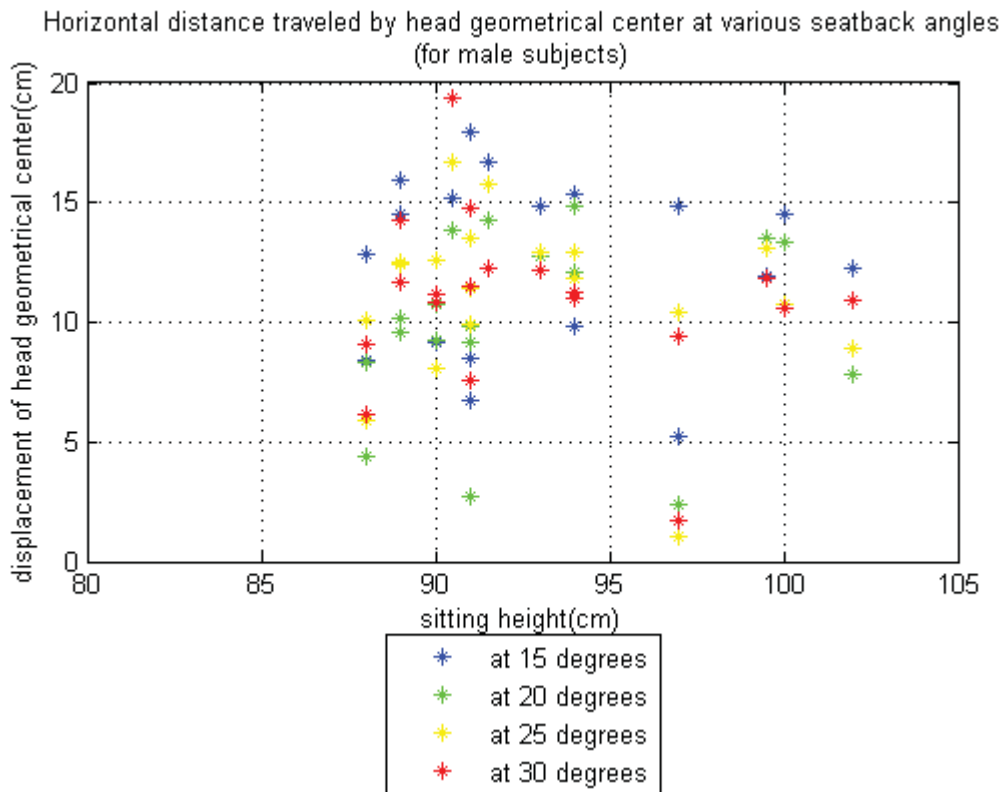


Figure 27 - Horizontal distance traveled by head geometrical center wrt occupant sitting height (For male subjects)

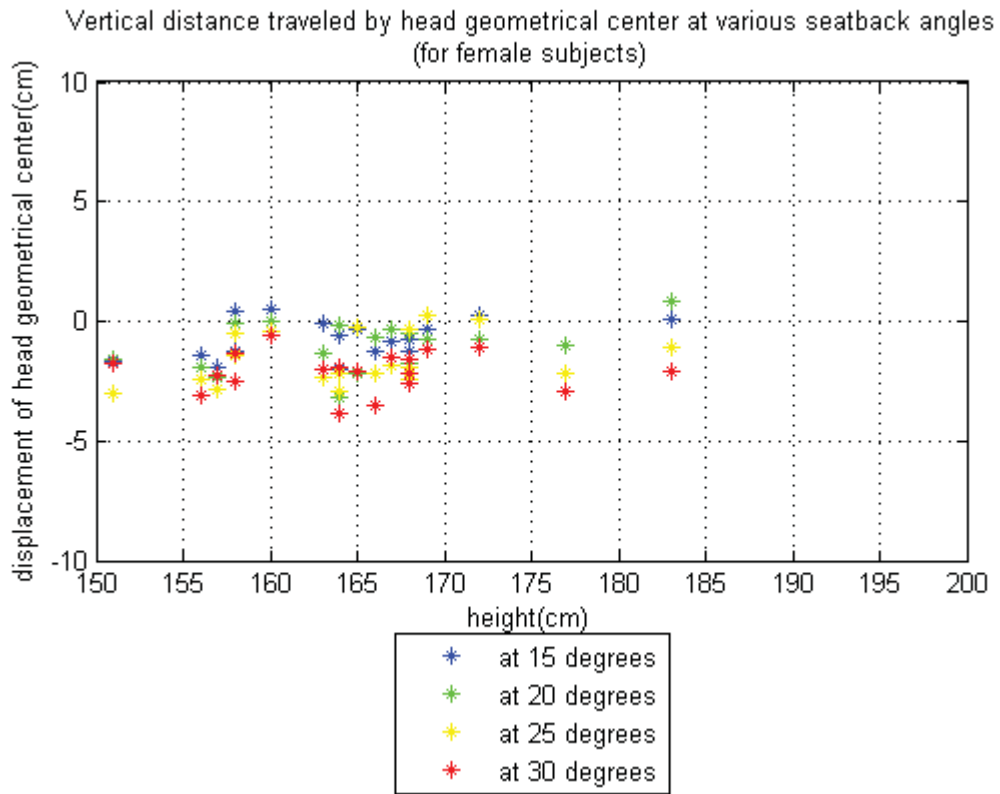


Figure 28 - Vertical distance traveled by head geometrical center wrt occupant height
(For female subjects)

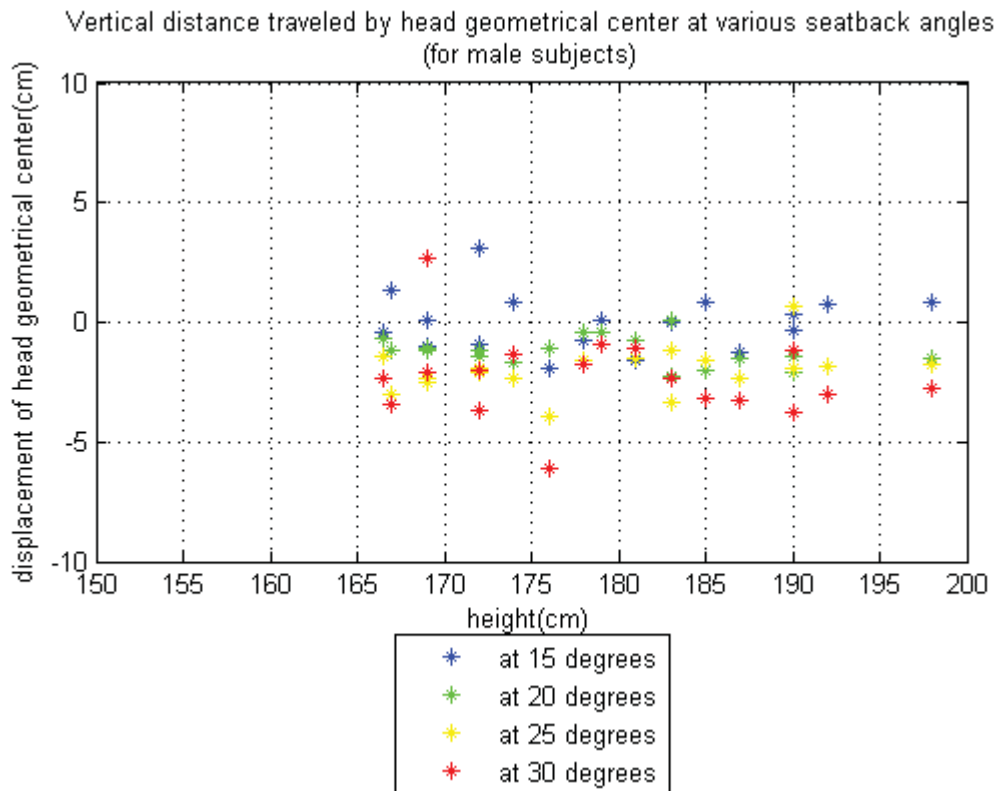


Figure 29 - Vertical distance traveled by head geometrical center wrt occupant height
(For male subjects)

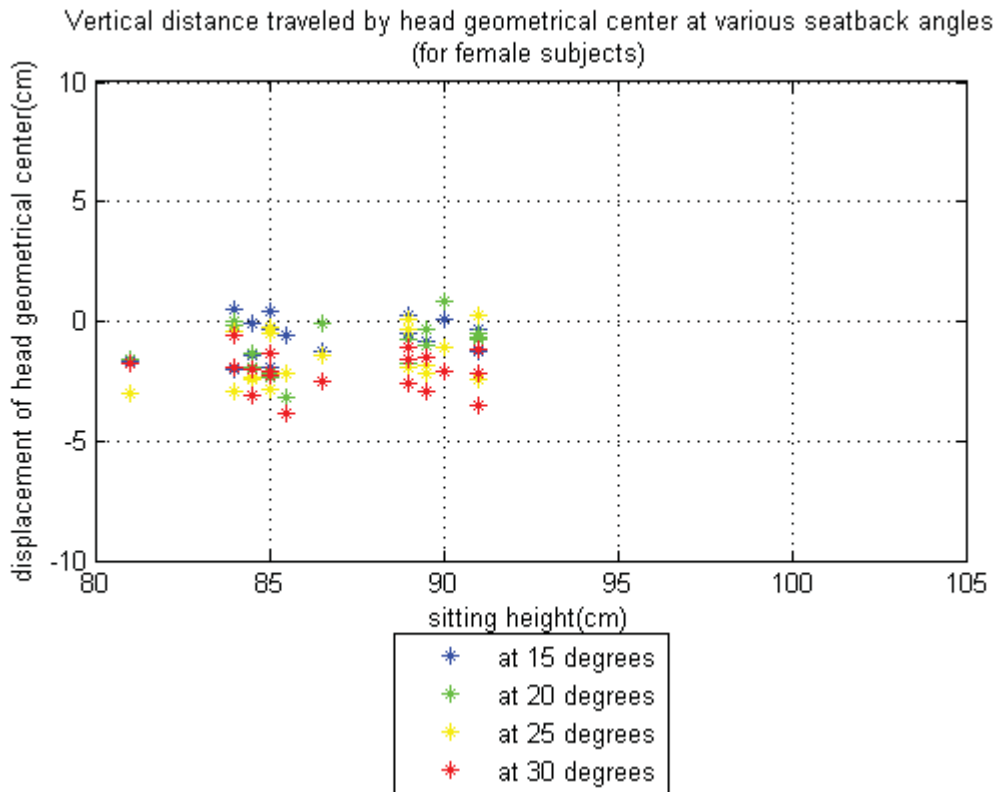


Figure 30 - Vertical distance traveled by head geometrical center wrt occupant sitting height (For female subjects)

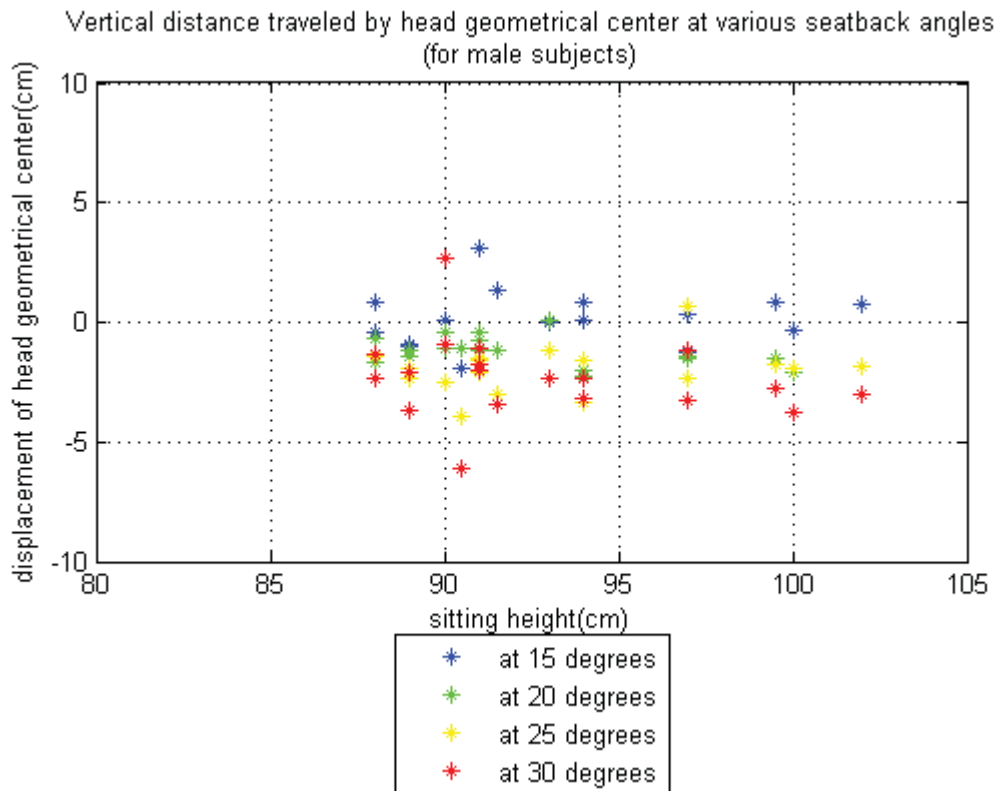


Figure 31 - Vertical distance traveled by head geometrical center wrt occupant sitting height (For male subjects)

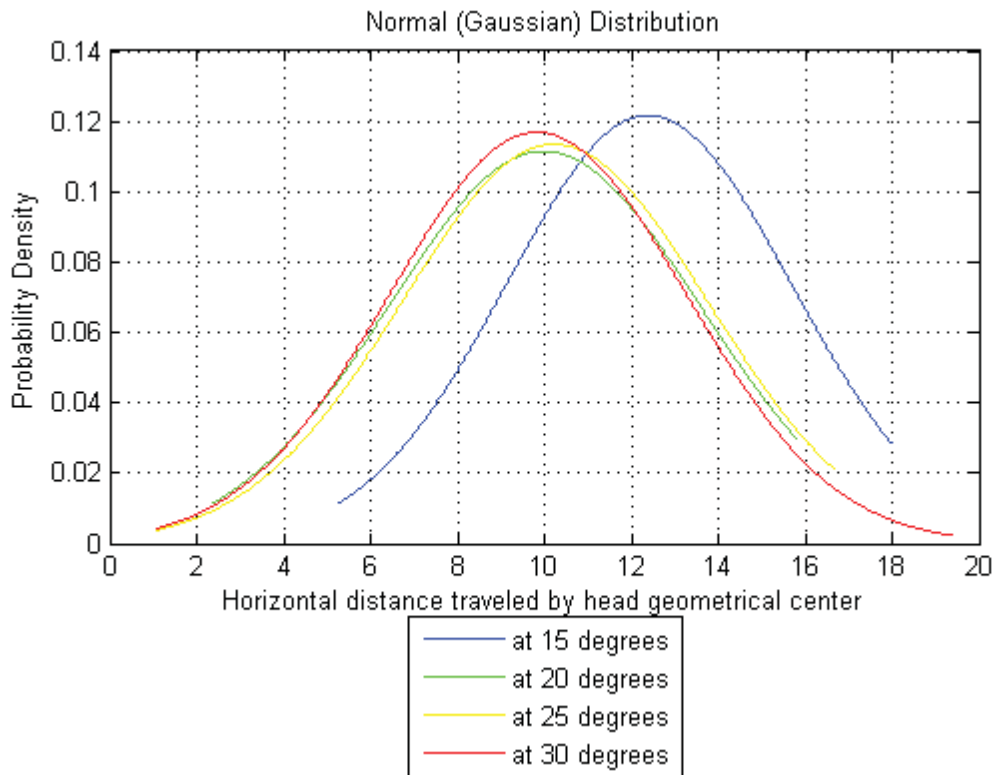


Figure 32 - Normal (Gaussian) distribution comparison of horizontal distance traveled by head geometrical center

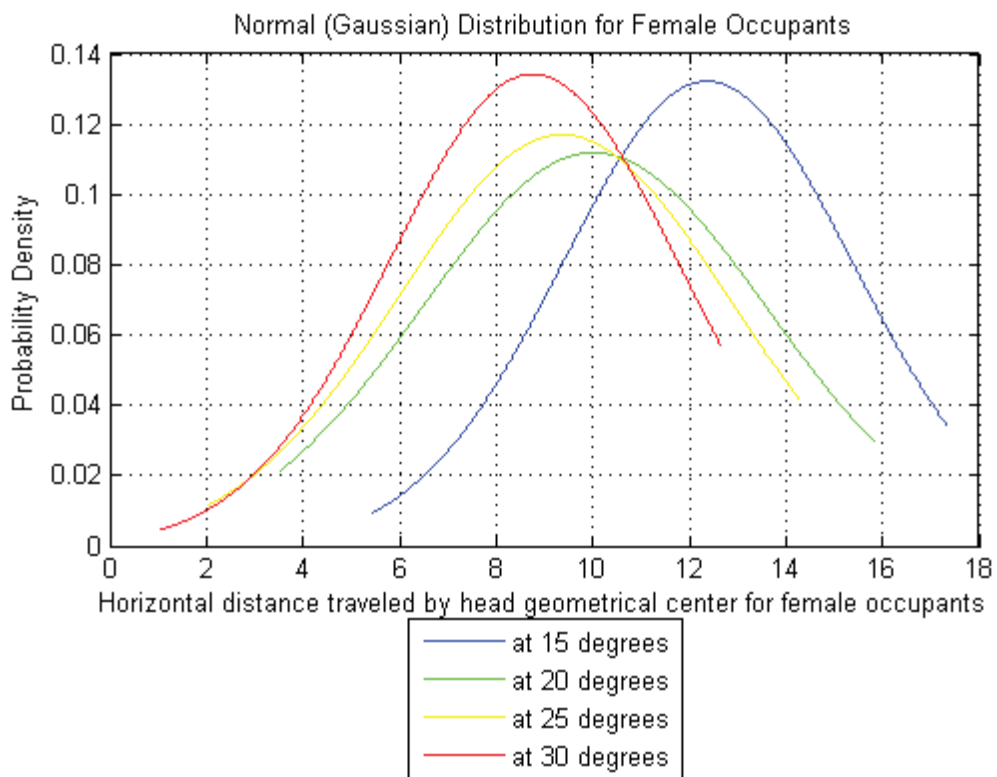


Figure 33 - Normal (Gaussian) distribution comparison of horizontal distance traveled by head geometrical center for female occupants

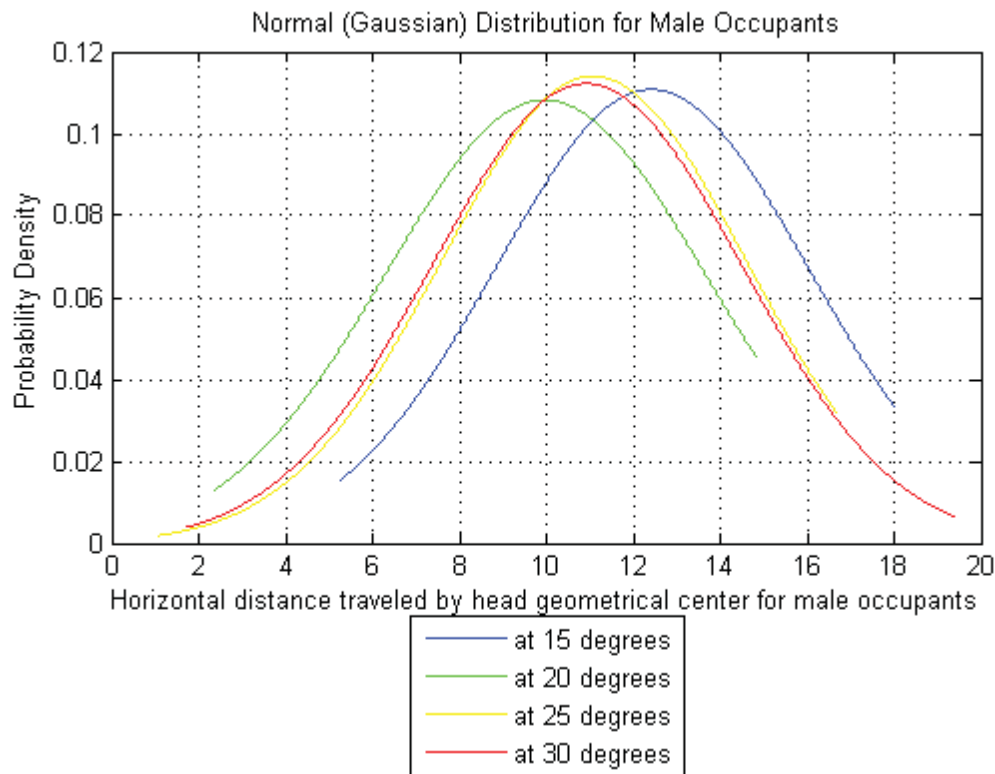


Figure 34 - Normal (Gaussian) distribution comparison of horizontal distance traveled by head geometrical center for male occupants

From the results it was seen in general that the distance traveled by the head geometrical center decreased with the increasing seatback angle, as opposed to the expectations and the results from the previous data from the literature. The reason for this result may be caused by subjects not extending their torsos maximally. People also have different flexibilities in their spines and the initial posture of the subjects can be different. People sit differently, which affects to freedom of movement on the seat. If the torso is bent forward a little bit for someone, then the horizontal displacement will be higher.

It was observed that at higher seatback angles especially at 25° and 30°, a considerable number of subjects leant on the seatback. Therefore, although one may expect that at higher seatback angles torso extension should be higher, the fact is that at these higher angles, many subjects leant their torsos on the seatback hence limiting torso extension. On the other hand, at lower seatback angles like 15° and 20°, occupant's torso is also at a more upright position and has more motion freedom. That is why, an increasing or decreasing trend in the amount of torso extension with respect to seatback angle, is not observed in the experiments.

4. COMPUTATIONAL STUDIES

To study the effects of the chosen car seat and head restraint design, vehicle rear crash simulations has been done on a car seat and occupant model, using the computer program Visual Nastran. The occupant model used in the simulations was taken from the 2 studies done by Himmetoğlu regarding multi-body human model and multibody head and neck model for rear impact simulations [52][53]. The mechanical properties of the basic seat model used in this thesis are based on two studies given in references [54] and [55].

The human and seat models was then modified for various seatback angles and added a different head restraint model for increased safety at said angles. In the study, all the other characteristics of the seat were kept constant while the head restraint properties of the seat were adjusted for the seatback angles that were chosen for this study. With the adjustment to the head restraint properties with respect to the seatback angle, it was aimed to obtain a safer car seat design at various seatback angles, unlike the common practice of optimizing a seat design for a standard seatback angle of 25° chosen by NCAP.

Since the aim was to optimize a car seat design that works well for a variety of seatback angles, simulation model has been set to 4 different seatback angles across the range of seatback angles (15°, 20°, 25° and 30°) and occupants seating positions are adjusted accordingly. For the adjustment of seating positions, reference pictures from a subject (close to 95th percentile male model), and the occupant model on the simulations is optimized accordingly. Although it can be seen that the seating position can vary greatly for each person and influence the results of a vehicle crash, this aim of this study is to be a starting point and a guide for further studies regarding safer vehicles and car seats for more diverse range of drivers and passengers. For the entirety of this study, around 110-120 simulations has been run, 70 of which were for the optimization of the HR (head restraint) model.

4.1. Mechanical Properties of the Car Seat

4.1.1. Head Restraint Model

In the head restraint model, a hysteresis model, as shown in Figure 35 is applied. In this model, when the deformation rate changes sign, the human head loads and unloads the head-restraint along the hysteresis slope until the corresponding loading and unloading curves are reached Head Restraint Model [56].

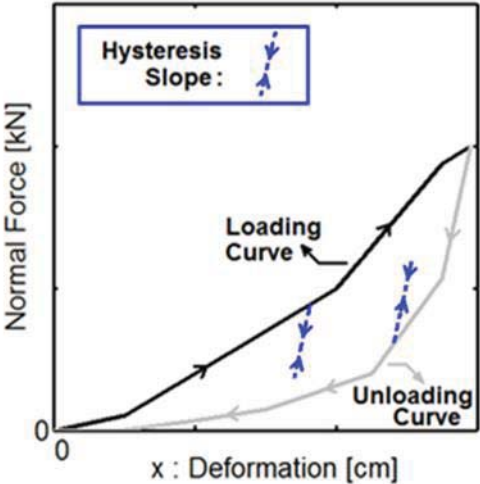


Figure 35 - Hysteresis model for the head-restraint

Mechanical properties of the head restraint used in the simulations are given in Figure 36. These mechanical properties are in accordance with the values obtained from the head restraint loading experiments done by D. C. Viano [57].

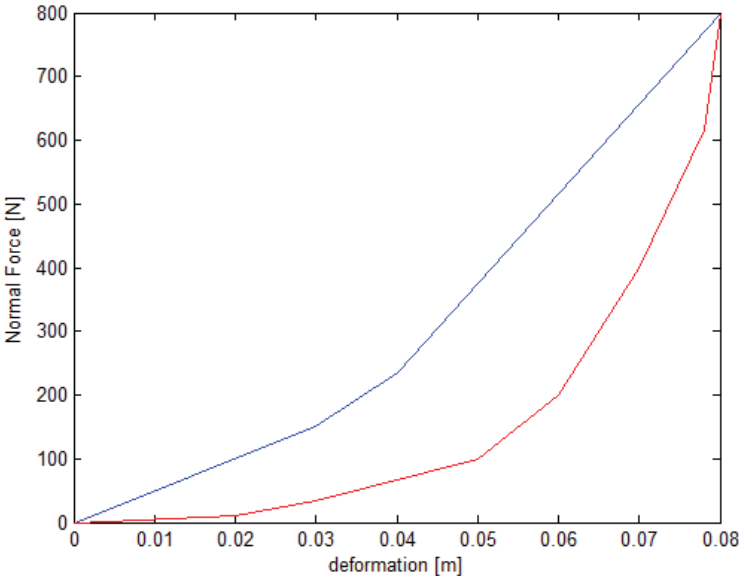


Figure 36 - Head restraint mechanical properties

4.1.2. Energy absorber at the bottom of the seat pan

The mechanical properties of the energy absorber at the bottom of the seat-pan are given below [56]:

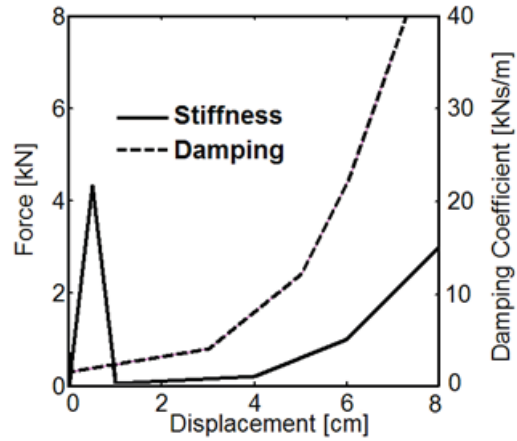


Figure 37 - Mechanical properties of the energy absorber at the bottom of the seat pan

4.1.3. Head-restraint damper at the top of the seatback

Stiffness properties of the head restraint damper are given in the figure below. Head restraint damper consists of spring and damper units connected in parallel. Damping properties of the damper is adjusted according to the seatback angle. More detailed explanation on how the values were obtained is given in the following chapters (damping simulations).

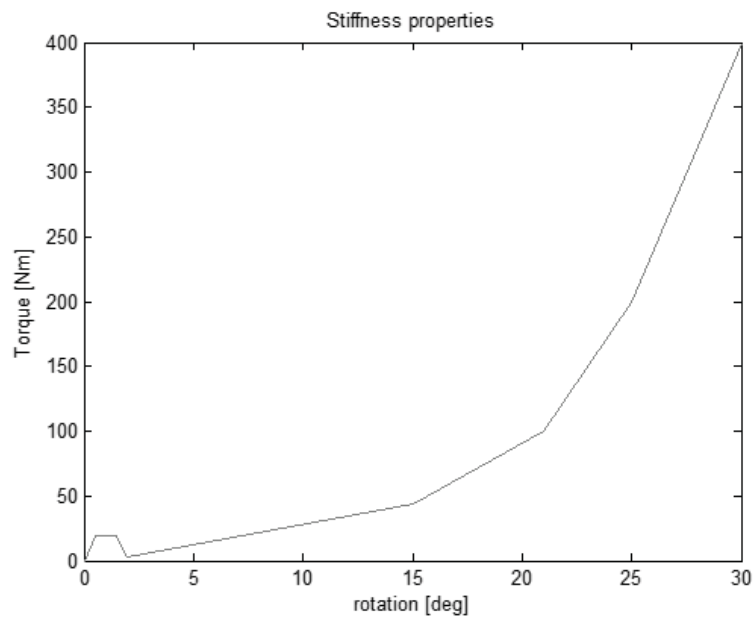


Figure 38 - Stiffness properties of the head restraint damper

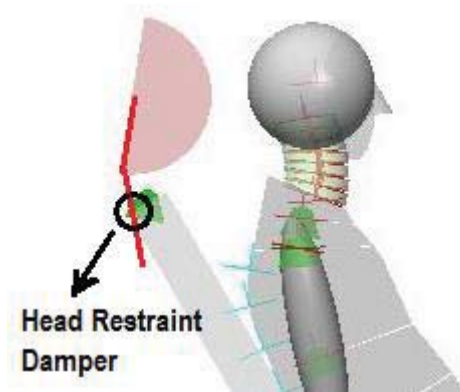


Figure 39 - Basic representation of the head restraint damper position

4.1.4. Recliner Mechanical Properties

The recliner used in the seat is a deformable component that provides energy absorption by way of plastic deformation. Stiffness properties provided by this recliner mechanism are given in Figure 40. The behavior of the recliner mechanism between 0-21° in the given stiffness graph is compatible with the real life standard car seat properties according to the results gotten by Quasistatic Seat Testing (QST) [57]. The reason for the increase in torque values after 21° is that after the plastic deformation of the components inside the recliner mechanism, stronger components of the recliner-seatback-seatpan connection prevents the seat from bending by providing higher torque.

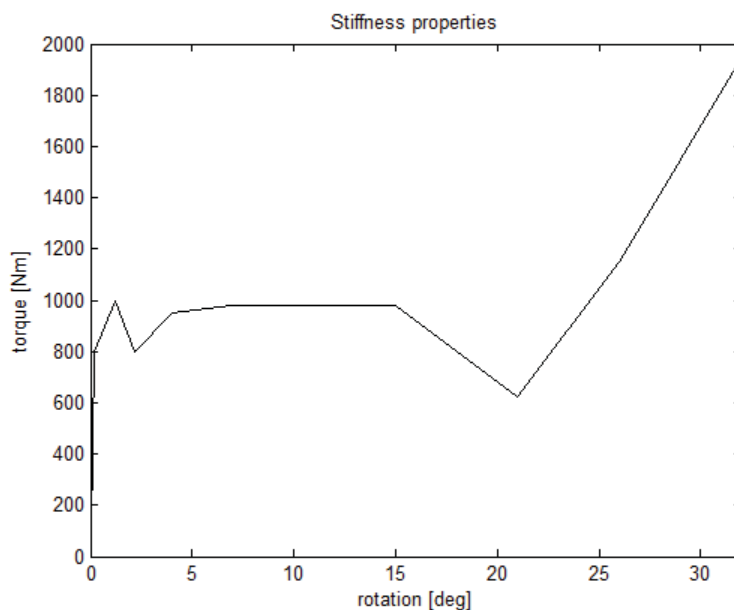


Figure 40 - Stiffness properties of the recliner mechanism

For rearward rotations at the recliner, a constant damping coefficient of 1 Nms/deg is used. This is an estimation of the rotational damping coefficient for the deformation of the recliner-mechanism in typical car-seats [56]. In the recliner, high damping (15 Nms/deg) is applied when the seatback start rotating forward (rebound motion), hence limiting rebound. This high damping is used for simulating the release of the stored elastic energy of the plastically deformed seatback and is compatible with seat tests of EuroNCAP in terms of rebound motion characteristics.

4.1.5. Seat Foam Mechanical Properties

The foam is present in the seat where torso meets the seatback. Stiffness and damping characteristics of the foam is given in the figures below. The mechanical properties of the foam are in actuality the combined characteristics shown by the foam and the suspension behind the foam. In the given figures the stiffness and the damping forces are shown and these forces represent the forces applied by foam+suspension to the torso through the seatback.

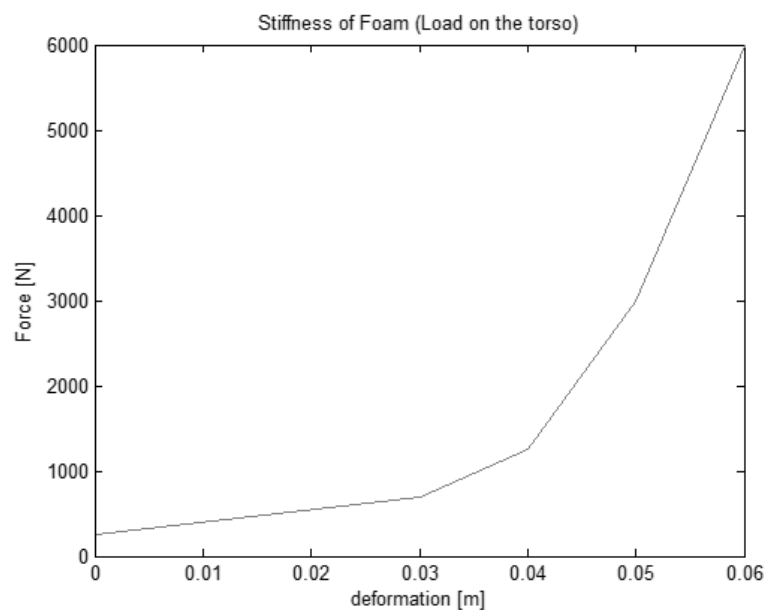


Figure 41 - Stiffness properties of the foam

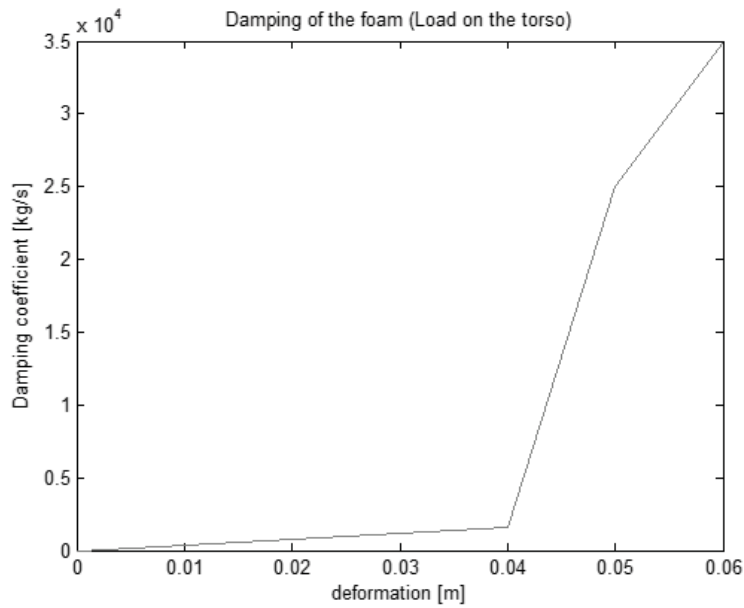


Figure 42 - Damping properties of the foam

The given foam properties are visually similar to the foams of the real car seats used in EuroNCAP tests. In the stiffness and damping values given in the above figures, force and damping values increase when the foam bottoms out. The reason for that increase is that in the case of bottom-out, the foam and the suspension are pushed completely.

4.1.6. Seatpan Angle of the Seat and H-Point Height

H-point can be considered as a relative location of an occupant's hip and is an important characteristic in a seat design. The H-point of the model used in the simulations was measured at 27.91 cm height from the floor.

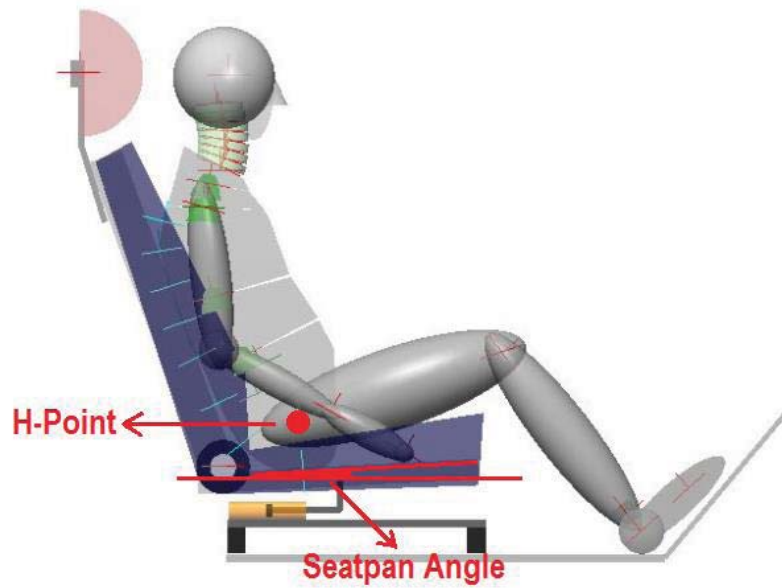


Figure 43 - H-Point and seatpan angle

Additionally, seatpan angle of the seat used in the simulations was 3° and the H point of the occupant model

4.2. Adjusted Seating Positions at 15° , 20° , 25° and 30° Seatback Angles

At the start of the simulations regarding seat's safety on different seatback angles, seating position of the occupant model had to be adjusted. Firstly the seatback has been set to 4 main seatback angles by changing the angle of the seatback model with the recliner considered as a base point.

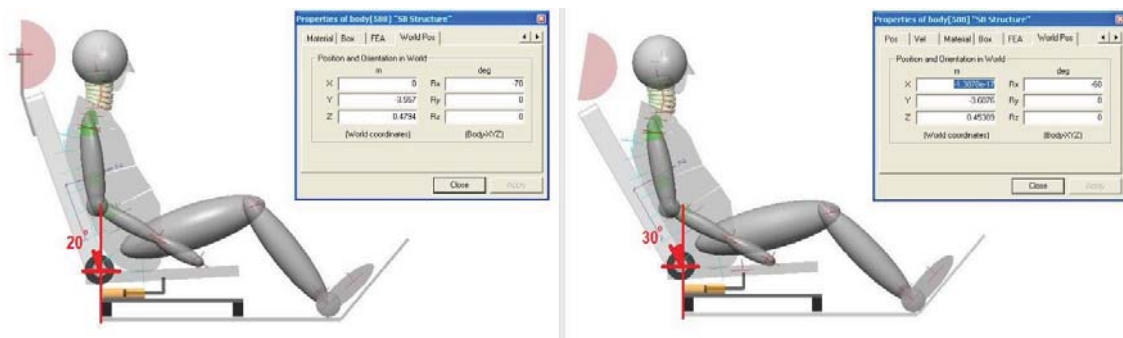


Figure 44 - Adjusting the seatback angle in the simulation

To adjust the occupant model to a natural seating position, sinking simulations has been done on each seatback positions.

For these sinking simulations, occupant model's joints (i.e. neck and torso joints that are supposed to stay facing forward) have been fixed as rigid joints, and after that the model has been lifted and dropped from around 2-3 centimeters above the seat, the simulation has been run as the model sank to the seat and all other joints has stabilized at a position. After the sinking simulations have been done on all seatback angles, the model's torso joints adjusted to more closely resemble the reference seating positions.



Figure 45 - Reference seating positions at various seatback angles

4.3. Selection of the Optimized Car Seat

As mentioned before, an optimized seat model from Himmetoğlu's pervious work was used for the simulations [54][55]. For the optimization process of the car seat, combination of various methods used for decreasing the neck injury risk on rear impacts were tested. The mechanisms tested were recliner (with and without an initial breakaway torque) and seatpan damper. The recliner used in the car seat absorbs some of the energy from the impact by a rotational motion to reduce the forces that affect the torso. The breakaway (torque) is used for preventing the recliner from activating at smaller torque values on the recliner, as in sudden speeding or breaks, occupant leaning back on the seatback or someone pulling the seatback from the behind (see Figure 40). It also helps the recliner absorb the initial forces before allowing the seatback's rotation.

Similarly, seatpan damper is also used for absorbing the impact's energy, but does so with linear motion. In this scenario the seatpan is allowed to move backwards while the force of the impact is gradually absorbed by the damper. The seatpan motion also avoids excessive seatback rotation at the initial stages of the impact. It increases the distance the occupant head and neck travels hence increasing the time for energy to dissipate and limiting the force in the neck.

In the simulations, the following combinations were tested for medium severity crash (IIWPG) and compared to each other to find the best seat model in terms of safety. In these simulations, the head restraint is fixed to the seatback. The car seat was optimized at 20° seatback angle and the backset of the occupant in the simulations was 5.8 cm. The criteria used for comparison per IIWPG standards are [52]:

- F_{shear} of C0/C1 on C1 vertebra: Should be between 30-190 N
- N_{km} : Should be between 0.15 and 0.55
- Orientation of T11/T12 (the joint between T11 and T12 vertebra): Should be less than 24°
- S-shape measures: Should be between -3.5 and 2.5

The given pictures show frozen frames from the simulations at (i) before the human model fully sinks into the seatback foam; the instant (ii) when the head first contacts the head restraint; the instant (iii) when the maximum seatback-rotation occurs (the maximum penetration of the head into the head restraint also occurs at around this moment); and the instant (iv) when the head just leaves the head restraint.

4.3.1. Seatpan damper is locked + recliner breakaway is removed (RONB):

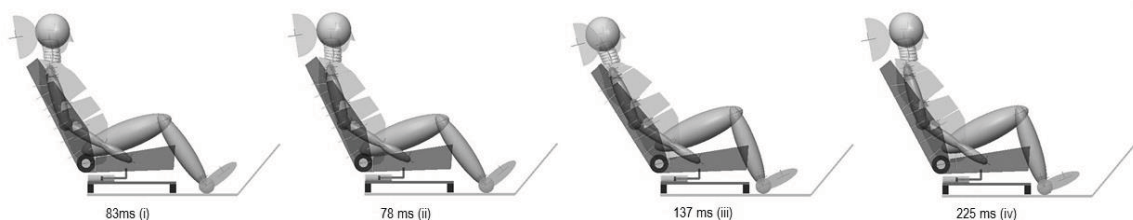


Figure 46 - Simulation for RONB seat

- Max F_{shear} of C0/C1 on C1: 147.57 N

- Max N_{km} : 0.476
- Max Orientation of T11/T12 : 25.613°
- S-shape measures: -2.992 min, 0.27987 max

Although the F_{shear} , N_{km} , relative angles and s-shape values are in the acceptable range, maximum orientation of T11/T12 joint is outside of the safe motion range and can cause an injury on person's torso.

4.3.2. Seatpan damper is locked + recliner with breakaway (ROWB):

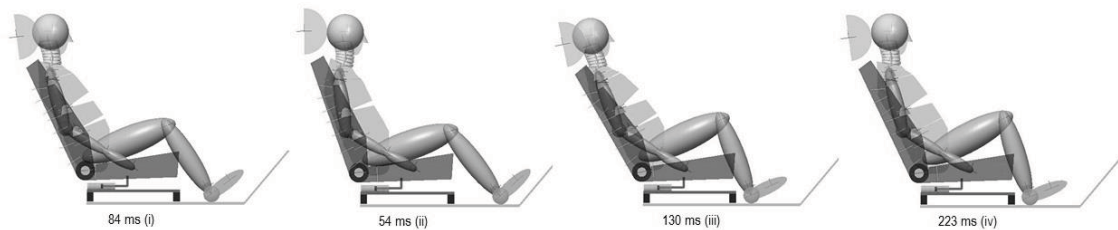


Figure 47 - Simulation for ROWB seat

- Max F_{shear} of C0/C1 on C1: 127.13 N
- Max N_{km} : 0.08928
- Max Orientation of T11/T12 : 24.027°
- S-shape measures: -1.5921 min, 0.27946 max

All the values of this combination can be considered acceptable, but the maximum orientation of T11/T22 is close to the acceptable value and has a low risk of injury.

4.3.3. Seatpan damper is active + recliner breakaway is removed (RSNB):

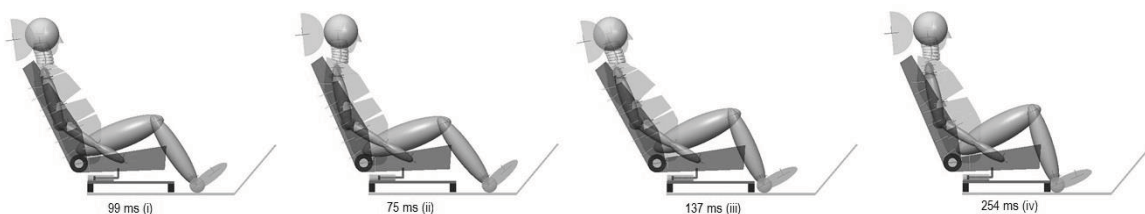


Figure 48 - Simulation for RSNB seat

- Max F_{shear} of C0/C1 on C1: 137.25 N

- Max N_{km} : 0.34982
- Max Orientation of T11/T12 : 23.596°
- S-shape measures: -1.7274 min, 0.03462 max

All the values in this simulation, but again the orientation of T11/T12 is close to the joint's ROM limit.

4.3.4. Seatpan damper is active + recliner with breakaway (RSWB):

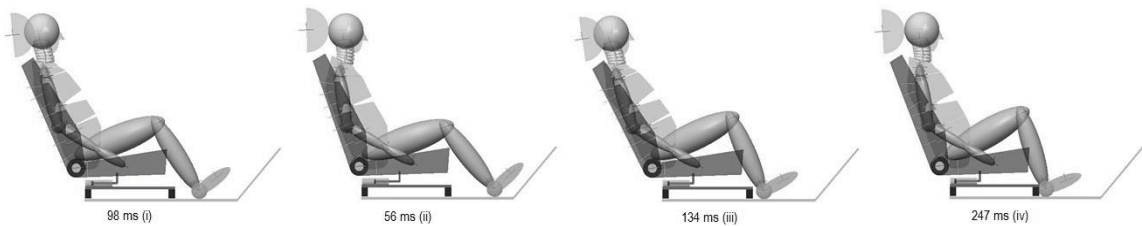


Figure 49 - Simulation for RSWB seat

- Max F_{shear} of C0/C1 on C1: 118.43 N
- Max N_{km} : 0.2426
- Max Orientation of T11/T12 : 20.665°
- S-shape measures: -0.93047 min, 0.34961 max

All the values in this simulation are in the acceptable range, and shows better values compared to the other combinations. F_{shear} , N_{km} and T11/T12 orientation values are considerably better than the other acceptable option RSNB, so the combination applied on this seatback is used for further studies regarding head restraint design.

4.3.5. Seatpan damper is active + recliner is locked (SOLR):

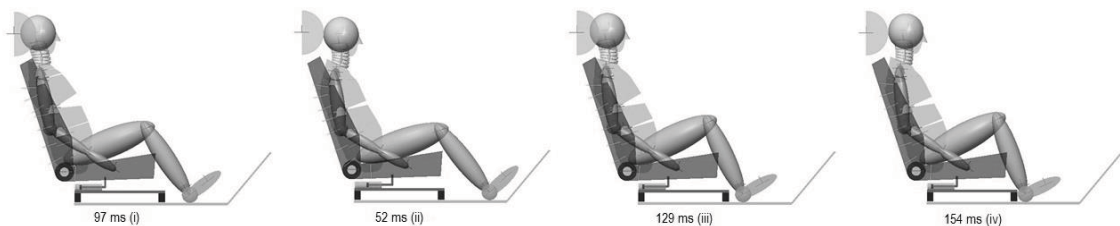


Figure 50 - Simulation for SOLR seat

- Max F_{shear} of C0/C1 on C1: 240.2 N
- Max N_{km} : 0.69523
- Max Orientation of T11/T12 : 25.276°
- S-shape measures: -2.9823 min, 1.3898 max

This combination has shown the worst results among the chosen combinations and isn't acceptable per NCAP criteria.

4.4. Performance of the Car Seat at Various Severities of Crash Pulses

The optimized car seat model was tested at 15°, 20°, 25° and 30° seatback angles against low, medium and high severity crash pulses. The optimization of the car seat was previously done at 20° seatback angle and to test it at different seatback angles, the HR (head restraint) was fixed to the seatback and after changing the angle of the seatback the occupant posture was adjusted accordingly. For different variations of the seatback angle, seating positions were adjusted with respect to the reference model's posture in Figure 45.

4.4.1. At 15° Seatback Angle

❖ TR16 (low severity) crash pulse:

- Max F_{shear} of C0/C1 on C1: 97.946 N
- Max N_{km} : 0.22612
- Max Orientation of T11/T12 : 14.471°
- S-shape measures: -0.5589 min, 2.8859 max

❖ IIWPG (medium severity) crash pulse:

- Max F_{shear} of C0/C1 on C1: 110.52 N
- Max N_{km} : 0.22638
- Max Orientation of T11/T12 : 15.4°
- S-shape measures: -0.7474 min, 2.1763 max

❖ **TR24 (high severity) crash pulse:**

- Max F_{shear} of C0/C1 on C1: 133.83 N
- Max N_{km} : 0.25485
- Max Orientation of T11/T12 : 18.425°
- S-shape measures: -3.0656 min, 2.2792 max

4.4.2. At 20° Seatback Angle

❖ **TR16 (low severity) crash pulse:**

- Max F_{shear} of C0/C1 on C1: 139.46 N
- Max N_{km} : 0.34863
- Max Orientation of T11/T12 : 20.239°
- S-shape measures: -1.0333 min, 0.29981 max

❖ **IIWPG (medium severity) crash pulse:**

The results are given in the previous part comparing various combinations' performances against IIWPG crash pulse. In the comparison, RSWB combination was chosen and is used in the further simulations.

❖ **TR24 (high severity) crash pulse:**

- Max F_{shear} of C0/C1 on C1: 160.63 N
- Max N_{km} : 0.45827
- Max Orientation of T11/T12 : 19.119°
- S-shape measures: -5.16 min, 1.8496 max

4.4.3. At 25° Seatback Angle

❖ **TR16 (low severity) crash pulse:**

- Max F_{shear} of C0/C1 on C1: 186.93 N

- Max N_{km} : 0.56132
- Max Orientation of T11/T12 : 24.346°
- S-shape measures: -2.2392 min, 0.22922 max

❖ **IIWPG (medium severity) crash pulse:**

- Max F_{shear} of C0/C1 on C1: 165.94 N
- Max N_{km} : 0.48016
- Max Orientation of T11/T12 : 24.899°
- S-shape measures: -2.4294 min, 0.26661 max

❖ **TR24 (high severity) crash pulse:**

- Max F_{shear} of C0/C1 on C1: 206.78 N
- Max N_{km} : 0.62395
- Max Orientation of T11/T12 : 22.539°
- S-shape measures: -3.7662 min, 1.3946 max

4.4.4. At 30° Seatback Angle

❖ **TR16 (low severity) crash pulse:**

- Max F_{shear} of C0/C1 on C1: 202.96 N
- Max N_{km} : 0.66918
- Max Orientation of T11/T12 : 23.845°
- S-shape measures: -3.247 min, 0.24268 max

❖ **IIWPG (medium severity) crash pulse:**

- Max F_{shear} of C0/C1 on C1: 202.74 N
- Max N_{km} : 0.64629
- Max Orientation of T11/T12 : 24.9°
- S-shape measures: -3.3839 min, 0.28165 max

❖ **TR24 (high severity) crash pulse:**

- Max F_{shear} of C0/C1 on C1: 197.96 N
- Max N_{km} : 0.61446
- Max Orientation of T11/T12 : 22.586°
- S-shape measures: -3.4353 min, 3.3111 max

4.5. Adaptation of the Head Restraint Model to the Simulations

It can be seen from the previous rear crash simulations that the lowest risk of head injury from selected seatback angles is at 20°. As it was explained in the previous chapters, backset is one of the major affecting factors for neck injury risk. To lower the risk of neck injury for other seatback positions, head restraint post's angle has been adjusted to result in a backset close to 5.5 cm.

To adapt this head restraint model, the joint connecting the head restraint to the seatback has been rotated forward or back depending on the original backset to set the distance between the head restraint and the head close to 5.5 cm.

The required angle change has been found through the computer program CATIA, using the reference 2D model prepared for the study of HR angle vs backset for the chosen 4 seatback angles. For each angle the head model has been kept fixed while the HR model was rotated to give the required backset. Then the round numbers of the angles obtained from the models has been applied to the seatback and head restraint models on the crash simulations.

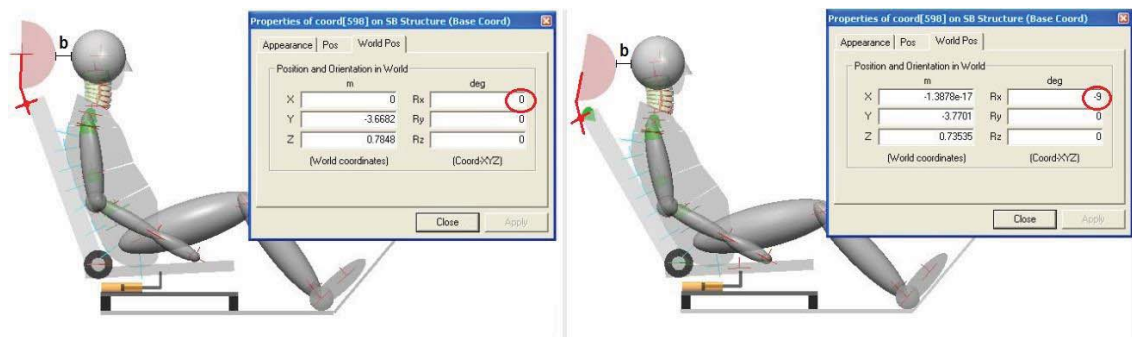


Figure 51 - Adjusting the head restraint position

The head restraint models were first tested for the middle severity crash pulse (IIWPG) and optimizations were done according to HR's performance on the aforementioned crash pulse. Final HR design was then tested against low and high severity crash pulses (TR16 and TR24) to check its general performance on different scenarios.

4.5.1. Simulations with Locked Head Restraint

The first simulations on the new seat models were done with the adjusted head restraint angles with fixed joint between the HR (head restraint) and the seatback.

The aim of this study was to mainly understand the effect of the angle of repose of the HR post and to observe what kind of affect the smaller backset would have while the other factors like the seating position, seatback angle and the distance of the upper back to the seatback was kept constant. In the simulation, the backset was decreased to 5.6 cm by rotating the HR from the joint placed where the HR post and seatback meets. After the HR position was adjusted, the joint was locked on the new position.

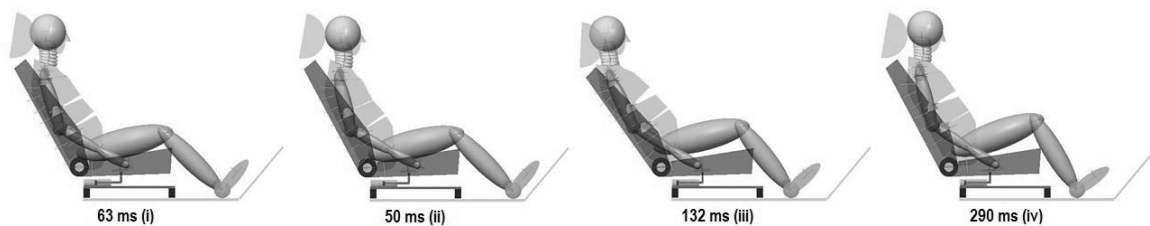


Figure 52 - Simulation with locked head restraint at 30° seatback angle

- Max F_{shear} of C0/C1 on C1: 266.14 N
- Max N_{km} : 0.50571
- Max Orientation of T11/T12 : 18.436°
- S-shape measures: -5.9999 min, 0.28161 max

It can be seen from the simulation results that while the smaller backset decreases the head's contact time the HR and provides an earlier support for the head, the sudden impact of the head to the HR without the help of back support can cause an increase in head normal force and cause a protrusion induced neck injury. Although it was seen from the simulations that the neck forces were smaller compared to the greater backset situations, short impact time can cause s-shape and result in neck injury.

To reduce the effects and cushion the force of this sudden impact, a damper was needed for the head restraint system.

4.5.2. Damping Simulations

To reduce the forces acting on the head and neck of the occupant, and reduce the risk of injury by absorbing part of the energy from the impact, a spring and damper mechanism was implemented to the head restraint model (Figure 39). After the first simulations with the constant damping and deciding on a rough approximation for the damping needed for reducing neck injury risk, variations added to the damping and stiffness values to further optimize the design. It was started with the previously determined minimum and maximum stiffness points with a linear increase in damping.

The optimal stiffness values were found by increasing and decreasing the values between minimum and maximum damping values depending on the results of each previous simulation, by determining the points where the peaks in normal force on the head caused by the head restraint, and adjusting the damping constant corresponding to the time the peak has occurred.

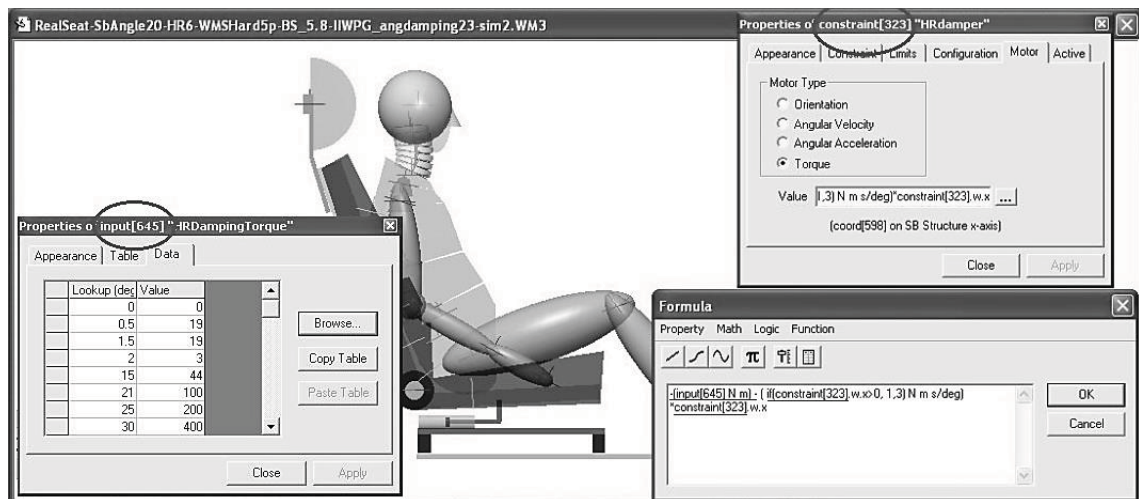


Figure 53 - Adjusting the damping ratio and stiffness for the head restraint

The optimization was done at 30° SB (seatback) angle which has the highest risk of injury to the neck at rear end accidents. Adjusting the damping rate for the other seatback angles to get the optimal results for each one has been done by changing the damping ratio for each angle.

While the more reclined seatback positions needed low damping ratio, higher damping ratios gave better results for more upright seatback positions.

4.5.2.1. Optimization at 30° Seatback Angle

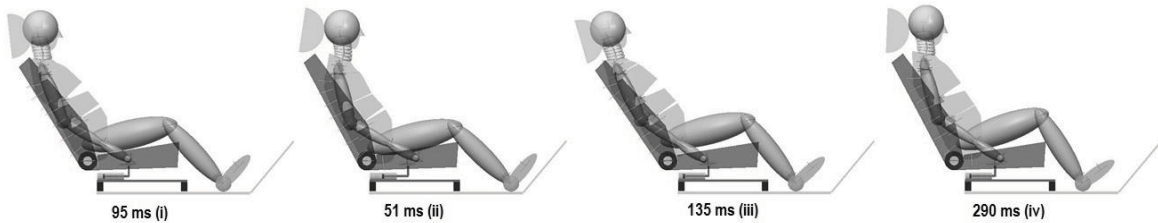


Figure 54 - Seatback 30° optimizations

- Max F_{shear} of C0/C1 on C1: 130.37 N
- Max N_{km} : 0.26967
- Max Orientation of T11/T12 : 22.418°
- S-shape measures: -4.2109 min, 0.28161 max

Damping ratio used for this HR position was 0.3 for rearwards motion and 0.1 for forward motion (to keep the HR from trying to return to its original position suddenly and pushing the head forward).

4.5.2.2. Optimization at 25° Seatback Angle

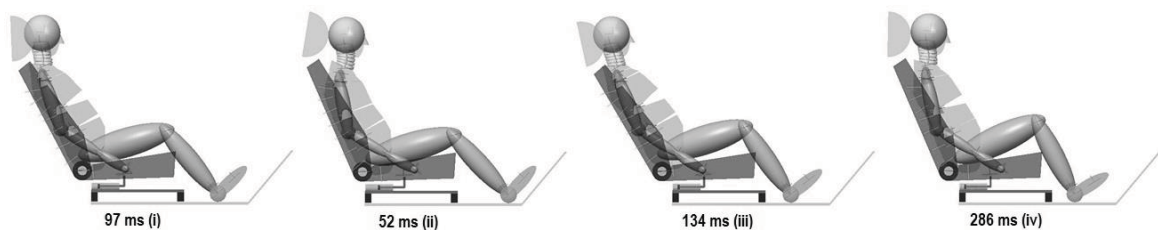


Figure 55 - Seatback 25° optimizations

- Max F_{shear} of C0/C1 on C1: 122.95 N
- Max N_{km} : 0.19311
- Max Orientation of T11/T12 : 22.569°
- S-shape measures: -3.3031 min, 0.26659 max

Damping ratio used for this HR position was 0.54 for rearwards motion and 0.18 for forward motion.

4.5.2.3. Optimization at 20° Seatback .Angle

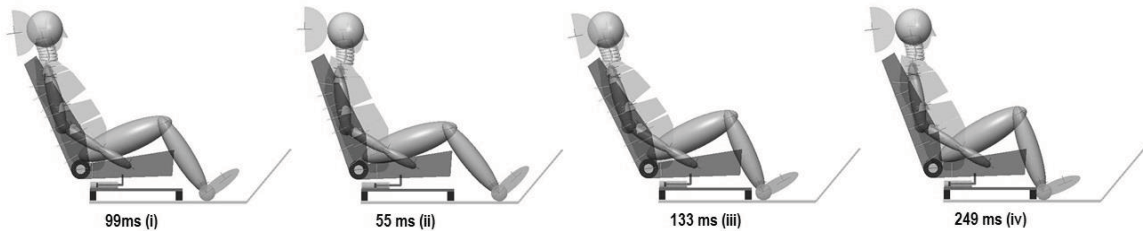


Figure 56 - Seatback 20° optimizations

- Max F_{shear} of C0/C1 on C1: 85.391 N
- Max N_{km} : 0.12562
- Max Orientation of T11/T12 : 21.103°
- S-shape measures: -0.82546 min, 1.1558 max

Damping ratio used for this HR position was 3 for rearwards motion and 1 for forward motion.

4.5.2.4. Optimization at 15° Seatback Angle

❖ At 5.5 cm Backset

- Max F_{shear} of C0/C1 on C1: 28.904 N
- Max N_{km} : 0.091931
- Max Orientation of T11/T12 : 18.354°
- S-shape measures: 0 min, 4.3213 max

At first the optimization at 15° seatback angle was tried with 5.5 cm backset as the other seatback angles, but to do that, the head restraint is rotated backwards relative to the seatback. This situation caused the HR to not have enough energy absorption for the forces on head and neck during the impact at lower damping ratios up to damping ratios that are high enough that the effects of damping aren't clearly seen in the results (such

as the HR mechanism acts as a rigid mechanism); thus resulting in higher s-shape values.

❖ At 4.5 cm Backset

After the results of 5.5 cm backset simulations, the backset at 15° SB was reduced to 4.5 cm. Although the lower backset values were expected to give better results, it wasn't preferred to reduce to backset further for the aim of keeping the backset value at comfortable driving region.

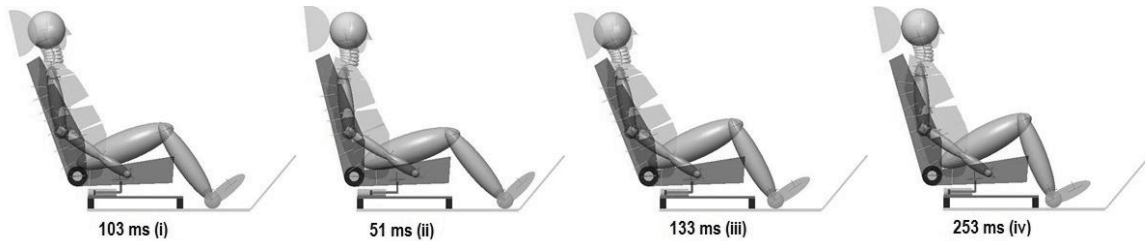


Figure 57 - Seatback 15° optimizations

- Max F_{shear} of C0/C1 on C1: 46.45 N
- Max N_{km} : 0.085306
- Max Orientation of T11/T12 : 17.231°
- S-shape measures: 0 min, 3.5084 max

It was seen that although the shear force on C0/C1 joint was higher, s-shape results for this condition were better than the previous try at 5.5 cm seatback, so this version was chosen as our final optimized version for further studies.

Damping ratio used for both HR positions at 15° SB angle was 3.6 for rearwards motion and 1.2 for forward motion

4.5.3. Performance on High and Low Severity Crash Pulses

4.5.3.1. At 30° Seatback Angle

❖ TR16 (low severity) crash pulse:

- Max F_{shear} of C0/C1 on C1: 121.93 N
- Max N_{km} : 0.24716
- Max Orientation of T11/T12 : 20.1°

- S-shape measures: -3.7256 min, 0.23907 max

❖ **TR24 (high severity) crash pulse:**

- Max F_{shear} of C0/C1 on C1: 135.55 N
- Max N_{km} : 0.49507
- Max Orientation of T11/T12 : 21.687°
- S-shape measures: -4.6082 min, 1.4975 max

4.5.3.2. At 25° Seatback Angle

❖ **TR16 (low severity) crash pulse:**

- Max F_{shear} of C0/C1 on C1: 108.07 N
- Max N_{km} : 0.23498
- Max Orientation of T11/T12 : 21.795°
- S-shape measures: -3.3587 min, 0.22624 max

❖ **TR24 (high severity) crash pulse:**

- Max F_{shear} of C0/C1 on C1: 121.8 N
- Max N_{km} : 0.45496
- Max Orientation of T11/T12 : 21.746°
- S-shape measures: -4.8763 min, 0.21775 max

4.5.3.3. At 20° Seatback Angle

❖ **TR16 (low severity) crash pulse:**

- Max F_{shear} of C0/C1 on C1: 101.22 N
- Max N_{km} : 0.22027
- Max Orientation of T11/T12 : 20.635°
- S-shape measures: -0.52726 min, 1.1073 max

❖ **TR24 (high severity) crash pulse:**

- Max F_{shear} of C0/C1 on C1: 137.47 N
- Max N_{km} : 0.42463

- Max Orientation of T11/T12 : 19.987°
- S-shape measures: -3.1353 min, 1.8304 max

4.5.3.4. At 15° Seatback Angle

❖ TR16 (low severity) crash pulse:

- Max F_{shear} of C0/C1 on C1: 71.885 N
- Max N_{km} : 0.16892
- Max Orientation of T11/T12 : 16.935 °
- S-shape measures: 0 min, 3.8311 max

❖ TR24 (high severity) crash pulse:

- Max F_{shear} of C0/C1 on C1: 117.75 N
- Max N_{km} : 0.27736
- Max Orientation of T11/T12 : 20.142°
- S-shape measures: 0 min, 3.1768 max

4.5.4. Comparison with the Experimental Results

4.5.4.1. Comparison of Distance Traveled by the Head

To evaluate the safety of the car seat design in terms of torso extension, the results were compared with the results of the torso extension experiment. For the comparison of the simulations and the experiments, the data related to the ones studied in the experiments were needed to be extracted or calculated. The data from the optimized models with the modified HR design with damping were used for the comparison.

For the calculation, related data were taken from the original seating position (Figure 58), and reclined position where the orientation of the torso joints are at greatest (Figure 60). To eliminate the effects of the seatpan motion and the recliner motion at the reclined coordinates of the occupant, the simulation was stopped at the reclined position after the crash, recliner rotation was reset and the occupant model's joints were adjusted to get it to the seating position (Figure 59).

Since the seatback angle in the experiment was fixed, reclined position is noted after the recliner is rotated back to zero with the occupant's body. After the related data was noted, the distance traveled by the head geometrical center was calculated. The coordinates for the calculations are;

C_0 : Middle point between T1 vertebra and the top of the sternum (C7/T1 at Figure 2) at the original seating position of the occupant at the start of the simulation

O_0 : Head geometrical center of the occupant at the original seating position of the occupant at the start of the simulation (Head C.G. at Figure 2)

C : Middle point between T1 vertebra and the top of the sternum at the adjusted seating position

O : Head geometrical center of the occupant at the adjusted seating position

C' : Middle point between T1 vertebra and the top of the sternum at the reclined position

O' : Head geometrical center of the occupant at the reclined position

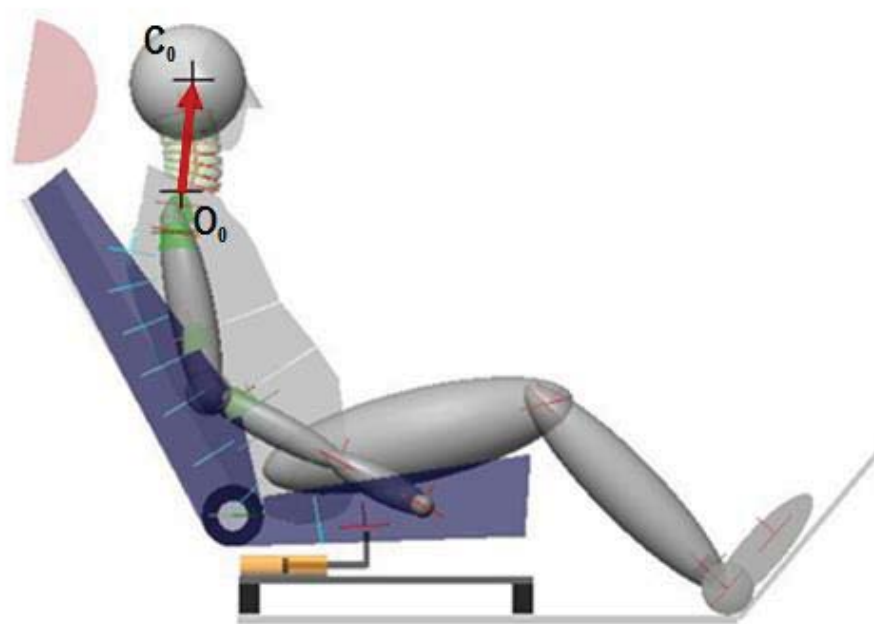


Figure 58 - Original seating position

After the related coordinates are noted, the vector \vec{r} (shown red in the Figure 58 and Figure 59) is calculated, and for the adjusted seating position moved to the new coordinate of O for further calculations.

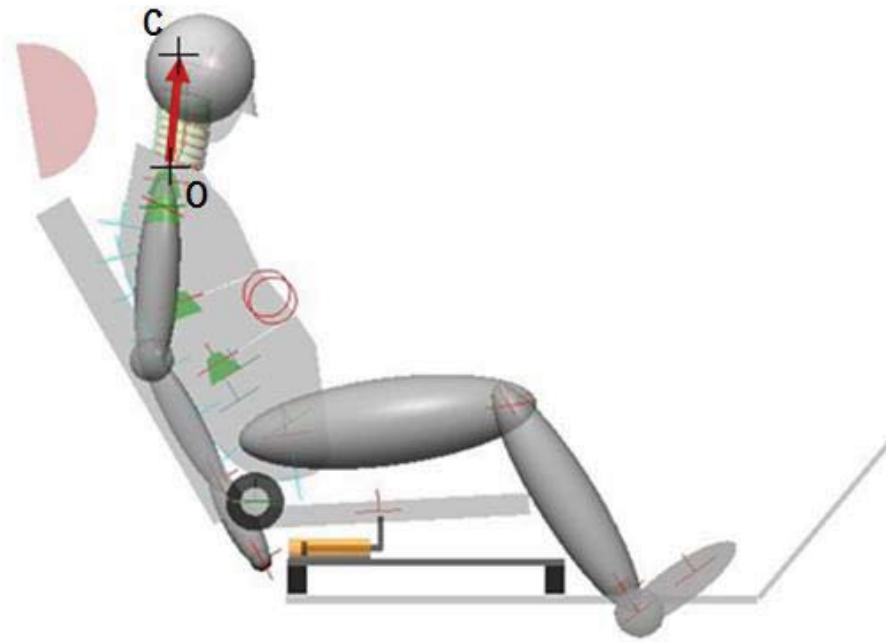


Figure 59 - Adjusted seating position

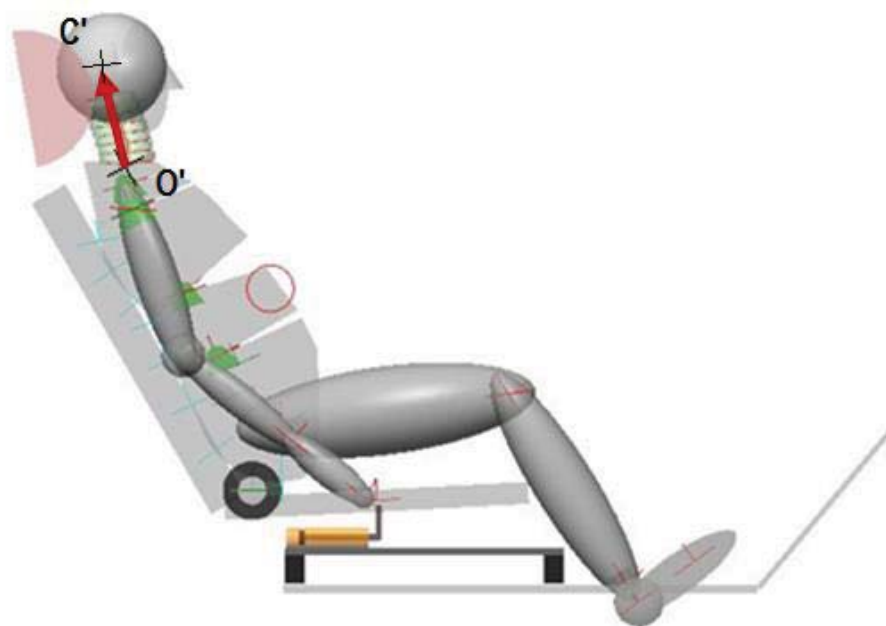


Figure 60 - Reclined position representing rear crash

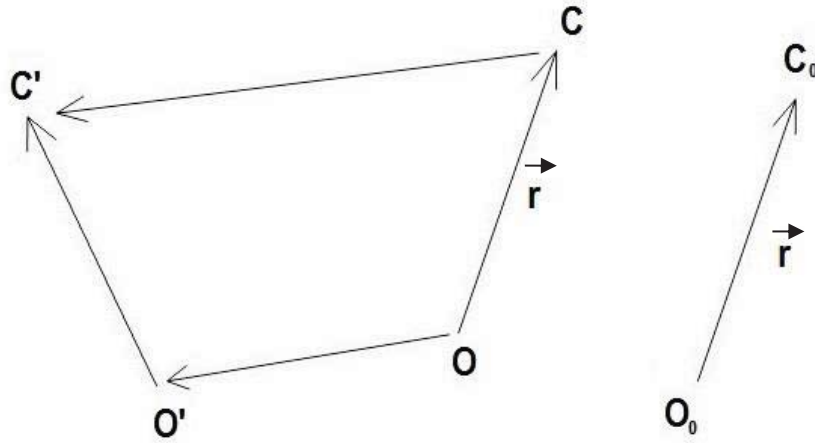


Figure 61 - Vectorial representation of the specified coordinates

To calculate the distance traveled by the head geometrical center (CC') the below formula was used; (y_c, z_c) being the coordinates of the head geometrical center and (y_o, z_o) being the coordinates of the center of torso 1:

$$\begin{aligned}\overrightarrow{OC} &= (y_c - y_o) * \vec{j} + (z_c - z_o) * \vec{k} = \vec{r} \\ \vec{r} &= \begin{bmatrix} (y_c - y_o) \\ (z_c - z_o) \end{bmatrix} \\ \overrightarrow{OO'} + \overrightarrow{O'C'} &= \overrightarrow{OC} + \overrightarrow{CC'} \\ \overrightarrow{CC'} &= \overrightarrow{OO'} + \overrightarrow{O'C'} - \vec{r}\end{aligned}$$

In which the $\overrightarrow{OO'}$ vector is calculated from the coordinates, and $\overrightarrow{O'C'}$ vector is calculated from the inclination angle of the vector (taken from the simulation data) and from the magnitude of $|\vec{r}|$;

$$\begin{aligned}\vec{r} &= |r| * (\cos\alpha * \vec{j} + \sin\alpha * \vec{k}) \\ \overrightarrow{O'C'} &= |r| * (\cos\theta * \vec{j} + \sin\theta * \vec{k})\end{aligned}$$

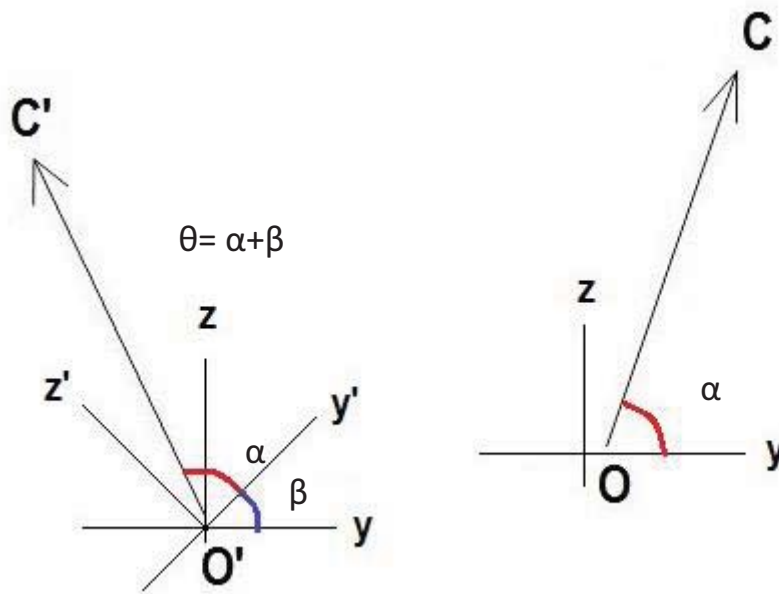


Figure 62 - Given angles of the specified vectors

The calculations are completed on Matlab for simulations of all seatback angles in 3 crash pulses.

Table 3 – Horizontal (Δy) and vertical (Δz) distances traveled by head geometrical center in simulations

	TR16 (cm) (low severity)	IIWPG (cm) (middle severity)	TR24 (cm) (high severity)
15° Seatback	$\Delta y = -2.64$ $\Delta z = 1.38$	$\Delta y = -5.84$ $\Delta z = 2.20$	$\Delta y = -4.98$ $\Delta z = 2.22$
20° Seatback	$\Delta y = -10.03$ $\Delta z = 1.26$	$\Delta y = -11.46$ $\Delta z = 1.07$	$\Delta y = -8.75$ $\Delta z = 1.39$
25° Seatback	$\Delta y = -13.44$ $\Delta z = 0.10$	$\Delta y = -15.26$ $\Delta z = -0.04$	$\Delta y = -12.98$ $\Delta z = 0.49$
30° Seatback	$\Delta y = -14.40$ $\Delta z = -2.10$	$\Delta y = -17.64$ $\Delta z = 0.79$	$\Delta y = -14.86$ $\Delta z = -1.61$

While it was seen from the results that the severity of the crush didn't have an observable effect on the horizontal or vertical distances traveled by head geometrical center, it was seen that for more reclined seatback angles, horizontal distance traveled was greater. It can be seen that the results for 15° and 20° SB angles are similar to the experiment results, while 25° and 30° SB angles gave greater horizontal distances than in the experiment.

Although it was preferable to get closer results to the experiment, rotational freedom of the head restraint allowed a greater freedom to the head. To reduce the distance, another simulation was run with higher damping ratio at 25° SB angle. While it was seen that the orientation of T11/T12 joint and the distance traveled by the head were decreased, the neck force was increased above the acceptable values.

Table 4 - Different damping values comparison (Δy horizontal and Δz vertical distances)

	Distance traveled by head geometrical center (cm)	Orientation of T11/T12 joint (degrees)	Neck Force (N)
Original damping	$\Delta y = -15.26$ $\Delta z = -0.04$	22.569°	122.95
Increased damping	$\Delta y = -12.47$ $\Delta z = 0.13$	20.656°	201.21

4.5.4.2. Different Posture Simulations

The previous simulations on the performance of the new head restraint design were done for typical driving position. Although our previous experiments showed that some occupants, especially passengers, sit more leaned back on the seatback; which is one of the reasons for getting lower values of horizontal distance traveled by head in the simulations. So there has been another 3 simulations at 25° seatback angle for different seating postures:

1. Leaned back position with same HR position and characteristics:

In the first simulation the human model is positioned in a more reclined position (with 1.8 cm backset), while the HR position and characteristics were kept the same. As a result, T11/T12 rotation was decreased, but the s-shape value was increased.

- Max F_{shear} of C0/C1 on C1: 138.02 N
- Max N_{km} : 0.23707
- Max Orientation of T11/T12 : 20.249°
- S-shape measures: -5.0125 min, 044775 max

The results of the torso extension calculations are also given below and are similar to experimental results. Horizontal and vertical distances travelled by the head geometrical center are as follows:

$$\Delta y = -10.78$$

$$\Delta z = -0.23$$

2. Leaned back position with reclined HR position and same characteristics:

In the second simulation, the HR was also reclined to keep the 5.6 cm backset while still keeping the same damping and stiffness characteristics. The result was that the neck forces and s-shape values were decreased, but the increased rearwards freedom on the HR caused an increase in T11/T12 rotation, thus increasing torso extension.

- Max F_{shear} of C0/C1 on C1: 76.492 N
- Max N_{km} : 0.12113
- Max Orientation of T11/T12 : 23.563°
- S-shape measures: -1.3881 min, 0.44777 max

Horizontal and vertical distances travelled by the head geometrical center have also shown an increase with respect to the smaller backset. The results are as follows:

$$\Delta y = -12.91$$

$$\Delta z = -0.45$$

3. Leaned back position with reclined HR position and adjusted characteristics:

In the third simulation, HR's damping and stiffness values were increased to adapt to the new occupant and HR position. As a result, the neck force was increased (in the range of acceptable values), s-shape was also in the reasonable range, and the T11/T12 rotation was decreased.

- Max F_{shear} of C0/C1 on C1: 143.46 N
- Max N_{km} : 0.34773
- Max Orientation of T11/T12 : 20.68°
- S-shape measures: -2.3813 min, 0.44782 max

Horizontal and vertical distances travelled by the head geometrical center have also decreased with respect to the version with lower damping ratio. The results are as follows:

$$\Delta y = -9.85$$

$$\Delta z = -3.66$$

This shows that by measuring the head and upper torso distances via sensors, the head restraint can be adjusted to optimum backset and suitable damping values, thus providing safety in a wider variety of situations.

5. RESULTS AND DISCUSSION

To better evaluate the results of the new HR (head restraint) design and see the advantages of the adaptations, performances of the seat with the new HR design and the original seat model without the changes to the HR were compared. The new HR design was implemented with a damper and optimized for various SB (seatback) angles. For 3 crash pulses, simulation results of both versions are given below.

5.1. Comparison of the Seat's Performance with and without the New HR design

5.1.1. TR16 Test Standards (Low Severity Crash)

Table 5 - Simulation results for TR16 crash pulse with the original car seat design

	Fsh (N)	Ftn (N)	Nkm	Orientation of T11/T12 (degrees)	NDI (S-shape) (degrees)	NIC
SB15	97.946	189.31	0.22612	14.471	Min: -0.25589 Max: 1.179	3.1371
SB20	139.46	160.08	0.34863	20.239	Min: -1.0333 Max: 0.29981	7.0334
SB25	186.93	260.14	0.56132	23.346	Min: -2.2392 Max: 0.22922	10.884
SB30	202.96	176.05	0.66918	23.845	Min: -3.247 Max: 0.24268	15.1420

Table 6 – Simulation results for TR16 crash pulse with the new HR design

	Fsh (N)	Ftn (N)	Nkm	Orientation of T11/T12 (degrees)	NDI (S-shape) (degrees)	NIC
SB15	71.885	117.92	0.16892	16.935	Min: 0 Max: 3.8311	3.5292
SB20	101.22	142.25	0.22022	20.635	Min: -0.52726 Max: 1.1073	6.9160
SB25	108.07	172.89	0.23498	21.795	Min: -3.3587 Max: 0.22624	7.8562
SB30	121.93	175.73	0.24716	20.1	Min: -0.25476 Max: 0.6017	10.387

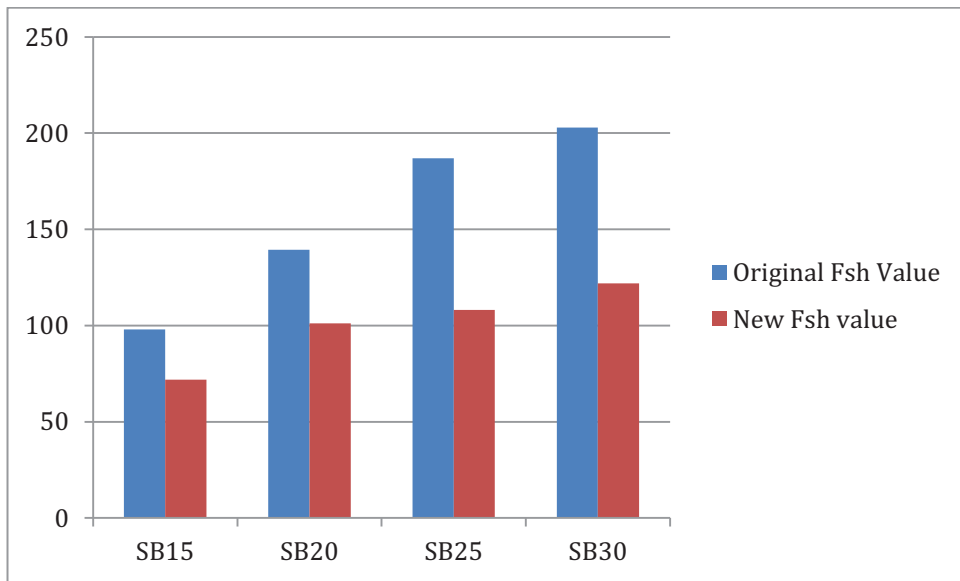


Figure 63 - TR16 Crash Pulse Fsh Comparison

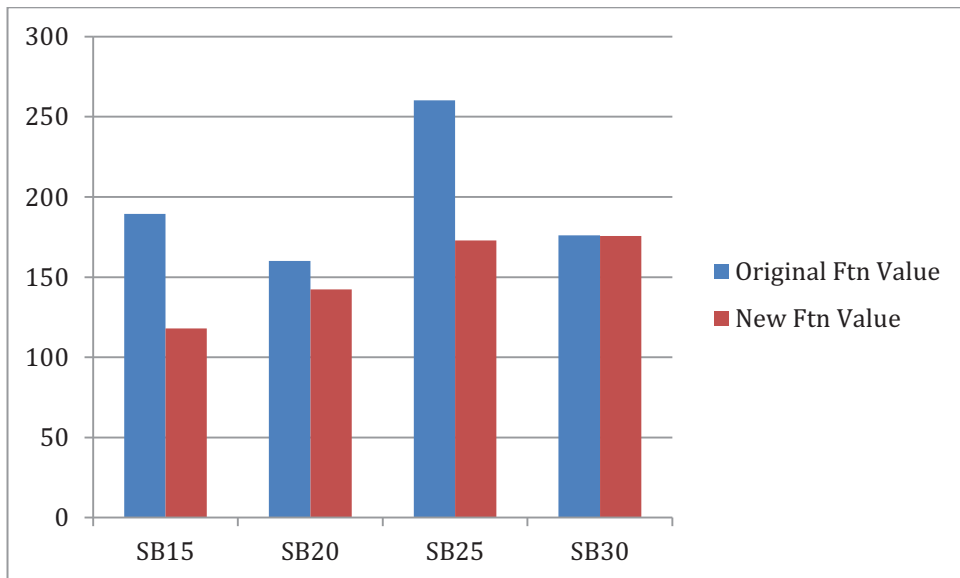


Figure 64 - TR16 Crash Pulse Ftn Comparison

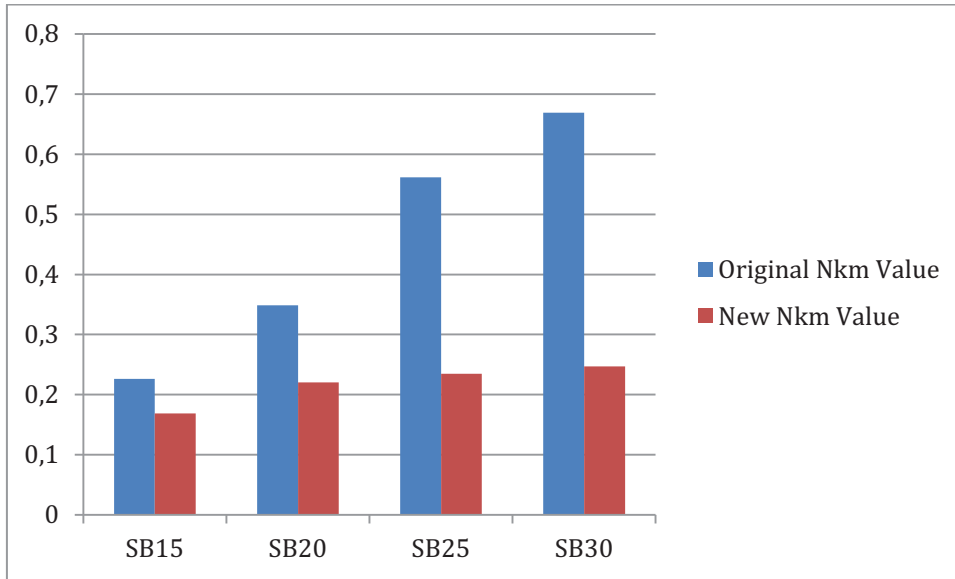


Figure 65 - TR16 Crash Pulse Nkm Comparison

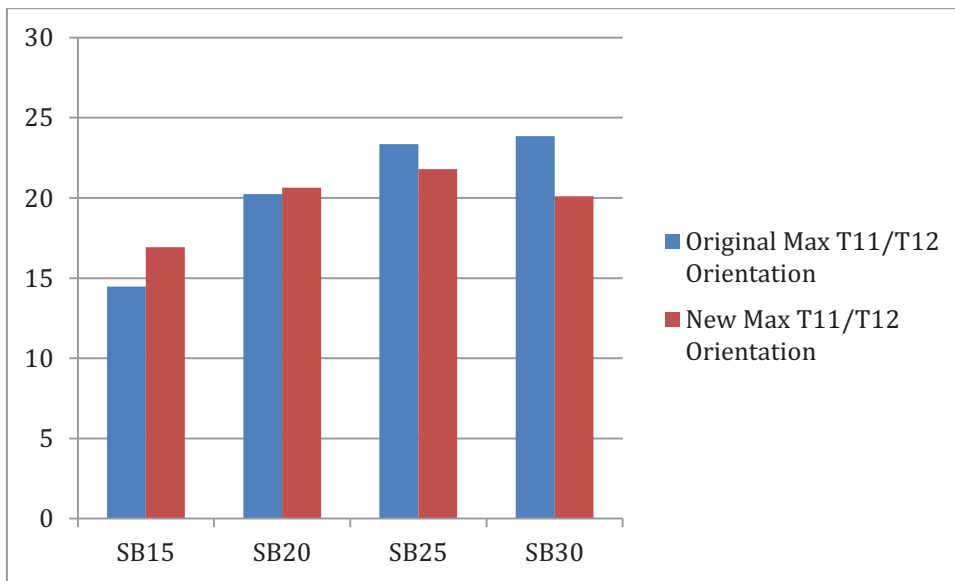


Figure 66 - TR16 Crash Pulse Torso Orientation Comparison

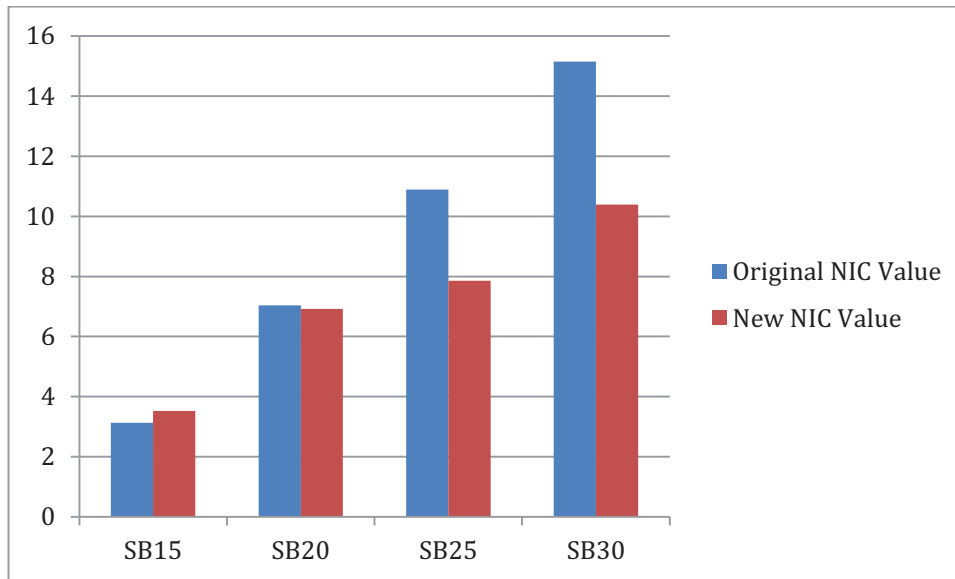


Figure 67 - TR16 Crash Pulse NIC Comparison

Although at lower seatback angles the damping increases the orientation of T11/T12, it can be seen that it greatly reduces the shear and tension forces and improve the Nkm and NIC values. Additionally even though the NDI values have been observed to increase, they are in the acceptable range and overall the new head restraint showed improved results in terms of injury prevention at TR16 crash pulse.

5.1.2. IIWPG Test Standards (Medium Severity Crash)

Table 7 - Simulation results for IIWPG crash pulse with the original car seat design

	Fsh (N)	Ftn (N)	Nkm	Orientation of T11/T12 (degrees)	NDI (S-shape) (degrees)	NIC
SB15	110.52	188.27	0.22638	15.4	Min: -0.7474 Max: 2.1763	3.7909
SB20	118.43	151.18	0.2426	20.665	Min: -0.93047 Max: 0.34961	9.0557
SB25	165.94	216.94	0.48016	24.899	Min: -2.4294 Max: 0.26661	14.3490
SB30	202.74	164.29	0.64629	24.9	Min: -3.3839 Max: 0.28165	14.0910

Table 8 - Simulation results for IIWPG crash pulse with the new HR design

	Fsh (N)	Ftn (N)	Nkm	Orientation of T11/T12 (degrees)	NDI (S-shape) (degrees)	NIC
SB15	46.45	163.62	0.085306	17.231	Min: 0 Max: 3.5084	4.3109
SB20	85.391	182.89	0.12562	21.103	Min: -0.82546 Max: 1.1558	8.9041
SB25	122.95	201.5	0.19311	22.569	Min: -3.3031 Max: 0.26659	11.8850
SB30	130.37	183.28	0.26967	22.418	Min: -4.2109 Max: 0.28161	10.5520

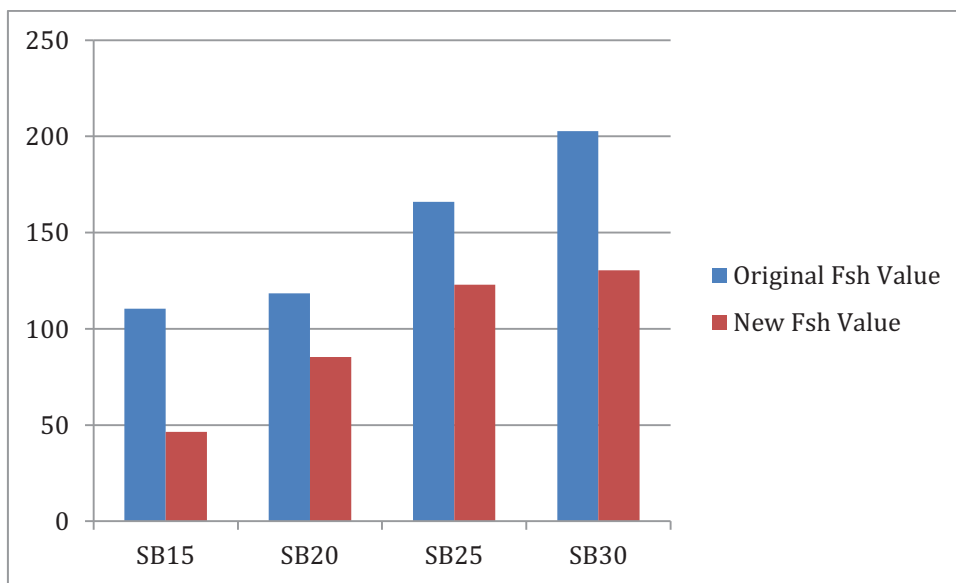


Figure 68 - IIWPG Crash Pulse Fsh Comparison

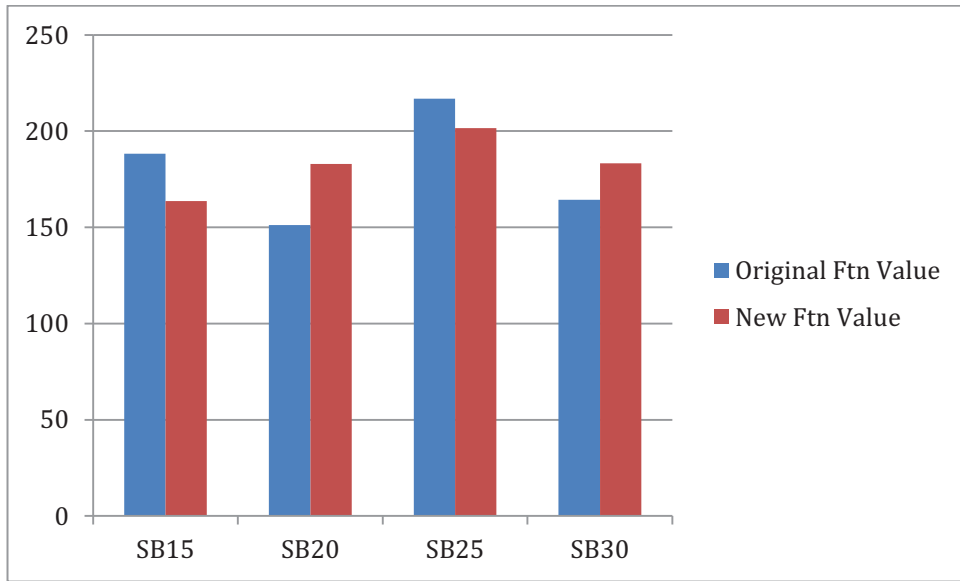


Figure 69 - IIWPG Crash Pulse Ftn Comparison

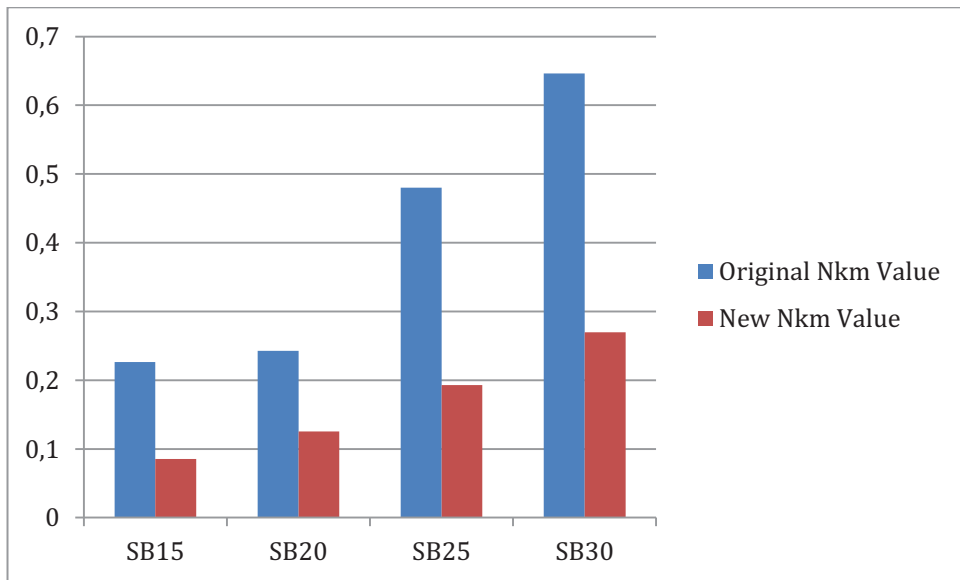


Figure 70 - IIWPG Crash Pulse Nkm Comparison

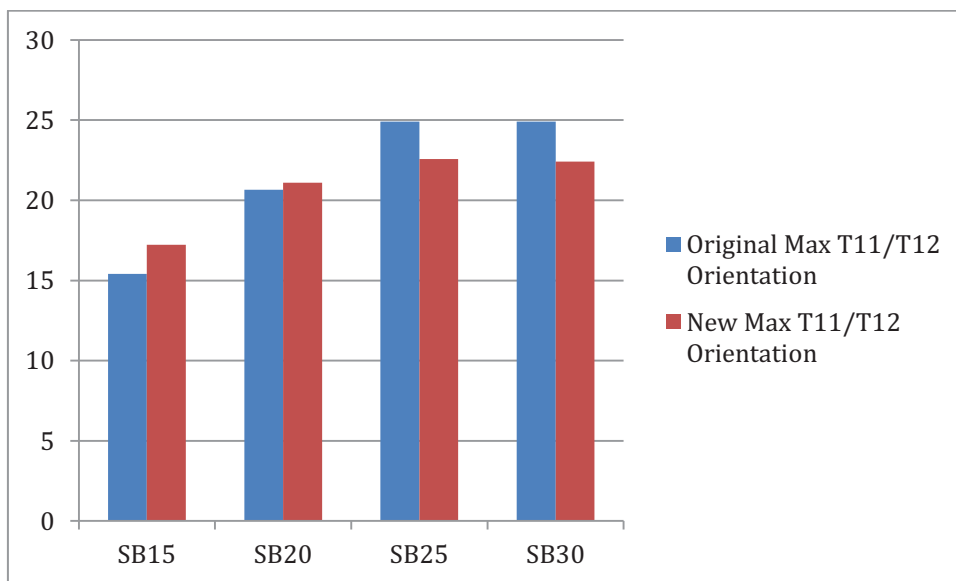


Figure 71 - IIWPG Crash Pulse Torso Orientation Comparison

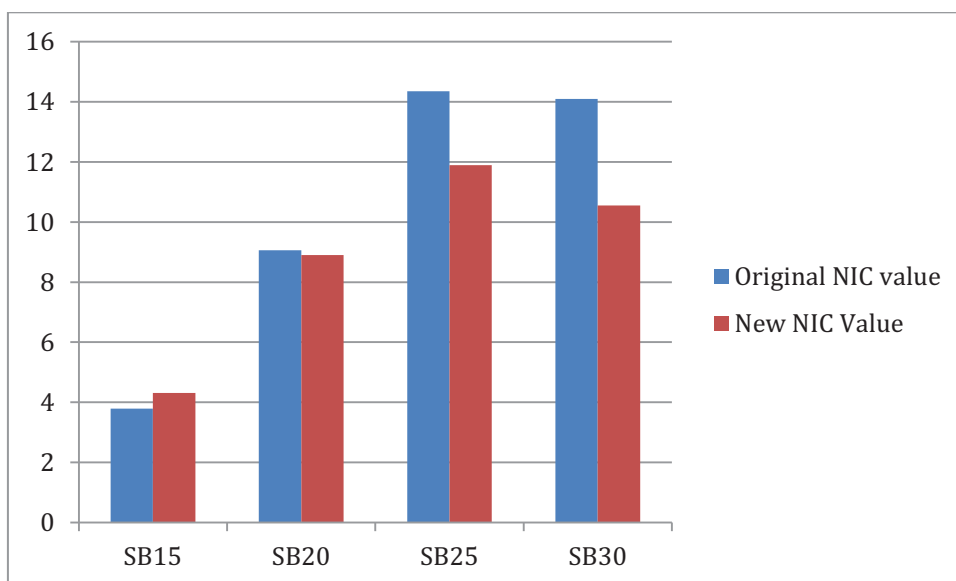


Figure 72 - IIWPG Crash Pulse NIC Comparison

Similarly to the TR16 crash pulse simulations, torso extension showed an increase at lower seatback angles while decreasing at above 20° seatback angles. While the tension force on the upper neck F_{tm} didn't exhibit a clear pattern, the values were in the acceptable range, and shear force F_{sh} was seen to have improved values.

As in the TR16 tests, NIC value was decreased in all 15° seatback angle. Despite increasing the NDI values also exhibit good results.

5.1.3. TR24 Test Standards (High Severity Crash)

Table 9 - Simulation results for TR24 crash pulse with the original car seat design

	Fsh (N)	Ftn (N)	Nkm	Orientation of T11/T12 (degrees)	NDI (S-shape) (degrees)	NIC
SB15	133.83	215.17	0.25485	18.425	Min: -3.0656 Max: 2.2792	6.1743
SB20	160.63	205.31	0.45827	19.119	Min: -5.16 Max: 1.8496	8.4844
SB25	206.78	168.47	0.62395	22.539	Min: -3.7662 Max: 1.3946	14.0080
SB30	197.96	189.66	0.61446	22.586	Min: -3.4353 Max: 3.3111	13.5680

Table 10 - Simulation results for TR24 crash pulse with the new HR design

	Fsh (N)	Ftn (N)	Nkm	Orientation of T11/T12 (degrees)	NDI (S-shape) (degrees)	NIC
SB15	117.75	217.71	0.27736	20.142	Min: 0 Max: 3.1768	4.5222
SB20	137.47	150.94	0.42463	19.987	Min: -3.1353 Max: 1.8304	8.6138
SB25	121.8	193.22	0.4596	21.746	Min: -4.8763 Max: 0.21775	11.4970
SB30	135.55	183.39	0.49507	21.687	Min: -4.6082 Max: 1.4975	10.0560

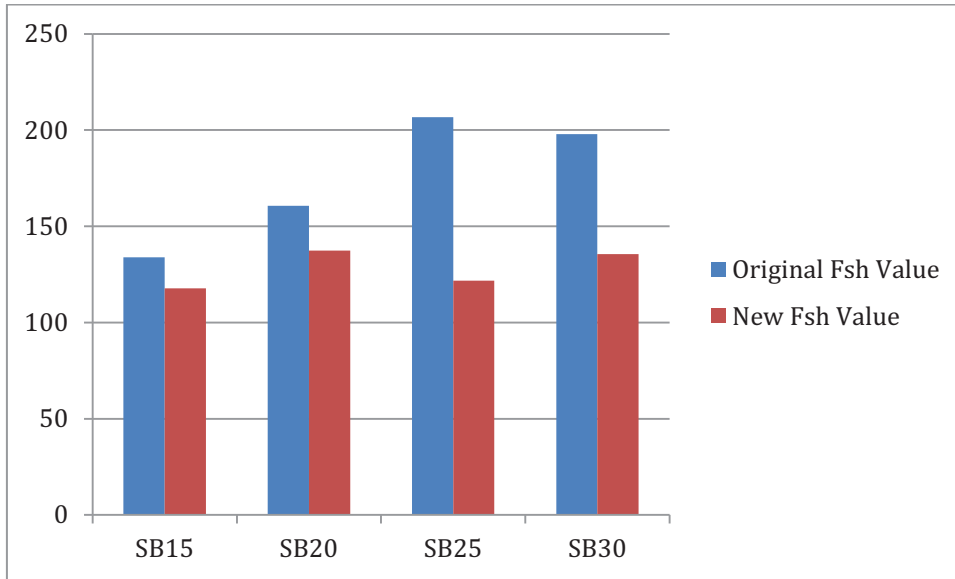


Figure 73 - TR24 Crash Pulse Fsh Comparison

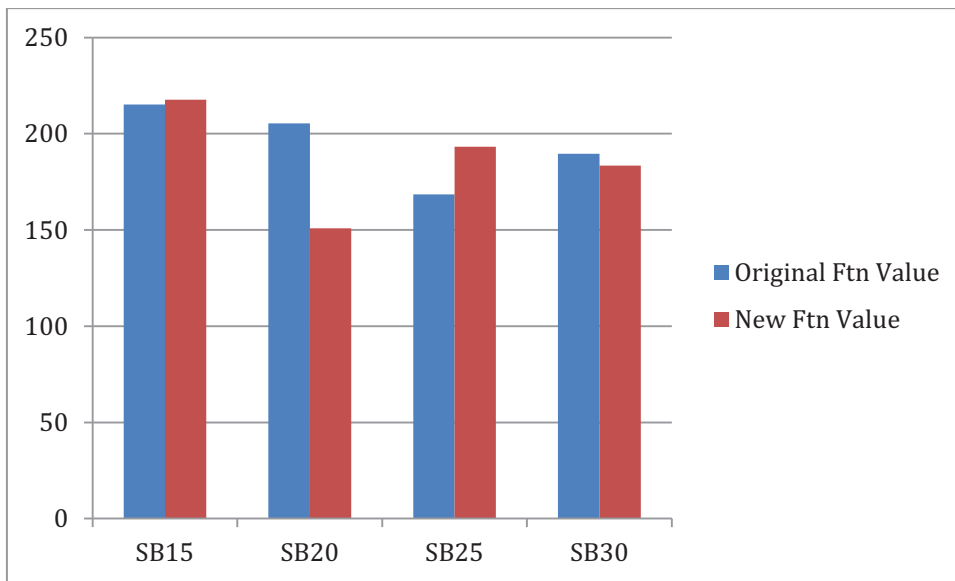


Figure 74 - TR24 Crash Pulse Ftn Comparison

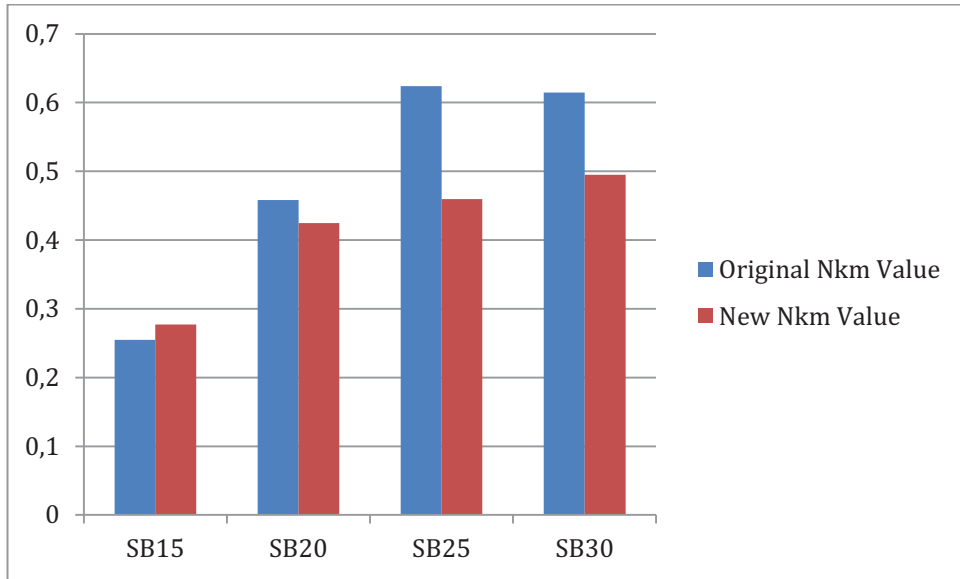


Figure 75 - TR24 Crash Pulse Nkm Comparison

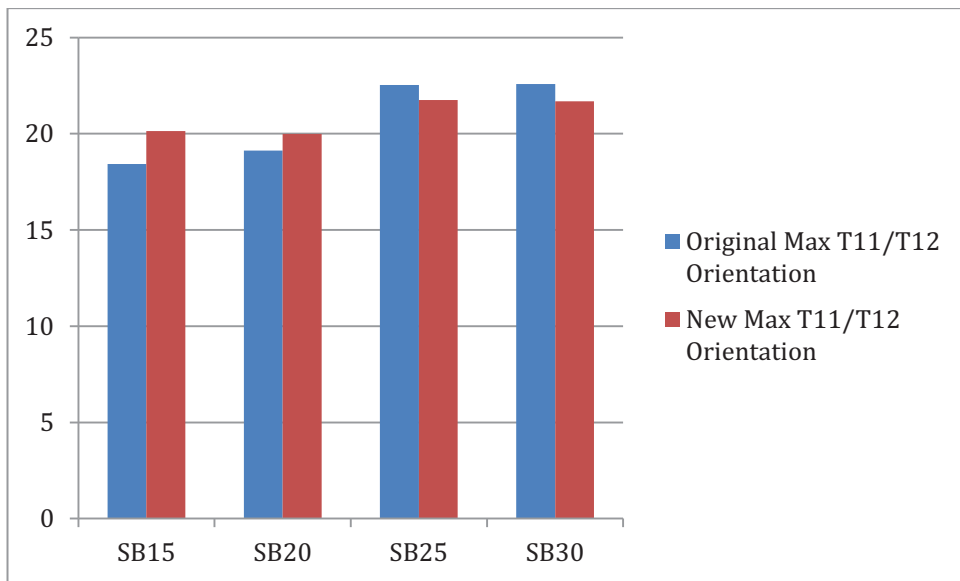


Figure 76 - TR24 Crash Pulse Torso Orientation Comparison

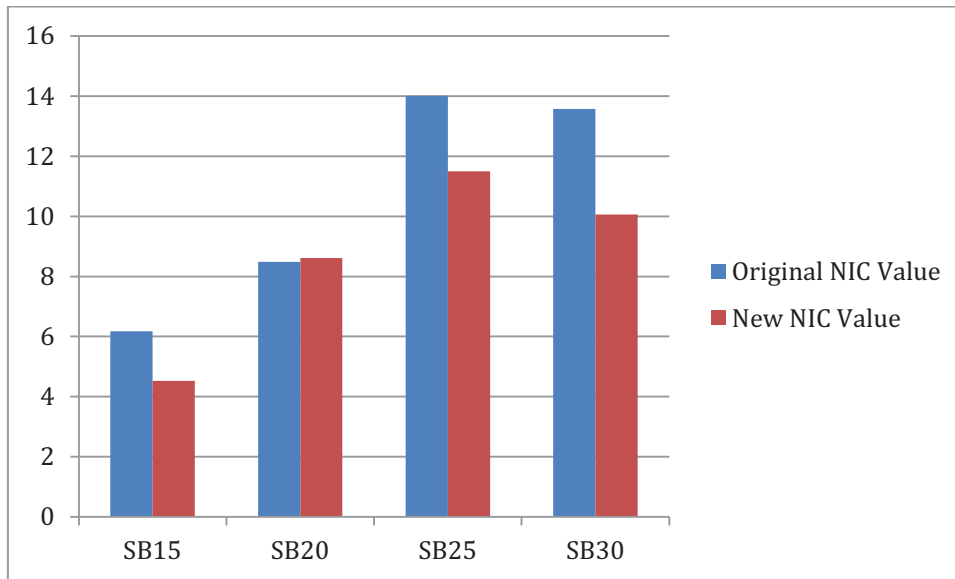


Figure 77 - TR24 Crash Pulse NIC Comparison

For TR24 crash pulse, Nkm values along with torso extension were increased below 20° while showing safer results at higher seatback angles. All NIC values except at 20° were improved for the new HR design with respect to standard HR simulations. While NDI and Ftn values didn't show a clear pattern of increase or decrease compared to the standard HR, Fsh values were greatly improved and overall injury risk was decreased at all angles.

5.2. Discussion

In the new head restraint design, the damping ratio and stiffness were optimized to give improved results across all seatback positions. To do that, a variable damping ratio was used. While at higher seatback angles lower damping ratios were used, the higher damping ratios were used for lower seatback angles. The reason for that was that at higher seatback angles the HR (head restraint) was closer to the head wrt seatback position, and the sudden impact without early support from backset and sufficient energy absorption on the head caused protrusion on the neck (pushing the head forward) and increased S-shape values. On the other hand, decreasing the damping ratio further, although reducing neck forces, also reduced the necessary support for the head and resulted in extension of the neck and increased torso extension.

As for the lower seatback angles, since the HR was already aligned with seatback or behind the seatback, further recline of the HR took away from head support and caused retraction and extension on the neck, also increasing S-shape values. Increasing the damping ratio further also increased the neck forces F_{sh} and F_{tn} . For improved results for all related injury criteria, optimized damping values were chosen for each seatback angle.

On the comparison of experiment and simulation values on torso extension, it was seen that although the simulation values were close to experiment values, the experiment values were seen to be a bit higher in general. The results for that are considered to be as follows:

- People can seat in very different positions. In the closer inspection of the experiment pictures, many people were seen to have sat at more reclined positions. It is thought that since a HR was absent in the car seat used in the experiments, people were more comfortable sitting reclined than they would be with a HR. Also outside of the driving environment and without the reasons like seeing the road above the dashboard, some people sat more like they would in a passenger seat. This sitting position reduces the movement freedom of the torso and reduces the torso extension.
- Since there wasn't a force pushing (or pulling) them towards the seatback, some people may not have pushed their torso to the seatback as much as they could.
- As can be seen in the numerical data below, range of motion of human vertebrae can vary greatly from person to person (Figure 78). This variation can affect the results of an experiment done with human subjects.

Vertebrae	Combined flexion–extension ROM (deg)
T1/T2	3–5 (4)
T2/T3	3–5 (4)
T3/T4	2–5 (4)
T4/T5	3–5 (4)
T5/T6	2–7 (4)
T6/T7	3–8 (5)
T7/T8	3–8 (6)
T8/T9	3–8 (6)
T9/T10	3–8 (6)
T10/T11	4–14 (9)
T11/T12	6–20 (12)
T12/L1	6–20 (12)
L1/L2	5–16 (12)
L2/L3	8–18 (14)
L3/L4	6–17 (15)
L4/L5	9–21 (16)
L5/S1	10–24(17)

Figure 78- The variation in the combined flexion– extension range of motions for voluntary sagittal rotations of the human thoracic and lumbar vertebrae [52]

6. CONCLUSION

- With the new HR (head restraint) design that utilizes a rotating HR post and damping, it was aimed to reduce the risk of injury at rear end accidents. Through optimization of backset and damping values at various seatback angles, the forces affecting the head and neck were reduced. By reducing the torso extension at T11/T12 joint at higher seatback angles, the risk of back injury and lower back pain were also reduced. Keeping the NDI and NIC at lower values also reduced the risk of whiplash injury. Therefore it was managed to design a HR concept that is both comfortable and safe at a variety of seatback angles.
- Although the study was done on a variety of seatback angles, typical seating positions were used for each variation. Sitting position is one of the major factors affecting injury risk unrelated to the seat's design. It is suggested for occupants to use the seat at lower seatback angles, use seatbelts adjust their HR heights properly and avoid leaning forward or sideways as much as possible regardless of seating position in the car and design of the car seat.
- The study on the safety of car seat in a variety of seatback angles is new in literature and there hasn't been a work that focuses on optimizing the seat at different seatback angles.
- The study on torso extension limits on a car seat is also new. A similar study wasn't found in the literature.
- For future work, the design of the HR can be improved for different scenarios. The HR design in this study was optimized for 50th percentile) (average size) male model in a typical driving position. Further simulations can be done for occupants of different postures and for different sitting positions. The new damping values can be optimized for occupants of smaller or greater postures, and passenger seating positions.

7. REFERENCES

- [1] Carlsson, A., “Addressing Female Whiplash Injury Protection - A Step Towards 50th Percentile Female Rear Impact Occupant Models”, Department of Applied Mechanics, Chalmers University of Technology, Gothenburg, Sweden, **2012**
- [2] Whiplashkommissionen Sweden, “The Whiplash Commission Final Report”, ISBN 91-975655-4-7, **2005**
- [3] Jakobsson, L., Lundell, B., Norin, H., Isaksson-Hellman, “I. WHIPS-Volvo’s Whiplash Protection Study. Accident Analysis & Prevention”, **2000**, 32:307–19
- [4] Matsubayashi K., Yamada Y., MotomiIyoda, Koike S., Kawasaki T., Tokuda M., “Development of Rear Pre-Crash Safety System For Rear-End Collisions”, Toyota Motor Corporation, Japan, 07-0146
- [5] Acar M., Clark S. J., Crouch R., “Smart head restraint system”, School of Mechanical and Manufacturing Engineering, Loughborough University, Leicestershire, LE11 3TU, UK
- [6] Giorgetta, M. Gobbi, G.Mastinu, **2009**, “Developing a ‘no-whiplash’ headrest”, Int. J. Vehicle Systems Modelling and Testing, Vol. 4, No. 3
- [7] AAAM, Association for the Advancement of Automotive Medicine, **1990**, The Abbreviated Injury Scale – **1990** Revision, Des Plaines, Illinois, USA
- [8] Spitzer, W.O., Skovron, M.L., Salmi, L.R., Cassidy, J.D., Duranceau, J., Suissa, S., and Zeiss, E., **1995**, Scientific monograph of the Quebec task force on whiplash-associated disorders: redefining ‘whiplash’ and its management. Spine, 20(8S)
- [9] Krafft, M., Kullgren, A., Ydenius, A., and Tingvall, C., **2001**, The Correlation Between Crash Pulse Characteristics and Duration of symptoms to the neck – Crash recording in real life rear impacts ‘In: Proc. of 17th ESV Conference’, Amsterdam, The Netherlands, Paper No 174.
- [10] Krafft, M., Kullgren, A., Malm, S., and Ydenius, A., **2005**, Influence of Crash Severity on Various Whiplash Injury Symptoms: A Study Based on Real-Life Rear-End Crashes with Recorded Crash Pulses ‘In: Proc. of 19th ESV Conference’, Washington DC, USA, Paper No 05-0363-O.
- [11] Yoganandan, N., Pintar, F.A., and Gennarelli, T.A., **2002**, Biomechanical Mechanisms of Whiplash Injury, Traffic Injury Prevention 3(2), 98-104
- [12] Boström O, Svensson MY, Aldman B, Hansson HA, Håland Y, Lövsund P, Seeman T, Suneson A, Sälsjö A, Örtengren T **1996** A New Neck Injury Criterion Candidate - Based on Injury Findings in the Cervical Spinal Ganglia after Experimental Neck Extension Trauma, Proc. IRCOBI Conf., Dublin (Ireland), pp. 123–136
- [13] Aldman B **1986** An Analytical Approach to the Impact Biomechanics of Head and Neck Injury, Proc. 30th Annual AAAM, Montreal, Quebec (Canada), pp. 446–454

- [14] Svensson MY, Aldman B, Lövsund P, Hansson HA, Sunesson A, Seeman T, Örtengren T, **1993a**, Pressure Effects in the Spinal Canal during Whiplash Extension Motion - A Possible Cause of Injury to the Cervical Spinal Ganglia, Proc. IRCOBI Conf., Eindhoven (The Netherlands), pp. 189–200
- [15] Örtengren T, Hansson HA, Lövsund P, Svensson MY, Suneson A, Saljo A, **1996**, Membrane Leakage in Spinal Ganglion Nerve Cells Induced by Experimental Whiplash Extension Motion: A Study in Pigs, J. Neurotrauma, Vol. 13, pp. 171–180
- [16] Svensson M Y, **2000** Comparison of car seats in low speed rear-end impacts using the BioRID dummy and the new neck injury criterion (NIC), Accid. Anal. Prev., Vol 32, No. 2, pp. 321–328
- [17] Kullgren A, Eriksson L, Boström O, Krafft M, **2003**, Validation of neck injury criteria using reconstructed real-life rear-end crashes with recorded crash pulses, Proc. 18th ESV Conf. (344), Nagoya (Japan), pp. 1–13
- [18] Linder A, Avery M, Kullgren A, Krafft M, **2004**, Real-world rear impacts reconstructed in sled tests, Proc. IRCOBI Conf., Graz (Austria), pp. 233–244
- [19] DeSantisKlinch K, Saul RA, Auguste G, Backaitis S, Kleinberger M, **1996** Techniques for Developing Child Dummy Protection Reference Values, NHTSA Docket No. 74–14
- [20] Kleinberger M, Sun E, Eppinger R, Kuppa S, Saul R, **1998**, Development of Improved Injury Criteria for the Assessment of Advanced Automotive Restraint Systems, NHTSA report
- [21] Schmitt K-O, Niederer PF, Muser MH, Walz F, **2004**, Trauma Biomechanics: Introduction to Accidental Injury, Springer-Verlag Berlin Heidelberg New York, ISBN 3-540-22299-5
- [22] Schmitt K-U, Muser M, Walz F, Niederer P, **2002**, Nkm – a proposal for a neck protection criterion for low speed rear-end impacts, Traffic Inj. Prev., Vol. 3, No. 2, pp. 117–126
- [23] Panjabi MM, Wang J-L, Delson N, **1999**, Neck Injury Criterion Based on Intervertebral Motions and its Evaluation Using an Instrumented Neck Dummy, Proc. IRCOBI Conf., Sitges (Spain) pp. 179–190
- [24] Viano D, Davidsson J, **2001**, Neck Displacements of Volunteers, BioRID P3 and Hybrid III in Rear Impacts: Implications to Whiplash Assessment by a Neck Displacement Criterion (NDC), Proc. IIWPG/IRCOBI Symposium, Isle of Man (UK)
- [26] RCAR-IIWPG seat/head restraint evaluation protocol, International Insurance Whiplash Prevention Group (IIWPG), **2008**
- [27] Himmetoglu, S. An evaluation of passive head-restraints with different stiffness and energy dissipation properties for whiplash mitigation. In Proceedings of the 7th International Expert Symposium on Accident Research (ESAR **2016**), Hannover, Germany, 9-10 June 2016, paper 1-03-02, 15pp.

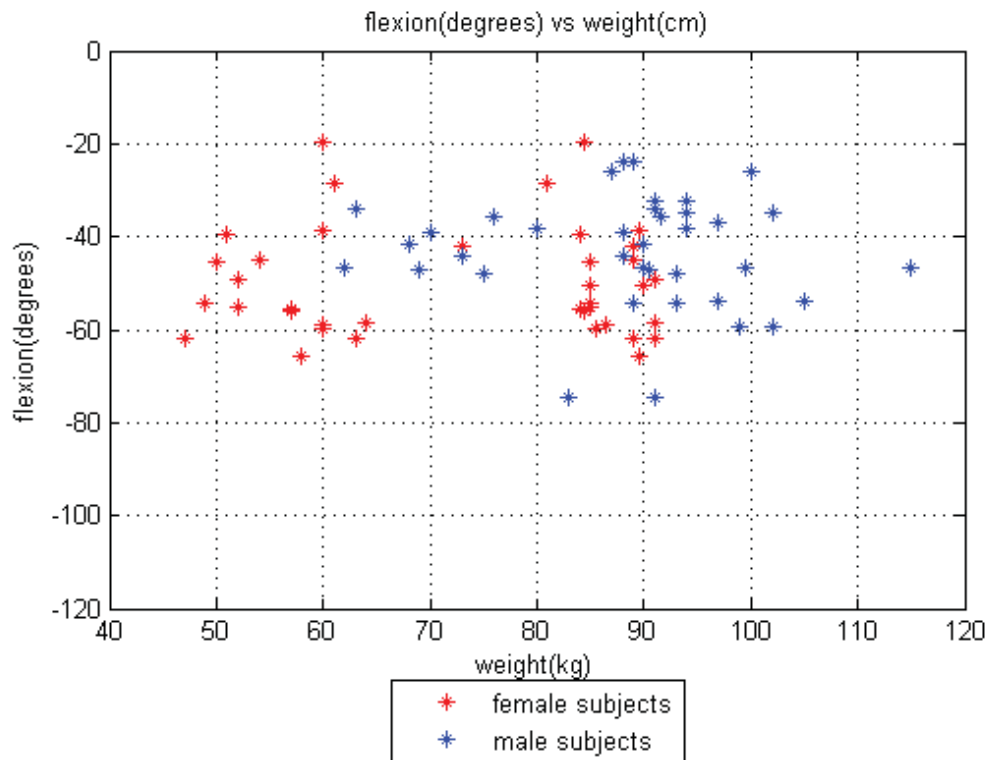
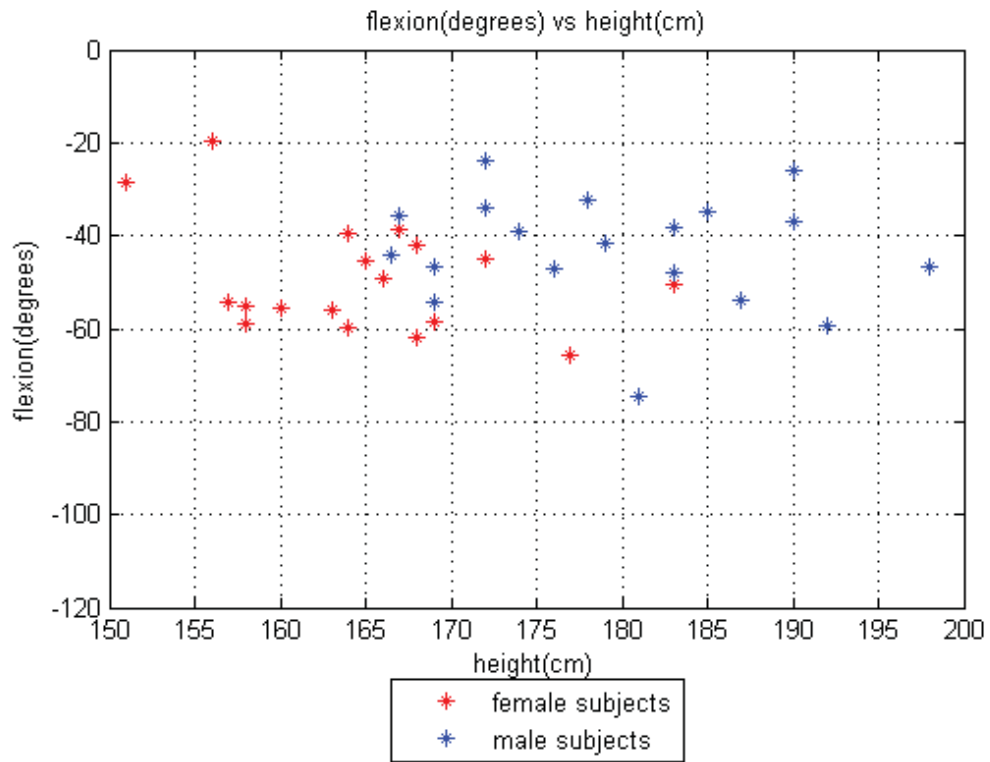
- [27] Heitplatz F, Sferco R, Tay P, Reim J, Kim A, Prasad P, **2003**, An Evaluation of Existing and Proposed Injury Criteria with Various Dummies to Determine Their Ability to Predict the Levels of Soft Tissue Neck Injury Seen in Real World Accidents, Proc. 18th ESV Conf., Nagoya (Japan), pp. 1–8
- [28] Linder, A., Avery, M., Krafft, M., and Kullgren, A., **2003**, Change of Velocity and Crash Pulse Characteristics in Rear Impacts: Real-World Data and Vehicle Tests ‘In: Proc. of 18th ESV Conference’, Nagoya, Japan, Paper No 285.
- [29] Hell, W., Langwieder, K., and Walz, F., **1998**, Reported soft tissue neck injuries after rear-end car collisions ‘In: Proc. of 1998 International IRCOBI Conference’, Göteborg, Sweden, 261-274.
- [30] Carlsson G, Nilsson S, Nilsson-Ehle A, Norin H, Ysander L, Örtengren R, **1985**, Neck Injuries in Rear End Car Collisions; Biomechanical Considerations to Improve Head Restraints, Proc. IRCOBI Conf., Göteborg (Sweden), pp. 277–289
- [31] Krafft M, Kullgren A, Lie A, Tingvall C, **2003**, The Risk of Whiplash Injury in the Rear Seat Compared to the Front Seat in Rear Impacts, Traffic Inj. Prev., Vol. 4, No. 2, pp. 136–140
- [32] Lundell B, Jakobsson L, Alfredsson B, Jernström C, Isaksson-Hellman I, **1998**, Guidelines for and the Design of a Car Seat Concept for Improved Protection Against Neck Injuries in Rear-End Car Impacts, Proc. Int. Congress and Exposition Detroit, Michigan (USA), Society of Automotive Engineers (SAE 980301), Warrendale, PA (USA)
- [33] Temming J, Zobel R, **1998**, Frequency and Risk of Cervical Spine Distortion Injuries in Passenger Car Accidents: Significance of Human Factors Data, Proc. IRCOBI Conf., Göteborg (Sweden), pp. 219–233
- [34] Minton R, Murray P, Pitcher M, Galasko CSB, **1997**, Causative Factors in Whiplash Injury: Implications for Current Seat and Head Restraint Design, Proc. IRCOBI Conf., Hanover (Germany), pp. 207–222
- [35] Jakobsson, L, **2004b**, Field Analysis of AIS1 Neck Injuries in Rear-End Car Impacts-Injury Reducing Effect of the WHIPS Seat, J. of Whiplash & Related Disorders, Vol. 3, No. 2, pp. 37–54
- [36] Sturzenegger M, Radanov BP, Di Stefano G, **1995**, The effect of accident mechanisms and initial findings on the long-term course of whiplash injury, J. Neurol., Vol. 242, No. 7, pp. 443–449
- [37] Farmer CM, Wells JK, Werner JV, **1999**, Relationship of Head Restraint Positioning to Driver Neck Injury in Rear-End Crashes, Accid. Anal. Prev., Vol. 31, No. 6, pp. 719–728
- [38] Szabo, T.J., **2000**, Influence of Seat Properties on Occupant Kinematics and Injury Potential in Low-Speed Rear Impacts, ‘In: Frontiers in Whiplash Trauma’, edited by Yoganandan, N., and Pintar, F.A., IOS Press, Amsterdam, 348-371.

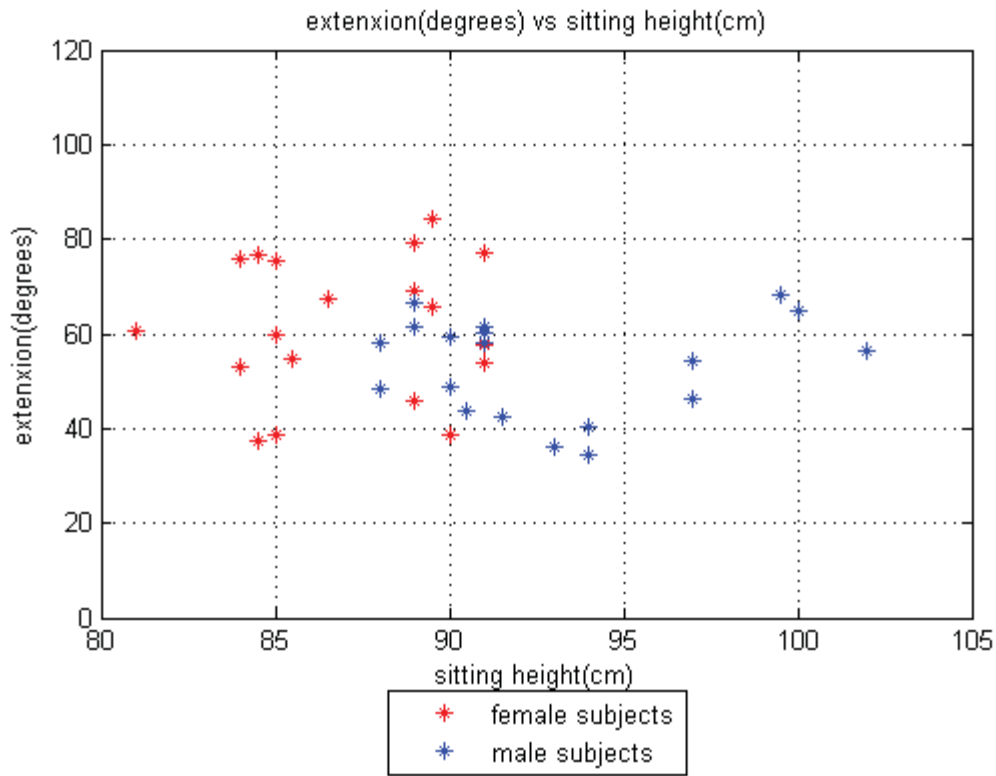
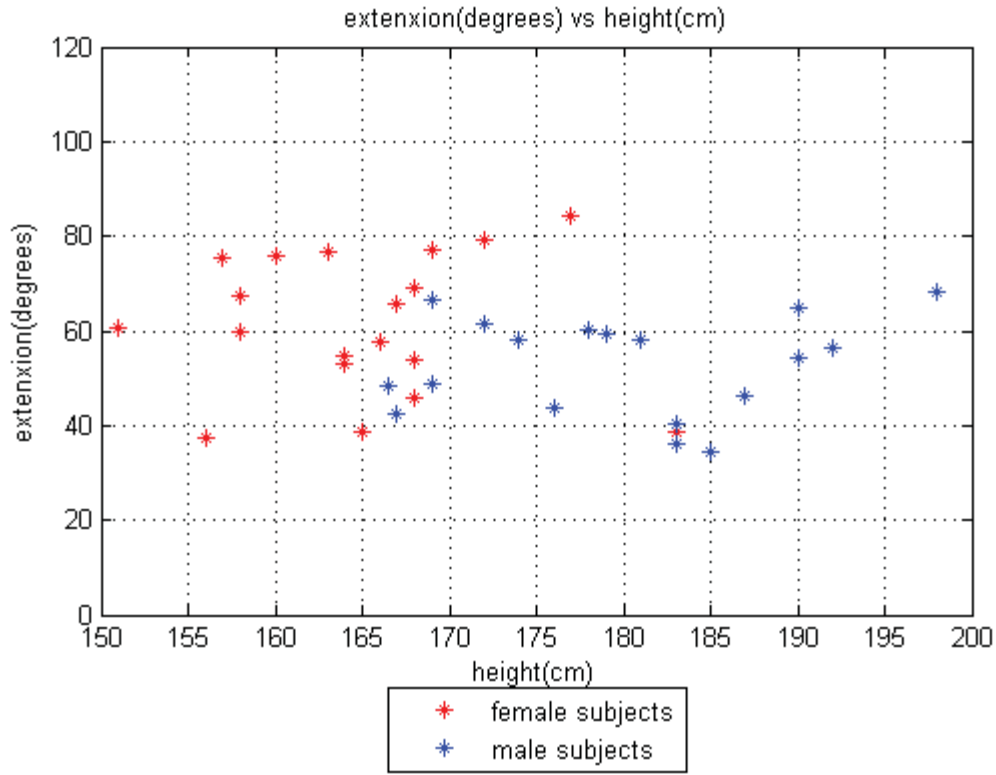
- [39] Parkin, S., Mackay, G.M., Hassan, A.M., and Graham, R., **1995**, Rear End Collisions and Seat Performance - To Yield or Not to Yield 'In: Proc. of the 39th Annual AAAM Conference', Vol. 4, Chicago, USA, 231-244.
- [40] Viano, D.C., **2003a**, Seat Properties Affecting Neck Responses in Rear Crashes: A Reason Why Whiplash Has Increased, *Traffic Injury Prevention* 4(3), 214-227.
- [41] Muser, M.H., Walz, F.H., and Schmitt, K.-U., **2002**, Injury Criteria Applied to Seat Comparison Tests, *Traffic Injury Prevention* 3(3), 224-232.
- [42] Romilly, D.P., and Skipper, C.S., **2005**, Seat Structural Design Choices and the Effect on Occupant Injury Potential in Rear End Collisions, SAE 2005-01-1294, Society of Automotive Engineers, Warrendale, PA
- [43] Viano, D.C., **2002**, Role of the Seat in Rear Crash Safety, Society of Automotive Engineers, Warrendale, PA
- [44] IIHS, **2005**, Insurance Institute for Highway Safety-Status Report, 40(2), 1-5.
- [45] IIWPG, **2006**, International Insurance Whiplash Prevention Group, RCAR-IIWPG Seat/Head Restraint Evaluation Protocol, Version 2.5
- [46] Latchford, J., Chirwa, C., Chen, T., and Mao, M., **2004**, The relationship of seat backrest angle of inclination and neck injury in low velocity rear impacts 'In: Proc. of ICrash 2004 Conference', San Francisco, USA, Paper No 2004-90.
- [47] Szabo, T.J., Voss, D.P., and Welcher, J.B., **2003**, Influence of Seat Foam and Geometrical Properties on BioRID P3 Kinematic Response to Rear Impacts, *Traffic Injury Prevention* 4(4), 315-323.
- [48] Watanabe, Y., Ichikawa, H., Kayama, O., Ono, K., Kaneoka, K., and Inami, S., **2000**, Influence of seat characteristics on occupant motion in low-speed rear impacts, *Accident Analysis and Prevention* 32(2), 243-250
- [49] Kaneko, N., Wakamatsu, M., Fukushima, M., and Ogawa, S., **2004**, Study of BioRID II Sled Testing and MADYMO Simulation to Seek the Optimized Seat Characteristics to Reduce Whiplash Injury, SAE 2004-01-0336, Society of Automotive Engineers, Warrendale, PA
- [50] Jakobsson, L., Lindman, M., Björklund, M, Victor, T., "Rear-End Impact – Crash Prevention and Occupant Protection", IRCOBI Conference , **2015**, IRC-15-90
- [51] Kolich M., Occupant Preferred Back Angle Relative to Head Restraint Regulations, **2010-01-0779**
- [52] Himmetoglu, S., Acar, M., Bouazza-Marouf, K., and Taylor, A. J. A multibody human model for rear-impact simulation. *Proc. IMechE, Part D: J. Automobile Engineering*, **2009**, 223(5), 623-638. DOI: 10.1243/09544070JAUTO985
- [53] Himmetoglu, S., Acar, M., Taylor, A. J., and Bouazza-Marouf, K. A multi-body head-and-neck model for simulation of rear impact in cars. *Proc. IMechE, Part D: J. Automobile Engineering*, **2007**, 221(5), 527-541. DOI: 10.1243/09544070JAUTO467

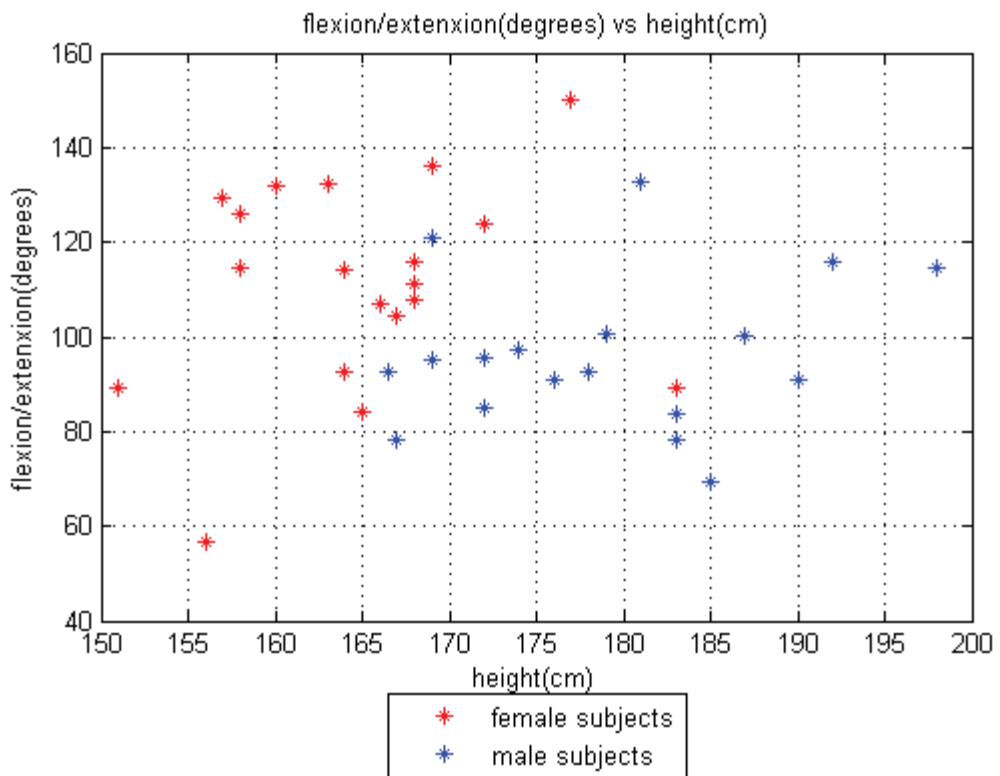
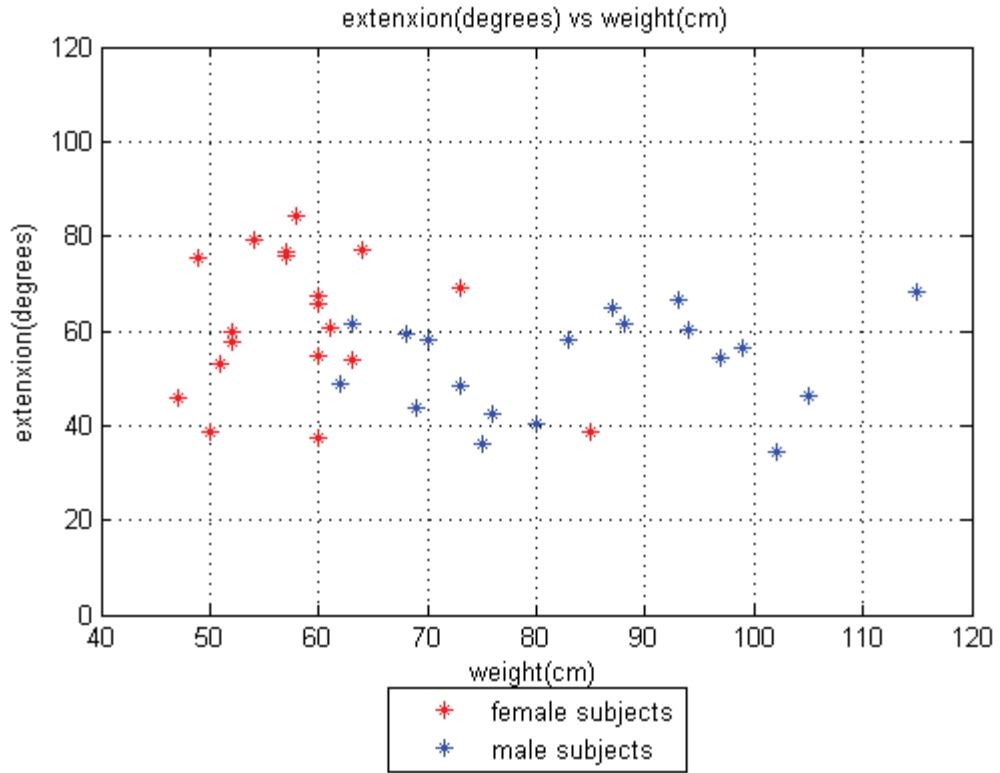
- [54] Himmetoglu, S. An adaptive car-seat to mitigate whiplash in rear impacts. In Proceedings of the 21st International Scientific Conference Transport Means 2017, Juodkrante, Lithuania, 20-22 September **2017**, pp. 32-38, ISSN 2351-7034.
- [55] Himmetoglu, S., Acar, M., Bouazza-Marouf, K., and Taylor, A. J. Car-seat design to improve rear-impact protection. Proc. IMechE, Part D: J. Automobile Engineering, **2011**, 225(4), 441-459. DOI: 10.1177/2041299110393188
- [56] Himmetoglu, S. An evaluation of passive head-restraints with different stiffness and energy dissipation properties for whiplash mitigation. In Proceedings of the 7th International Expert Symposium on Accident Research (ESAR 2016), Hannover, Germany, 9-10 June **2016**, paper 1-03-02, 15pp.
- [57] D C Viano, Role of the seat in rear crash safety, Society of Automotive Engineers, Warrendale, PA, USA, **2002**.)
- [58] Gordon, C.C., Churchill, T., Clauser, C.E., Bradtmiller, B., McConville, J.T., Tebbetts, I., and Walker, R.A. Anthropometric Survey of U.S. Army Personnel: Methods and Summary Statistics, Final Report, Yellow Springs, Ohio, **1989**
- [59] McCaffrey, L., LeFebvre, R., Defoyd, B., Directional Preference Protocol: Centralizing Neck, Shoulder and Arm Pain, WSCC Clinics Protocol, Western States Chiropractic College, Portland, Oregon, **2008**

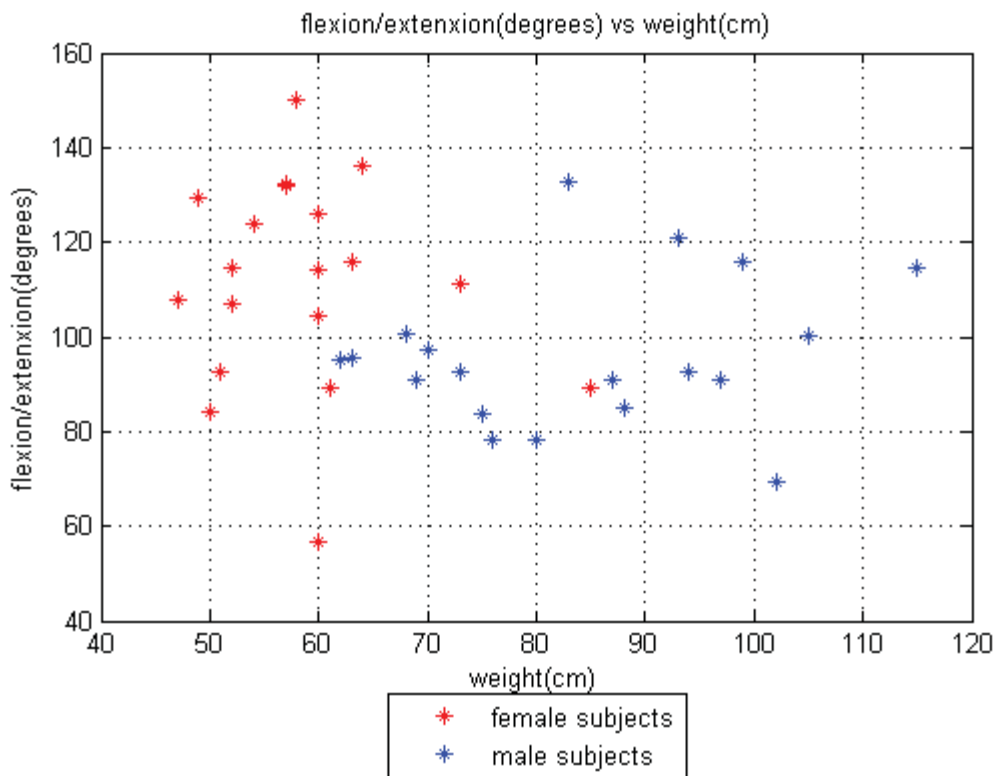
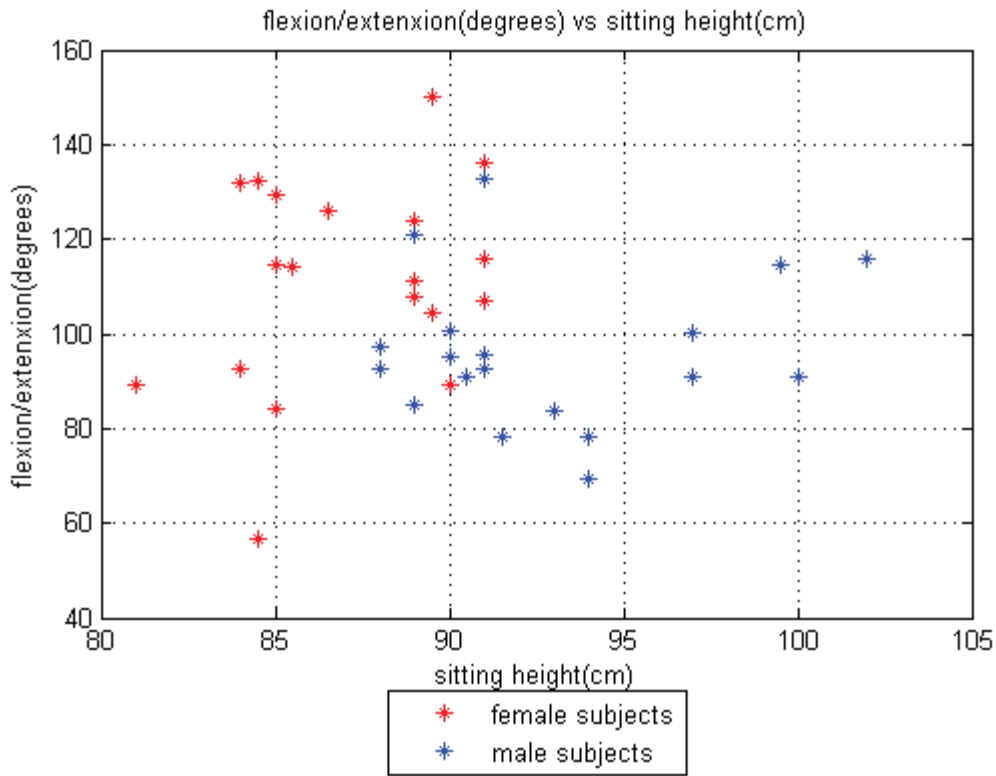
APPENDIX

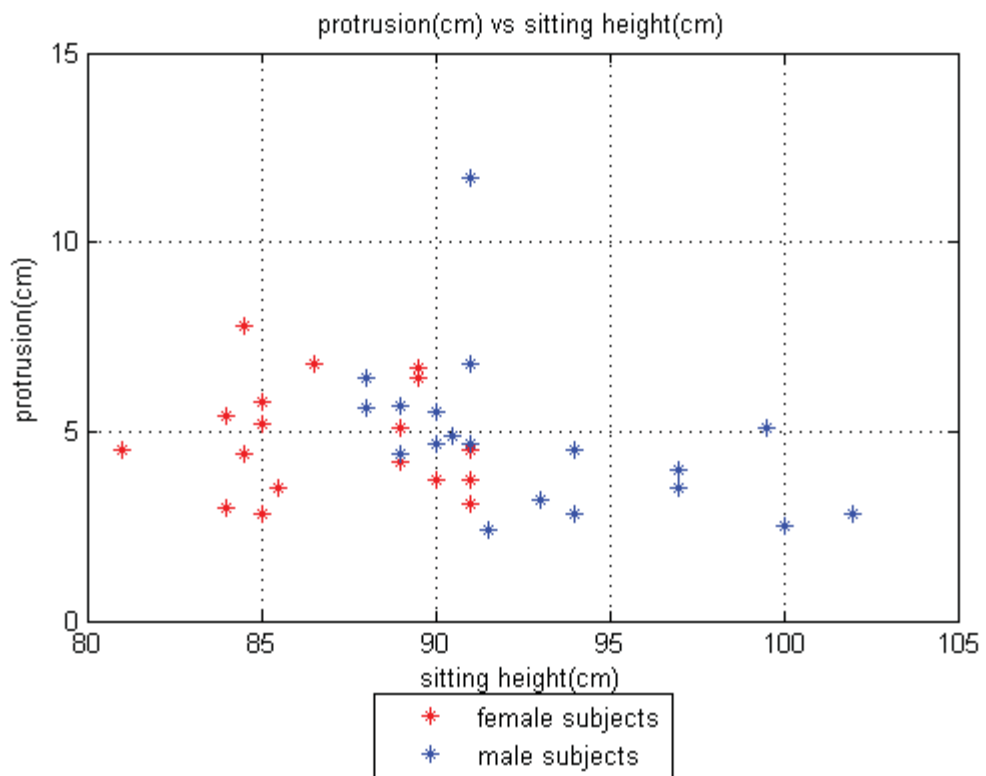
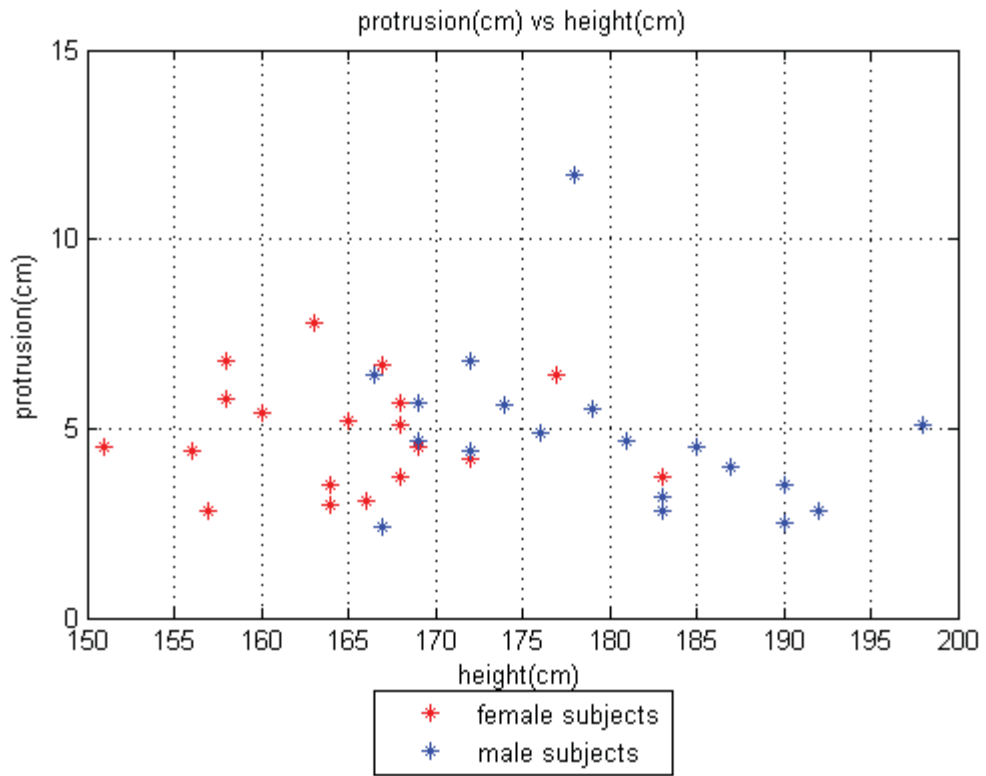
APPENDIX 1 – RANGE OF MOTION STUDY OF NECK

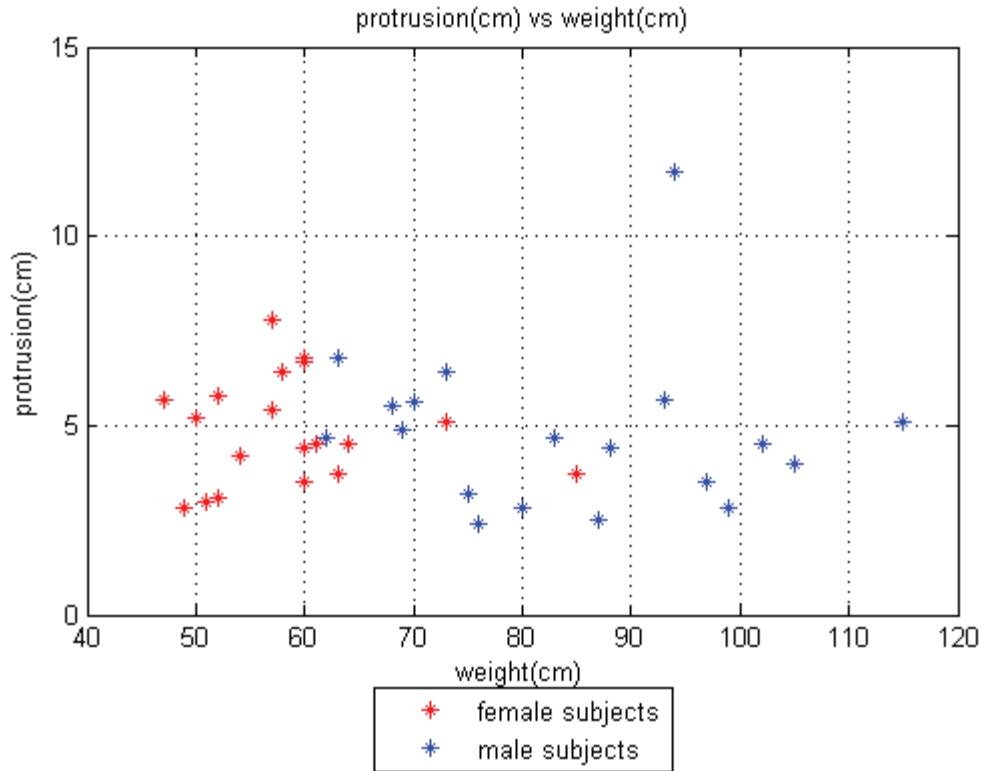












On the closer study of resulting graphs, it can be seen that height and sitting height doesn't have a clear relation to extension or flexion. Although on total neck ROM regarding flexion + extension, female subjects seemed to have a higher average than male subjects. The variation of height, sitting height and gender also didn't seem to have an effect on protrusion. Weight also didn't have effect on neck ROM measured from the experiment.



HACETTEPE UNIVERSITY
GRADUATE SCHOOL OF SCIENCE AND ENGINEERING
THESIS ORIGINALITY REPORT

HACETTEPE UNIVERSITY
GRADUATE SCHOOL OF SCIENCE AND ENGINEERING
TO THE DEPARTMENT OF MECHANICAL ENGINEERING

Date: 16/07/2019

Thesis Title / Topic: Smart Car Seat Design for Safety and Comfort

According to the originality report obtained by my thesis advisor by using the *Turnitin* plagiarism detection software and by applying the filtering options stated below on 16/07/2019 for the total of 79 pages including the a) Title Page, b) Introduction, c) Main Chapters, d) Conclusion sections of my thesis entitled as above, the similarity index of my thesis is 6 %.

Filtering options applied:

1. Bibliography/Works Cited excluded
2. Quotes included
3. Match size up to 5 words excluded

I declare that I have carefully read Hacettepe University Graduate School of Science and Engineering Guidelines for Obtaining and Using Thesis Originality Reports; that according to the maximum similarity index values specified in the Guidelines, my thesis does not include any form of plagiarism; that in any future detection of possible infringement of the regulations I accept all legal responsibility; and that all the information I have provided is correct to the best of my knowledge.

I respectfully submit this for approval.

Date and Signature

Name Surname: Cansu Karabeyoğlu

Student No: N14323726

Department: Mechanical Engineering

Program: Mechanical Engineering

Status: Masters Ph.D. Integrated Ph.D.

16.07.2019

ADVISOR APPROVAL

APPROVED.

Asst. Prof. Dr. Selçuk
Himmetoğlu

(Title, Name Surname, Signature)

CURRICULUM VITAE

Name, Surname : Cansu Karabeyođlu
Place of Birth : ŐiŐli, İstanbul
Date of Birth : 1992
Marital Status : Single
E-mail address : cansukarabeyoglu@gmail.com
Foreign Language : English, German

EDUCATION

B.Sc. : Hacettepe University Mechanical Engineering
Department Automotive Engineering Program (2010/2015)
M.Sc. : Hacettepe University Mechanical Engineering
Department (2015/2019)

Work Experiences

Promec Engineering Co. Ltd. - Mechanical Design and Test Systems Department
(01.2018/-)
Artec Advanced Research Technologies Co. Ltd. – R&D Engineer (03.2016/06.2016)